Anti-lymphangiogenic compounds as novel treatment strategies in dry eye disease

Inaugural Dissertation

zur
Erlangung des Doktorgrades
Dr.nat.med
der Medizinischen Fakultät
und
der Mathematisch-Naturwissenschaftlichen Fakultät
der Universität zu Köln

vorgelegt von

Laura Schöllhorn
aus: Aachen

Köln
2016

Berichterstatter/Berichterstatterin:	Prof. Dr. Thomas Langmann Prof. Dr. Ines Neundorf
Tag der letzten mündlichen Prüfung:	12. Januar 2017

“Du machst das nicht für uns…
Du machst das für dich!”

Hans Dieter und Rosi Schöllhorn

Inhaltsverzeichnis

Zusammenfassung

Das Trockene Auge ist eine der häufigsten Erkrankungen der Augenoberfläche, die vor allem ältere Menschen betrifft. Patienten, die an einem trockenen Auge leiden, berichten von Symptomen wie Trockenheit, Reizung, und einer verschlechterten Sehschärfe, die mit einem Verlust der Lebensqualität einhergeht. Auch wenn die Immunpathogenese in den letzten Jahren intensiv diskutiert wurde, kann auf Grund der vielen verschiedenen Auslöser und der Komplexität der Erkrankung noch immer keine kausale Therapie angeboten werden. Somit ist die Identifizierung neuer Behandlungsstrategien von wesentlicher Bedeutung.

Neuere Daten lassen vermuten, dass das antiangiogene Privileg, welches die Transparenz der Hornhaut und somit die Sehschärfe bewahrt, im Verlauf der Erkrankung gestört wird und es zu einer selektiven und spontanen kornealen Lymphangiogenese kommt. Diese pathogene Veränderung ist bereits als Risikofaktor im Bereich der Hornhauttransplantation identifiziert worden. Dabei stellen die Lymphgefäße den afferenten Arm eines Immunreflexbogens dar, indem sie den Transport von antigenem Material und Antigen-präsentierenden Zellen zu den drainierenden Lymphknoten ermöglichen.

In Bezug auf das trockene Auge gibt es erste Hinweise die korneale Lymphangiogenese als die mögliche Verbindung zur adaptiven Immunantwort angenommen, so dass Strategien, die die Lymphangiogenese modulieren, eine Chronifizierung verhindern bzw. den Krankheitsverlauf verbessern können. Eine erste Studie, in der der pro-lymhangiogene Faktor VEGF-C mit Hilfe eines prä-klinischen Medikaments inhibiert wurde, zeigte sowohl eine verminderte Entzündung als auch eine geringere Epitheliopathie.

Im Zuge dieser Arbeit wurde diese Hypothese weiter untersucht. Dazu wurde das bereits zugelassene Medikament Aflibercept hinsichtlich seiner Effizienz, die korneale Lymphangiogenese sowie die T-Zell-vermittelte Immunantwort im Mausmodell des trockenen Auges zu modulieren, getestet. Es wurden zwei verschiedene experimentelle Modelle des trockenen Auges, welche die zwei klinischen Hauptklassen widerspiegeln, verwendet: dass akut induzierbare Desiccating Stress Model, welches durch Umweltfaktoren induziert wird, und das neue, chronische Autoimmunmodell, welches durch eine autoimmune Exokrinopathie der Tränendrüsen induziert wird. Letzteres musste neu etabliert und entwickelt werden und ahmt nicht vollständig die menschliche Pathologie des Sjögren‘s Syndrom nach, spiegelt jedoch die autoimmun getriebene Entzündung und die entstehende Infiltration der Tränendrüsen wieder. Damit wurde ein neues „subklinisches“ Modell des trockenen Auges etabliert. Aflibercept wurde dementsprechend nur im etablierten Desiccating Stress-Modell getestet. Die vorgestellten Ergebnisse lassen vermuten, dass die korneale Lymphangiogenese keine übliche phänotypische Veränderung zu sein scheint, da es in keinem der Experimente mit dem Modell des trockenen Auges induziert werden konnte. Trotz allem führte die Behandlung mit Aflibercept zu einer veränderten, z.T. abgeschwächten Immunantwort. Die vorliegende Arbeit kann die Hypothese einer wichtigen neuen Rolle der

pathologischen kornealen Lymphangiogenese in der Pathogenese des trockenen Auges nicht bestätigen. Es wird jedoch ein neues subklinisches Modell des autoimmunen trockenen Auges etabliert und die grundsätzliche Machbarkeit einer Immunmodulation beim trockenen Aue durch anti-VEGF Therapie gezeigt. Damit ergeben sich zukünftig möliche neue Therapieansätze bei Patienten mit trockenem Auge.

Abstract

Dry eye disease (DED) is one of the most common ocular surface diseases, affecting millions of individuals. Over the last years it became a public health disorder, concerning especially the elderly. Patients who suffer from dry eye, report symptoms like dryness, irritation and decreased visual acuity leading to a loss of life's quality.

Even if the underlying immunopathogenesis has been verified in recent years more and more accurately, no causal treatment is available due to the various factors triggering dry eye disease and its self-intensifying viscious circle. Artificial tears and anti-inflammatory eye drops are nowadays the conventional therapy. Thus the identification of new treatment strategies is essential.

Recent data suggest that the anti-angiogenic privilege, which maintains the transparency of the cornea and preserves high visual acuity, is disturbed in DED leading to a selective and spontaneous outgrowth of lymphatic vessels. These vessels are known as risk factor for corneal graft rejection representing the afferent arm of the immune reflex arc and are shown to enable the access of antigenic material and antigen presenting cells (APCs) to the corneal draining lymph nodes. Thus, with respect to dry eye disease, corneal lymphangiogenesis is speculated to represent the potential link to the adaptive immune response and strategies modulating the lymphangiogenesis could preserve a normal phenotype or improve the disease outcome. A first study, testing blockade of pro-lymphangiogenic VEGF-C by a subclinical drug, revealed a suppressed inflammation and epitheliopathy associated with DED.

Hence, adopting this approach, we tested the hypothesis whether the already approved anti-VEGF compound Aflibercept can modulate corneal lymphangiogenesis as well as the T-cell mediated immune response occurring in dry eye disease. Therefore, two different experimental models, reflecting two major classes of clinical dry eye were contemplated to be used: the reproducible acute inducible desiccating stress model induced due to environmental stress and the novel experimental autoimmune Dry eye model induced due to a specific autoimmunological exocrinopathy of the lacrimal glands.

Regarding the latter, a new self-generated protocol had to be established to induce a "subclinical" model of experimentally autoimmune dry eye. Since it is beyond the frame of this work to show the whole establishment, only the last attempts are shown and discussed concerning the induction of dry eye. The described protocol does not fully mimic the human pathology seen in Sjögren's Syndrome dry eye, but reflects the autoimmunological destruction and the inflammatory infiltration of the lacrimal glands. Thus, testing Aflibercept was only performed in the desiccating stress model.

The results presented provide evidence, that corneal lymphangiogenesis does not seems to be a common phenotypical event in DED as it could not be induced in any of the experiments. However, treatment with Aflibercept leads to an altered immune response.

In summary, this work does not confirm the hypothesis of an important pathogenic role of corneal lymphangiogenesis in inflammatory dry eye disease, at least in the desiccating stress model.

Nonetheless, anti-VEGFs strategies allow for modulation of the immune response in dry eye disease thus opening new treatment avenues for future therapy of dry eye patients.

1. Introduction

Dry eye disease (DED) is one of the most common ocular surface diseases, affecting millions of individuals. With a prevalence of about 5-35% and an incidence of 21.6% [1], dry eye increasingly becomes a public health disorder with a high financial burden [2], concerning especially the elderly [3] [4] [5].

Dry eye disease is defined as a disorder of the lacrimal functional unit (LFU) [6] [7]; a more specialized subunit of the ocular surface system [8] [9]. It can be triggered by several multifactorial factors and manifests itself with several symptoms and severity levels. Thereby the underlying immune reaction is amplified by a self-intensifying vicious circle [9]. Beside symptoms of dryness, irritation and decreased visual acuity, patients suffering from dry eye undergo a loss of life's quality.

Despite the increased understanding of the underlying pathogenesis, no causal treatment is available. Artificial tears are the conventional and first-line treatment nowadays. Therefore, the identification of new approaches and potential therapeutics is essential.

In the following sections of the introduction, the anatomical structures and the ocular immune privilege of the ocular surface are discussed. Furthermore, the definition, the classification, the current treatment strategies and the state of the research regarding dry eye are summarized. Furthermore, the used therapeutic Aflibercept is described.

1.1. The ocular surface system

The ocular surface system is described as an integrated system, including the "*wet-surfaced and glandular epithelia of the cornea, conjunctiva, lacrimal gland, accessory lacrimal glands, nasolacrimal duct and meibomian gland, and their apical and basal matrices, linked as a functional system by both continuity of epithelia, by innervation, and the endocrine and immune systems* "[8] [9].

Based on the direct system's exposition to the environment, including desiccation, injury and pathogens, several protective mechanisms are provided by the ocular surface system to maintain its integrity. As the smooth wet surface is responsible for most of the refractive power, the protection and maintenance of its components is the primary function of the ocular surface system. Thus its name is linked to its primary function [9].

Within the ocular surface system, a more specialized unit can be defined: the lacrimal functional unit *"comprising lacrimal glands, ocular surface (cornea, conjunctiva and meibomian glands) and lids, and the sensory and motor nerves that connect them"* [6] [7]. Its overall function is to maintain the clarity of the ocular surface, which in turn depends on surface homeostasis and the integrity of the tear film which provides lubrication and a proper environment for epithelial cells [10]. Defined by Stern et al. the lacrimal functional unit *"controls the major components of the tear film in a*

regulated fashion and responds to environmental, endocrinological, and cortical influences." [6] [7] [11]. Stimulation of the corneal nerve endings of the sensory afferent nerves triggers impulses which integrate in the central nervous system through the ophthalmic branch of the trigeminal nerve; in turn generating efferent impulses terminating the optimal tear quantity and composition (see Fig. 1).

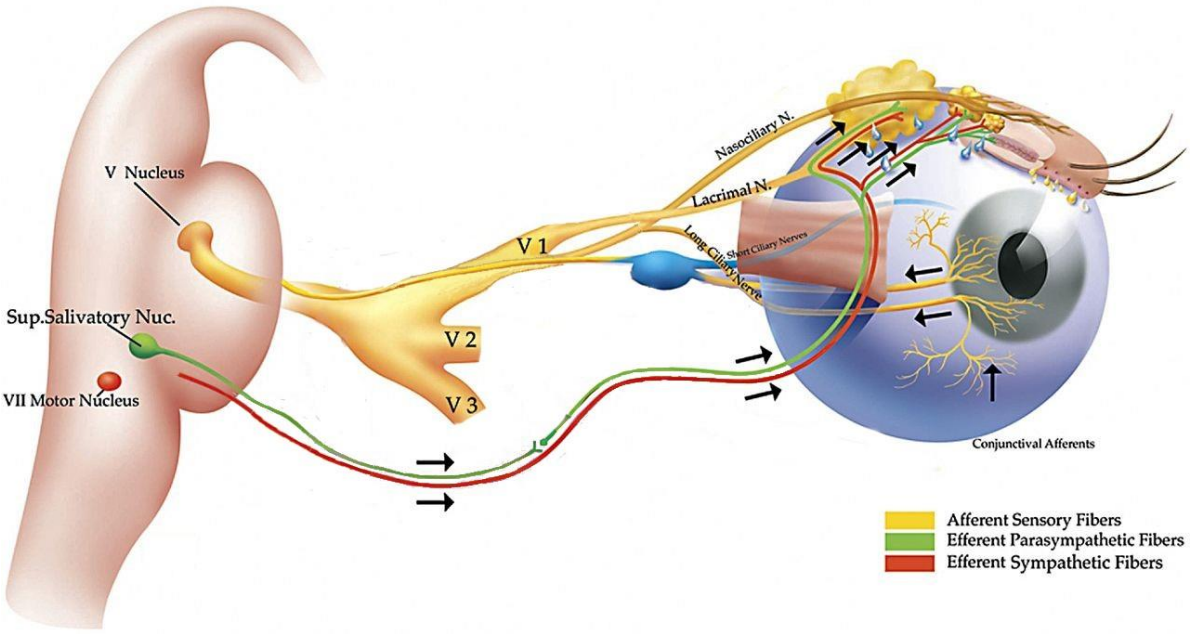

Fig. 1: Schematic illustration of the lacrimal functional unit. Stimulation of the corneal nerve endings triggers afferent impulses which integrate through the ophthalmic branch of the trigeminal nerve (V1, V2, V3) into the central nervous system. This in turn generates efferent impulses that stimulate the secretion of a healthy tear film, terminating the optimal tear quantity and composition. Illustration adapted from Beuermann *et al.* The lacrimal functional unit in *Dry eye and Ocular Surface Disorders* [7] [11].

Damage to any components of the lacrimal functional unit results in an unstable and unrefreshed tear film leading to e.g. tear film break-up causing optical aberrations, reduced tear volume, elevated tear osmolarity, and a reduced clearance of proinflammatory mediators and proteases.
Despite disturbance of the tear film, dysfunctional corneal and conjunctival cells are the most common reasons for ocular surface disorders and their pathological changes [12].

1.2. Anatomical components of the lacrimal functional unit

1.2.1. The cornea

The cornea consists of five different layers which are arranged anterior to posterior as follows: the squamous non-keratinized epithelium, the anterior limiting lamina (Bowman's layer), the corneal stroma (substantia propria), the posterior limiting lamina (Descement's membrane) and the corneal endothelium (see Fig. 2). The outer mucous layer of the corneal epithelium thereby acts as a border to the external environment, whereas the corneal endothelium acts as an internal border to the anterior chamber.
To enable the light to proceed through the eye onto the retina the cornea has to be transparent, thus it is devoid of blood and lymphatic vessels. This is referred as "angiogenic privilege" of the eye [13] and will be discussed in a separated chapter (see 1.3.4)

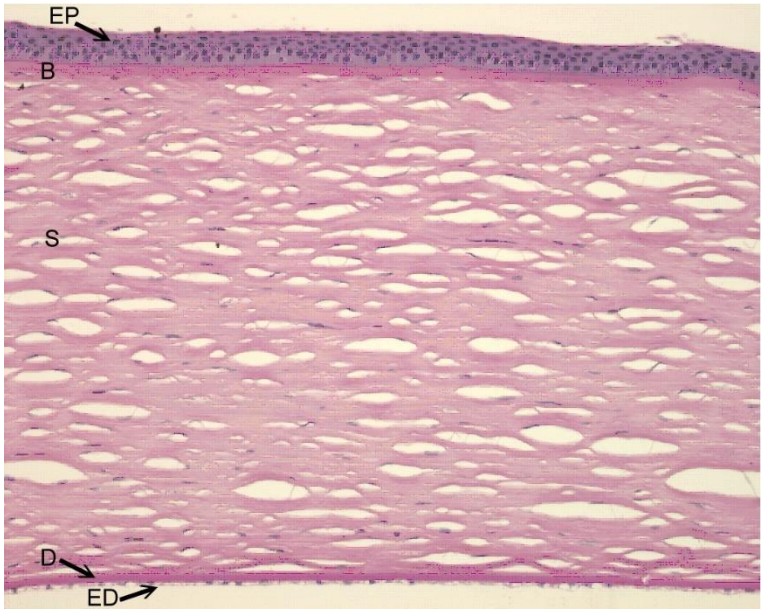

Fig. 2: Histological section of a healthy cornea. It consists of five different layers: the corneal epithelium (EP), the Bowman's layer (B), the stroma (S), the Descement's membrane (D) and the corneal endothelium (ED).

The corneal epithelium is composed of five to six cell layers, 50 - 60 µm thick in humans and the superficial cells are flattened and enucleated [14] [15] [16]. In healthy eyes it is devoid of melanocytes and immunocompetent cells are only located at the outer edge. Desmosomes hold the adjacent cells together whereas the cells of the underlying basal lamina are held together by hemidesmosomes and anchoring filaments [16]. The anterior surface, exposed to the environment, has a specialized structural framework of microvilli and microplicae whose layer of secreted mucus (glycocalyx) support the interaction with several factors like immunoglobulins [17]. Further on, it

enables the aqueous phase of the tear film to attach to the hydrophobic non-wettable corneal epithelium [18].
As maintaining the integrity of the ocular surface is essential for vision, cell replication on the cornea is managed rapidly by mitotic activity. New cells from the limbal basal layer are recruited by the amoeboid movements of the cells in the wounded area, whereby the regenerative response is correlated to severity of damage. [19] [20].

1.2.2. The limbal area

The intervening transition area between the bulbar conjunctiva/sclera and the cornea is called corneal limbus or limbal area. It is the anatomical structure wherein the corneal epithelium becomes continuous with the conjunctival epithelium and the corneal stroma becomes continuous with the sclera (corneoscleral junction). Descement´s membrane and Bowman´s layer of the cornea end at this region.
Loops and arcades of the conjunctival blood and lymphatic capillaries appear throughout this tissue, leading to the involvement in multiple processes like nourishment of the peripheral cornea, immunosurveillance, and hypersensitivity responses. Furthermore, the corneoscleral region accommodates ocular surface progenitor cells (stem cells) in its basal epithelium [21] [22].

1.2.3. The conjunctiva

The conjunctiva is a thin translucent mucous membrane fusing the epithelium of the eyelids at their margin with the corneal epithelium at the limbal area. Until the limbal area it covers up the sclera where the transition towards the corneal epithelium begins.
Goblet cells, integrated in the conjunctival epithelium, are responsible for the production of gel-forming mucins [18] providing the adherence of the tear film to the corneal and conjunctival epithelium.
Intraepithelial dendritic (Langerhans) cells function as sentinels, whereas the subepithelial vascularized tissue contains immunocompetent cell e.g. mast cells, lymphocytes, eosinophils and plasma cells.

1.2.4. The lacrimal glands

The lacrimal gland is a branched tubuloacinar exocrine gland. It secrets electrolytes, proteins, mucins and water into the tear film whereby its right composition and amount is essential for a

healthy ocular surface. In humans it is located in the bony orbit of the eye. It is divided into two lobes, a small palpebral and the large orbital portion. The orbital portion has fine interlobular ducts which unite to form three to five main excretory ducts, transversing the palpebral lobe. It consists of acinar, ductal and myoepithelial cells and the lobules are separated by interlobular fibrovascular tissue [23]. Due to external environmental influences and the adaptive needs of the surface epithelia, the lacrimal gland must be able to quickly adjust the composition of the tear film. This is accomplished by afferent sensory nerves which transmit the stimuli of the cornea and the conjunctiva to the central nervous system from where it is forwarded via the efferent parasympathetic and sympathetic nerves to the lacrimal glands [24].

1.2.5. The corneal tear film

In a simplified way, the corneal tear film is composed of three layers secreted by lacrimal and meibomian glands as well as the corneal and conjunctival epithelia (see Fig. 3).
The superficial lipid layer is secreted by the meibomian glands. It consists of nonpolar lipids covering amphipathic polar lipids [25]. The former provides a barrier function at the air interface whereas the latter are in contact with the intermediate aqueous layer of the tear film providing structural stability. This layer is secreted by the lacrimal glands and contains electrolytes, ions, water and several antimicrobial proteins (further described in the following section). The deep hydrophilic mucin layer of the tear film is secreted by the goblet cells and also the corneal and conjunctival epithelial cells [26]. This layer is not wiped away by blinking. As mentioned before, membrane spanning mucins interact with the glycocalyx of the corneal epithelium enabling the tear film to stick on the hydrophobic non-wettable cornea [8] [16].

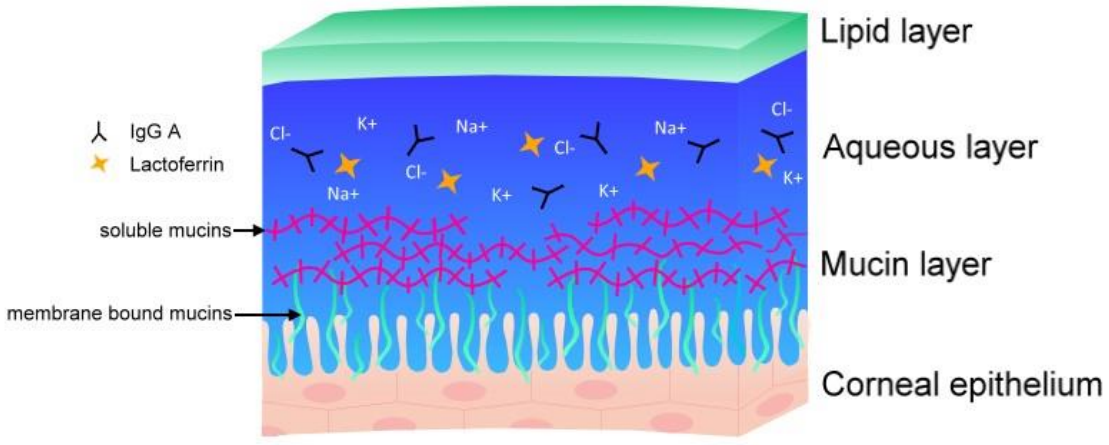

Fig. 3: Scheme of the corneal tear film, composed of three layers: the superficial lipid layer, the intermediate aqueous layer and the deep hydrophilic mucin layer.

1.3. Ocular immune privilege

The eye including all its tissues and compartments of the visual axis has to be transparent to enable light's passage on the retina where visual response is initiated. Thus, challenges from external environment have to be recognized and processed in a way that transparency is not affected.
To balance the amount of inflammation to clear pathogens and the amount of tissue destruction the eye possesses a unique ocular immune privilege [27] which is maintained by anatomical and physical barriers, an immunoregulatory and immunosuppressive microenvironment, the anterior chamber associated immune deviation (ACAID) and the angiogenic privilege.
Thereby site- and tissue-specific mechanisms regulate both, the induction and the expression of innate and adaptive immune response.

1.3.1. Anatomical and physical barriers of the eye

The anterior segment of the eye which is highly vulnerable to pathogens is protected by a multilayer barrier system including the corneal epithelium and the tear film. Numerous antimicrobial proteins (lysozyme, lactoferrin, defensins, secretory IgG and complement factors C3 and C4) in the tear film provide a passive innate response while Toll-like receptors (TLR's) on corneal and retinal epithelial cells provide an active innate immune response.
Furthermore, the blood: retina barrier and the absence of lymphatic vessels in the cornea prevents the fast migration of immunopathogenic cells into and from the eye, regulating the adaptive immune response.

1.3.2. Immunoregulatory and immunosuppressive microenvironment

The immune-privileged microenvironment of the eye consists of several constitutive expressed soluble and cell-bound immunoregulatory and immunosuppressive factors that mediates both, innate and adaptive immunity.
Soluble factors secreted into the aqueous humor (AqH) directly inhibit the activation of innate immunity: Transforming growth factor β (TGF-β) [28] and soluble Fas ligand (FasL) are shown to inhibit neutrophil activation; macrophage migration inhibitory factor (MIF) is shown to inhibit natural killer cells (NK cells) activity [29] [30]; calcitonin gene-related peptide is demonstrated to inhibit macrophages [31] and complement regulatory factors (CD46, CD55, CD59) are shown to inhibit complement activation [32].
With regard to the adaptive immunity it could be demonstrated that AqH inhibits T cell activation and differentiation *in vivo* without affecting lysis by fully functional cytotoxic T cells [33]. In addition,

it is demonstrated that immunopathogenic T cells passing through the cornea, the iris pigment epithelium (IPE) or the retinal pigment epithelium (RPE) are neutralized by apoptosis due to direct cell contact with membrane bound FasL [34] [35] or converted in their immunological function to regulatory T cells by constitutively expressed TGF-β or CD86 [36] [37].

1.3.3. ACAID

Despite the local features mentioned above, the eye possesses an actively regulated deviant systemic immune response against eye-derived antigens; the so called anterior chamber associated immune deviation (ACAID). This specialized immune response is characterized by the suppression of CD4+ T helper 1 (T_{H1}) and T_{H2} cells as well as a suppressed generation of B cells which would secrete complement fixing antibodies. Elimination of pathogens is achieved by primed CD8+ cytotoxic T cells and B cells producing non-complement fixing antibodies in the absence of inflammation while antigen-specific regulatory T cells (Tregs) inhibit the induction of T cell-mediated immunity.
Based on animal studies ACAID is shown to arise because indigenous intraocular APCs (e.g. macrophages and dendritic cells distributed in the stroma and the anterior chamber surrounding structures (iris and ciliary body)) [38] [39] capture eye-derived antigens and migrate through the blood stream to the thymus and the marginal zone of the spleen [40] [41] [42]. Within the thymus they evoke the induction of natural killer T cells (NKT cells) which also migrate to the spleen. At this site, ocular APCs as well as NKT cells [43] [44], marginal zone B cells [45] [46] and naive antigen specific CD4+ and CD8+ T cells congregate. Together, they create a microenvironment that is rich in the cytokines TSP1 [47], TGF-β [48] and interleukin 10 (IL10) [49].
Within these cell clusters two distinct populations of Tregs emerge [50] [51]: CD4+ Tregs, which inhibit the initial induction of naive T cells into T_{H1} cells and CD8+ Tregs, which suppress the T_{H1}-mediate immunity, such as delayed-type hypersensitivity (DTH). Thus, CD4+ Tregs act at the afferent arm of the ACAID in the secondary lymphoid compartment, whereas CD8+ Tregs act at the efferent arm of the ACAID in the periphery, including the eye.
Accordingly, ACAID results in a prolonged acceptance of corneal allografts [52] and solid tissue in the anterior chamber as well as the induction of a systemic tolerance to eye-derived antigens.

1.3.4. Angiogenic privilege of the cornea

To assure visual acuity the healthy cornea is transparent and devoid of blood and lymphatic vessels. This phenomenon is highly conserved in all vertebrates and actively maintained by the so called , angiogenic privilege [13] [53] [54] [55] [56].

It was demonstrated that corneal epithelium cells express soluble forms of the three major vascular endothelial growth factor (VEGF) receptors (sVEGFR-1, sVEGFR-2, sVEGfR-3) acting as a decoy receptor for the hem- and lymphangiogenic factors VEGF-A, VEGF-C, and VEGF-D [57] [58] [59] [60]. In addition endothelial cells of the cornea serve as pumps which remove fluid from the corneal stroma to the aqueous humor to keep the cornea dehydrated [61]. Fluid influx and storage in the stroma would cause irregulations in the tightly packed collagen lamellae and keratocyte network leading to increased light scatter [62] and gaps where vessels could grow in-between the lamellae [63] [64].
Further on several endogenous antiangiogenic factors like endostatin and thrombospondin, located at the epithelial basement membrane, as well as plasminogen derived angiostatin and serine protease inhibitor pigment epithelium derived factor (PEDF) maintain the corneal angiogenic privilege [65] [66] [67] [68] [69] [70] [71] [72] [73]. Endostatin causes endothelial cell cycle arrest in G1, blocks vascular endothelial growth factor (VEGF) induced mitogenic and motogenic activities in endothelial cells [65] [66], and was recently demonstrated to have an effect on lymphangiogenesis [74]. Thrombospondin exerts a strong anti-angiogenic effect via several mechanism [67] [68] and is also important for corneal alymphaticity [75] [76]. Angiostatin was shown to inhibit and regress corneal neovascularization [70]. Furthermore, it is involved in corneal avascular wound healing and downregulates endothelial cell proliferation and migration [69] [71]. PEDF is responsible for excluding vessels from invading the cornea, the vitreous and the retina [73].
Moreover the generated avascularity acts as an anatomical barrier suppressing both arms of the immune reflex arc [77] [78] maintaining the ocular immune privilege. Blood vessels providing a route of entry for immune effector cells (efferent arm) as well as lymphatic vessels enabling the effective access of antigens and APCs to the regional lymph nodes (afferent arm) are physically separated from the cornea, ending at the limbal area (see 1.2.2) [79].

1.4. Dry eye disease

1.4.1. Definition, classification, therapy

2007, on a follow-up consensus meeting of the International Dry Eye Workshop (DEWS 2007), the original definition of dry eye by Lemp [80] was updated to a more broaden definition reflecting not only the newest research but also the multifaceted aspects of the disease:
“Dry eye is a multifactorial disease of the tears and the ocular surface that results in symptoms of discomfort, visual disturbance, and tear film instability with potential damage to the ocular surface. It is accompanied by increased osmolarity of the tear film and inflammation of the ocular surface.” [9].

In accordance to that dry eye is recognized as an disturbance of the lacrimal functional unit (LFU), with tear hyperosmolarity and tear film instability as the main driving forces in the self-intensifying vicious circle of DED [9]. Tear hyperosmolarity leads to the activation of inflammation on the ocular surface, followed by the release of inflammatory molecules into the tears [81] [82] [83]. As a consequence, the ocular surface epithelium is damaged, characterized by cell death due to apoptosis [84], loss of goblet cell density [85], and disturbance of mucin expression [86]. The following tear film instability exacerbates the ocular surface hyperosmolarity and completes the vicious circle (see Fig. 4).

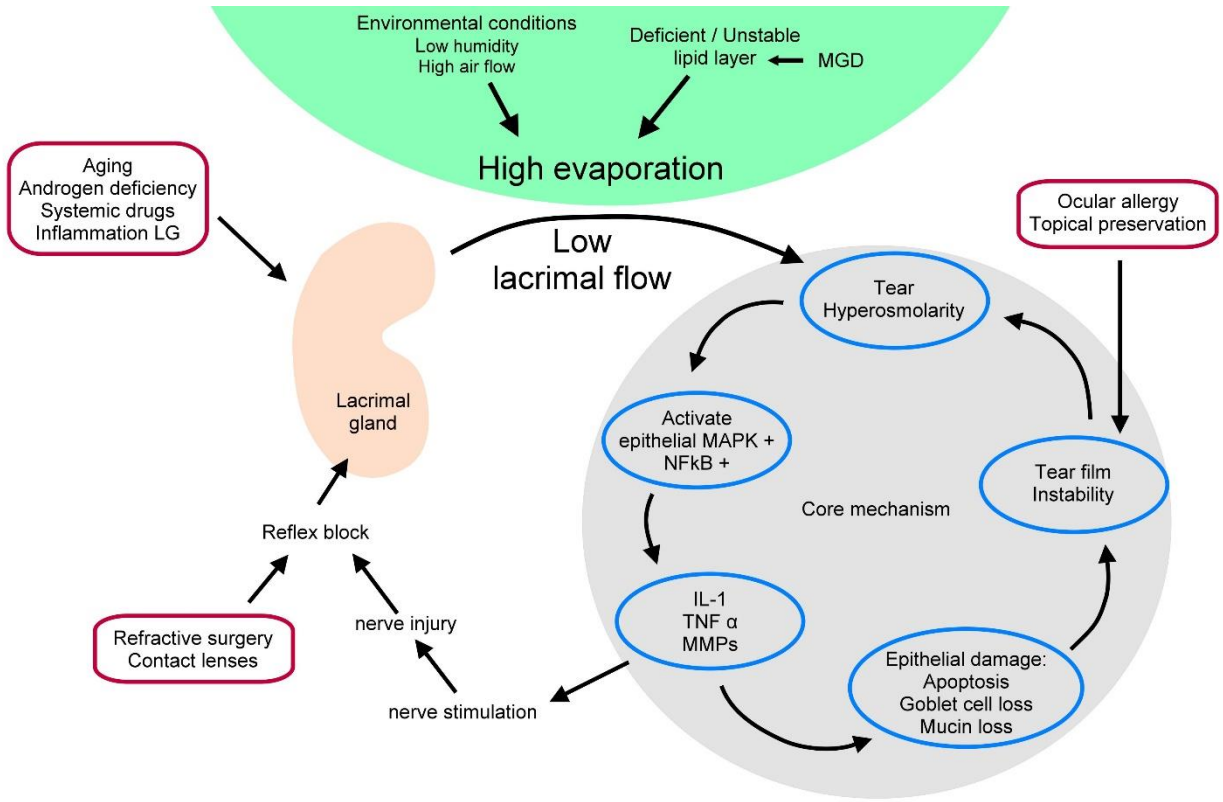

Fig. 4: Schematic mechanism of DED. Tear hyperosmolarity and tear film instability are the main forces in the self-intensifying vicious circle of dry eye. The core mechanisms are shown on the right. Tear hyperosmolarity leads to the activation of inflammation and the subsequent release of inflammatory molecules into the tears. The following corneal epithelium damage is characterized by cell death due to apoptosis, loss of goblet cell density, and disturbance of mucin expression. This in turn leads to tear film instability, which exacerbates ocular surface hyperosmolarity and completes the vicious circle. Possible risk factors are represented in the outer red circles. Adapted from DEWS (2007) [9].

Risk factors for the development of dry eye have a wide variety, resulting either in tear hyperosmolarity or in tear film instability or both. Aging, androgen deficiency, systemic drugs and local inflammatory reactions could have a direct influence on the lacrimal flow rate whereas due to

refractive surgery or wearing contact lenses a neurosensory blockade of the lacrimal flow could be induced. Environmental conditions like low humidity and high air flow as well as a deficient or unstable lipid layer due to meibomian gland dysfunction (MGD) leads to a high evaporation of the tear film. All these conditions lead to an increased tear osmolarity. In addition, several etiologies, like ocular allergy or topical preservative use, could initiate tear film instability without the prior occurrence of a tear film hyperosmolarity.

Classification of dry eye disease can either be performed by severity, since different severities need different treatment regime or by etiopathological factors, reflecting the secretory elements involved in disease induction. Using the latter, dry eye disease can be classified in two main groups: aqueous tear-deficient dry eye (ADDE) and evaporative dry eye (EDE) [9].
ADDE arises through a failure of lacrimal gland function, resulting in a reduced tear secretion and volume. This in turn leads to a tear hyperosmolarity, inducing inflammatory responses of the epithelial cells. Due to the underlying immune response, ADDE is divided in two subclasses: Sjögren's syndrome dry eye (SSDE) and non-Sjögren's syndrome dry eye (NSSDE). SSDE is caused by an exocrinopathy in which lacrimal and salivary glands are targeted by an autoimmune reaction. Autoreactive T and B cells infiltrate the lacrimal and salivary glands, inducing cell death of acinar and ductual cells. As a result of the local inflammation, autoantigens are expressed by epithelial cells [87] and tissue specific T cells are retained [88]. NSSDE proceeds without any autoimmune features. Lacrimal gland deficiency mostly occurs due to age-related conditions, like decreased tear volume and flow, increased osmolarity [89], decreased tear film stability [90] or an alteration in the lipid layer [91].
In contrast, EDE is characterized by a normal lacrimal secretory function with a coupled excessive evaporation rate. Thereby intrinsic causes like meibomian gland dysfunction or extrinsic causes like contact lenses are described to induce EDE.

Patient who suffer from DED are likely to report symptoms of dryness, irritation, decreased visual acuity, contrast sensitivity and a loss of quality of life. Further on, compensatory responses like increased reflex tearing, blinking and meibomian gland secretion are reported.
Patients suffering aqueous tear deficiency have decreased tear film stability and tear volume. These individuals have several therapeutic options in form of artificial tears. They are applied topically to the ocular surface and viscosity, retention time and adhesion to the ocular surface of the artificial tears are determined by the polymers they based on. Common polymers are hyaluronic acid, cellulose esters, polyvinyl alcohol, povidone and carbomers. As chronic forms of DED remain due to an immune-based inflammation, topically applied corticosteroids are prescribed as effective short-term therapeutics. They block inflammatory pathways, including proinflammatory cytokine and chemokine secretion, synthesis of matrix metalloproteinases and prostaglandins as well as cell adhesion molecule expression. Cyclosporine-A (Restasis®, Allergan; Ikervis®, Santen) are the only

FDA approved therapeutics used for DED. Cyclosporine is a fungal-derived peptide, which inhibits nuclear translocation of cytoplasmic transcription factors and the production of inflammatory cytokines. But, however, so far no causal therapies are available to cure DED.

1.4.2. Current research

Based on the current knowledge, non-Sjögren's Syndrome dry eye is understood as a chronic inflammatory disorder, wherein the innate as well as adaptive immunity of the ocular surface are activated.

As mentioned above, increased evaporation or tear hyperosmolarity causes ocular surface inflammation. Due to the osmotic stress to the ocular surface epithelium, early innate effectors are activated, representing the afferent arm of the immune response.

Natural killer cells are shown to accumulate by 1 day of desiccating stress, representing an early source of Interferon γ (IFN-γ), IL-6, IL-23 and IL-17 [92] [93]. IFN-γ upregulates the expression of the intracellular adhesion molecule 1 (ICAM-1) on epithelial and endothelial cells and together with IL-17 it contributes to corneal barrier disruption [94] [95] [96].

Due to elevated epithelial apoptosis Toll-like receptor (TLR) activation is induced, and mitogen-activated protein kinase (MAPK) pathways and NFκB signaling are activated in epithelial cells [81] [97] [98] [99]. MAPK activation stimulates these cells to produce several proinflammatory cytokines; e.g. IL1-β, TNF-α and IL-8, as well as several MMPs (MMP-1, -3, -9, -10 and -13) [81] [100] [98].

IL1-β and TNF-α are demonstrated to amplify the innate immune response by upregulating the expression of costimulatory molecules like CD80/86, MHC class II antigens and CC chemokine receptor 7 (CCR7) on resident APCs, like dendritic cells (DCs) and macrophages [101]. In addition, both promote the expression of several chemokines (e.g., CCL3, CCL4, CCL5, CXCL9, CXCL10) [102] [103] [104] [105] as well as of ICAM-1 on epihelial cells [106] [107].

Activated antigen-bearing APCs represent the link between innate and adaptive immune response, since they migrate toward the draining lymph nodes where they stimulate cognate naive T cells, reflecting the efferent arm of the immune response. APC trafficking is dependent on CCR7 signaling [108] and seems to be enhanced by isolated corneal lymphangiogenesis demonstrated to occur in experimental induced non-Sjögren's Syndrome dry eye [109] [110] [111] as well as in Sjögren's Syndrome dry eye [76].

CD4+ T_{H1}, CD4+ T_{H17} T cells as well as CD8+ T cells are nowadays understood as the primarily effector cells of the immunopathogenesis [112] [113], which additionally is associated with an inefficient function of regulatory T cells (Tregs) [114]. While Treg homeostasis is not affected, their potential to suppress effector T cells is reduced and restricted to the T_{H1} T cell subpopulation [114]. Migration out of the lymphoid compartment of activated T cells toward the site of inflammation is

shown to be primarily mediated by CCR5 as well as CXCR3 [113]. T cell infiltration is facilitated by elevated expression of lymphocyte function-associated antigen 1 (LFA-1) on these T cells coupled to the increased expression of its binding partner ICAM-1 on epi- and endothelial cells [96] [106] [107]. At the ocular surface, these cells secret IFN-γ (T_{H1} T cells) and IL-17 (T_{H17} T cells). Increased expression of both derivates has been reported on human and murine ocular surface and are demonstrated to correlate with epithelial cell apoptosis, increased corneal permeability and squamous metaplasia of the corneal surface [94] [95] [112] [115] [116].

In addition, dry eye could manifest itself as an inflammatory autoimmune disorder, known as Sjögren's Syndrome dry eye [9]. In this case it is described as an autoimmune epithelitis, wherein the exocrine glands (salivary and lacrimal glands) are infiltrated by lymphocytic and plasma cells as well as monocytic inflammatory cells [117] [118], leading to a glandular destruction of the tissue. Thereby, the underlying exocrinopathy can be encountered alone, like in the primary Sjögren's Syndrome dry eye or in association with other autoimmune disorders, like rheumatoid arthritis (secondary Sjögren's Syndrome dry eye) [9].

Regarding possible autoantigens, itself little is known. Putative autoantigens have been identified in sera of patients suffering from Sjögren's Syndrome dry eye including type 3 muscarinic acetylcholine receptor, ribonucleoprotein Ro52 and 60 (anti-Sjögren's Syndrome antigen A, (SS-A/Ro)), La 48 (anti-Sjögren's Syndrome antigen B, (SS-B/LA)) and αFodrin [119] [120] [121] [122]. Nonetheless, a specific initiating autoantigen is still not identified.

1.4.3. Dry eye disease and corneal lymphangiogenesis

Only recently, experimental studies in a desiccating stress model of non-Sjögren's Syndrome dry eye as well as in an autoimmune model reflecting Sjögren's Syndrome dry eye revealed the isolated ingrowth of lymphatic vessels, but not blood vessels, into the physiologically avascular cornea [109] [110] [111] [118] [76].

It was demonstrated that the lymphatic area was increased 14 days after desiccating stress while lymphangiogenic VEGF-D and VEGFR-3 levels were increased earliest on day 6. In addition, an increased homing of mature CD11b positive APCs to the corneal draining lymph nodes as well as an increased recruitment of CD11b positive monocytic cells to the cornea was detectable [109].

Furthermore, using the mouse cornea micropocket assay, IL17, one of the predominantly secreted inflammatory cytokines in DED, was demonstrated to directly induce corneal lymphangiogenesis [123]. Thus, the corneal angiogenic privilege [13] which maintains the transparency of the cornea and preserves high visual acuity is disturbed in DED.

As lymphatics were conduits that provide the access of APCs and antigenic material from the cornea to the draining lymph nodes [124] [125] it is assumed that strategies modulating lymphangiogenesis could preserve a normal phenotype or improve the disease outcome.

First studies that have adopted this approach, revealed a significantly reduced corneal lymphangiogenesis, a weakened immune response and disease progression. Thus *in vivo* blockade of IL17 in the desiccating stress model demonstrated a significantly decreased corneal lymphangiogenesis and epitheliopathy [123]. Same results were reached by systemically blockade of VEGF-C, leading to a significant reduction in lymphatic vessels, epitheliopathy and CD11b positive monocytic cells in the cornea [110].

Despite these findings, corneal lymphangiogenesis is shown to be the primary risk factor for corneal allograft rejection [126] and inhibiting lymphangiogenesis before and after keratoplasty significantly increases the outcome of corneal transplantation [127] [128] [129]. Coincident, cervical lymphadenectomy (the surgical excision of draining lymph nodes) results in 90% graft survival after high-risk keratoplasty [130].

Hence, anti-lymphangiogenic therapies may be a novel effective therapeutic tool to diminish severity of DED.

1.5. Aflibercept

Aflibercept is a recombinant fusion protein with a molecular weight of approximately 115 kilo Daltons. It is composed of the Fc portion of human IgG1 fused to portions from the human extracellular VEGFR 1 and 2 domains [131]. It serves as a soluble decoy receptor binding VEGF-A, -B, and placenta growth factor (PIGF) [132]. As an ophthalmic agent, it is FDA-approved for neovascular age-related macular degeneration, macular edema and diabetic retinopathy. Human safety profile and efficacy studies demonstrated a good tolerance without any drug-related ocular or systemic adverse events and due to its high affinity blocking properties (between 0.36 and 39 pM) it allows an extended dosing interval up to 8-week interval. Further on, Aflibercept is shown to bind murine VEGF-A with a K_D of 0.5 pM [132], making it a suitable compound used in several murine experimental models.

Thus, Aflibercept is already shown to suppress choroidal and subretinal neovascularization by subconjunctival and intravitreal administration [133] [134]. Furthermore, it is demonstrated to inhibit both, corneal hem- and lymphangiogenesis by systemically application in the murine inflammatory suture-induced neovascularization model as well as after keratoplasty [127] [128] [129] [135] [126]. Furthermore, a sufficient penetration through the cornea of topical administered Aflibercept was demonstrated in the model of corneal neovascularization induced by chemical burn in rats [136].

1.6. Scope of the thesis

Recent data indicate that the anti-angiogenic privilege of the cornea is disturbed in DED, leading to a selective and spontaneous lymphangiogenesis. Lymphatic vessels were already shown to be the primarily risk factor for corneal graft rejection in animal models of corneal transplantation [126], representing the afferent arm of the immune reflex arc enabling the access of antigenic material and APCs to the corneal draining lymph nodes.

Our hypothesis was that anti-lymphangiogenic compounds could interfere in the vicious circle of dry eye disease by modulating the lymphangiogenesis as well as the T cell mediated immune response, thereby preserving a normal phenotype or improving the disease outcome.

To test this, 2 different models reflecting the two major classes of dry eye were contemplated to be used:

1) the novel, herein developed experimental autoimmune Dry eye model induced due to a specific autoimmunological exocrinopathy of the lacrimal glands reflecting Sjögren's Syndrome dry eye.
2) the established acute desiccating stress model induced due to environmental stress reflecting non-Sjögren's Syndrome dry eye.

In both models the efficiency of Aflibercept to modulate dry eye related lymphangiogenesis was contemplated to be tested by topical as well as systemic application. Therefore, clinical evaluation of epitheliopathy and tear secretion, immunohistochemical analysis of corneal neovascularization as well as flow cytometry analysis of corneal lymph nodes were performed.

2. Material

2.1. Reagents

Tab. 1

Reagents	*Manufacturer*
Acetone	Carl Roth GmbH & CO KG
Albumin bovine fraction V	BDH chemicals
Bovine serum albumin, 2% (w/v)	Carl Roth GmbH & Co KG
Collagenase from Clostridium histolyticum, Type IA	Sigma-Aldrich Chemie GmbH
DAKO® fluorescent mounting medium	DAKO Diagnostic
Eosin G 1% (v/v)	Carl Roth GmbH & CO KG
Ethanol 70%(v/v)	Otto Fischar GmbH und Co. KG
Formaldehyde, 5% (v/v)	Otto Fischar GmbH und Co. KG
Fluorescein Alcon® 10% (w/v)	Alcon Pharma GmbH
Freund's Adjuvant, Complete	Sigma-Aldrich Chemie GmbH
Freund's Adjuvant, Incomplete	Sigma-Aldrich Chemie GmbH
Hematoxylin	Morphisto
Hanks'Balanced Salt solution	gibco® by life technologies™
Hepes Buffer, BioWhittaker®, 1M	Lonza
Medium, DMEM (1X) + GlutaMAX™	gibco® by life technologies™
Mycobacterium Tuberculosis H37 Ra, Desiccated	BD *Difco*™
Neo-Mount® mounting medium, anhydrous	Merck Millipore
Pertussis toxin from Bordetella pertussis	Sigma-Aldrich Chemie GmbH
Phosphate buffer saline (PBS)	
Red blood cell lysis buffer	Sigma-Aldrich Chemie GmbH
Sodium chloride (NaCl), 0.9% (w/v)	B. Braun Melsungen AG
(−)-Scopolamine hydrobromide trihydrate	Sigma-Aldrich Chemie GmbH
Xylene	Carl Roth GmbH & Co KG

2.2. Consumables and Equipment

Tab. 2

Consumables and Equipment	*Manufacturer*
Autoclave, Labklav 25	SHP Steriltechnik AG
Anesthesia machine, UNO	UNO BV
Precision balance, Sartorius M-pact AX6202	Sartorius AG
Analytical balance, Sartorius, Competence CP64	Sartorius AG
Culture plates, CELLSTAR®, 6-well	Greiner Bio One International GmbH
Cell strainer, EASYstrainer™, 40 µm	Greiner Bio One International GmbH
Centrifuge, Refrigerated Benchtop, Sigma® 4K15C	Sigma Laborzentrifugen GmbH
Centrifuge, Refrigerated Benchtop, Heraeus® 16	Thermo Fisher scientific
Centrifuge, Benchtop, Galaxy MiniStar	VWR International GmbH
Cover slip	Carl Roth GmbH + Co KG,
Counting chambers according to Neubauer 0.1 mm depth, 0.0025 mm²	Karl Hecht GmbH&Co KG,
Cold light source KL 1500 LCD	Schott AG
Digital camera ColorView III	Olympus, Soft Imaging Solutions GmbH
Digital camera XM10	Olympus
Flow cytometer, guava easyCyte™ HT, benchtop	Merck Millipore
Flow cytometer, Canto	BD
Fluorescence microscope BX51	Olympus Optical Co., Hamburg,
Freezer, Forma 906, -86°C	Thermo Fisher scientific
Fridge, G 521008, -20°C	Liebherr International Deutschland GmbH
Fridge, UK1720, 4°C	Liebherr International Deutschland GmbH
Glassware	Schott AG
Gloves, Peha-soft® nitrile powderfree	Paul Hartmann AG
Homogeniser, Precellys® 24	Bertin Technologies

Instrument cleaning Fluid; Guava ICF®	Merck Millipore
Illuminator Intensilight C-HGFI	Nikon Instruments Europe B.V.
Magnetic stirrer, heatable, VMS-A	VWR International GmbH
Microscope Illumination, Stereo, KL1500 compact	Schott AG
Microscope slides, Superfrost Ultra Plus®	Thermo scientific
Microscope, Primovert	Carl Zeiss Microscopy, LLC
Microtom, Microm HM400	Histo Serve
Needle, Eclipse ™ ,23G 1“ (0.6 x 25 mm)	Becton, Dickinson and Company
Needle, Sterican®, 30G 1/2“ (0.3 x 12 mm)	B. Braun Melsungen AG
Ocular sticks, Pro-ophta®, 5 mm ø	Lohmann & Rauscher GmbH & Co. KG
Papertowels, Kolibri	igeia
Phenol red threads, Zone Quick®	Showa Yakuhin Co., LTD
Pipette controller, accu-jet®pro	Brand GMBH + CO KG
Pipettes, Eppendorf® Research plus	Eppendorf
Pipettes, Glass Pasteur	Brand GMBH + CO KG
Pipettes, serological (5 ml, 10 ml, 25 ml)	Sarstedt AG
Pipette tips	Sarstedt AG
Precellys Ceramik-Kit 1.4 / 2.8 mm	PEQLAB Biotechnologie GmbH
Scalpel, disposable, No.11	FEATHER Safety Razor Co., Ltd.
Spectrophotometer, Epoch Microplate reader	Bio-Tek
Stereomicroscop, SMZ168TP	Motic Deutschland GmbH
Syringe, Dispomed®, fine dosing, 1 ml	Dispomed Witt oHG
Tubes, Flow cytometry, 5 ml	Sarstedt AG
Tubes, micro (1.5 ml, 2 ml)	Sarstedt AG
Ultrasonic processor, Vibra cell™ 72434	Bioblock scientific
Vortex Mixer, analog	VWR International GmbH

2.3. Antibodies

Tab. 3

Antibodies/Isotype Controls		*Manufacturer*
rat anti *mouse* CD4	APC conjugated	eBioscience
rat anti *mouse* CD8b	FITC conjugated	Biolegend
armenian hamster anti *mouse* CD11c	FITC conjugated	Biolegend
rat anti *mouse* CD11b	FITC conjugated	AB Serotec
rat anti *mouse* MHC2	PE conjugated	BD Bioscience
rat anti *mouse* CD45	PE conjugated	BD Bioscience
rabbit anti *mouse* Lyve-1	unconjugated	AngioBio
rat anti *mouse* CD31	FITC conjugated	BD Bioscience
goat anti rabbit Cy3		Dianova
rat IgG2aκ	APC conjugated	eBioscience
rat IgG2bκ	FITC conjugated	eBioscience
armenian hamster IgG	FITC conjugated	Biolegend
rat IgG2b	FITC conjugated	BD Bioscience
rat IgG 2a κ	PE conjugated	eBioscience
7-AAD Viability staining solution		Biolegend
rat anti *mouse* CD16/CD32 (Mouse BD Fc Block™)		BD Bioscience
Aflibercept (Eylea®), 40 mg / ml		Bayer AG

2.4. Commercially available Kits

Tab. 4

Kits	*Manufacturer*
Pierce™ BCA Protein Assay Kit	Thermo Fisher Scientific
Nuclear extract Kit	Actif motif ®

2.5. Surgical instruments

Tab. 5

Surgical instruments	*Manufacturer*
Scissor, Metzenbaum	F.S.T., Heidelberg, Germany
Spring scissor, Student Vannas, straight	F.S.T., Heidelberg, Germany
Forcep, Sudent Dumont #5	F.S.T., Heidelberg, Germany

2.6. Animals

For all animal experiments, female C57BL/6NCrl mice from Charles River Laboratories, Germany aged 6-8 weeks were used. All animal protocols were approved in accordance with the Association for Research in Vision and Ophthalmology's Statement for the Use of Animals in Ophthalmology and Vision Research.

2.7. Software

Tab. 6

Software	*Manufacturer*
Cell Sense	Olympus Soft Imaging solutions GmbH
FlowJo Version 10.0.7	FlowJo
Gen5™ Datenanalyse-Software	Biotek
Guava Easy Cyte, Version 3.7.4	Merck Millipore
InStat 3, Version 3.10	GraphPad Software Inc.
Prism6, Version 6.05	GraphPad Software Inc.

3. Methods

3.1. Animal experimental techniques

The local animal care committee in accordance with the Association for Research in Vision and Ophthalmology's Statement for the Use of Animals in Ophthalmology and Vision Research approved all animal protocols. As mice were purchased from external sources, they were housed for one or two weeks to acclimate.

3.1.1. Experimental autoimmune Dry eye model

First, Complete Freund's adjuvant (CFA, 1 mg / ml, Sigma-Aldrich Chemie GmbH) was adjusted to a concentration of 2.4 mg / ml by adding desiccated Mycobacterium tuberculosis (BD *Difco*™). Next, equal volumes of lacrimal gland homogenate (240 µg / 100 µl per mouse, for preparation see 3.6.1) and CFA (240 µg / 100 µl per mouse) were sonificated on ice to form an emulsion.
After mice were deeply anesthetized (see 3.1.3) each mouse received 200 µl of the emulsion in total: 100 µl were injected subcutaneous (s.c.) on the base of the tail and 50 µl were injected s.c. in each flank. Furthermore, to increase immune onset mice received 2 µg Pertussis toxin (PTX, Sigma-Aldrich Chemie GmbH) intraperitoneally (i.p.). Control mice received an emulsion consisting of adjusted CFA mixed only with PBS. All mice were kept under standard animal housing.
On day 7 mice received a booster injection (BI). Therefore, equal volumes of lacrimal gland homogenate (240 µg / 100 µl per mouse) or PBS were mixed with Incomplete Freund's adjuvant (IFA) and sonificated on ice to form an emulsion. Under anesthesia each mouse received 200 µl of the emulsion in total: 100 µl were injected s.c. on the base of the tail and 50 µl were injected s.c. in each flank.
Short-term analysis (until day 14) (see Fig. 5) as well as long-term analysis (until day 56) (see Fig. 6) of immunization were performed. Short-term analysis comprise clinical evaluation of epitheliopathy and tear secretion on day 0, 3, 7, 10 and 14. Morphometric analysis of corneal neovascularization, flow cytometry analysis of corneal draining lymph nodes as well as the lacrimal glands were performed on day 7, 10 and 14. Long-term analysis comprise clinical evaluation of epitheliopathy and tear secretion on day 14, 21, 28, 35, 42, 49, and 56. Morphometric analysis of corneal neovascularization, flow cytometry analysis of corneal draining lymph nodes as well as the lacrimal glands were performed on day 14, 28, 42, and 56. Histochemical analysis of inflammatory infiltrates in lacrimal gland sections were performed on day 56.

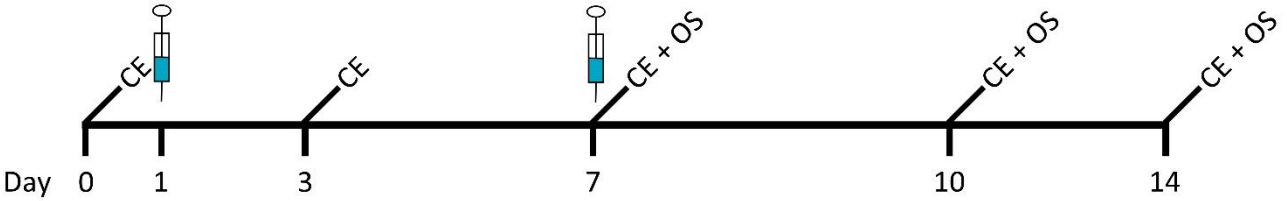

Fig. 5: Scheme of short-term immunization. Initial immunization on day 1 and booster injection on day 7 are indicated by syringes. Clinical evaluation (epitheliopathy and tear secretion; CE) was performed on day 0, 3, 7, 10 and 14. On day 7, 10 and 14 organs required for subsequent analysis were collected (organ sampling; OS).

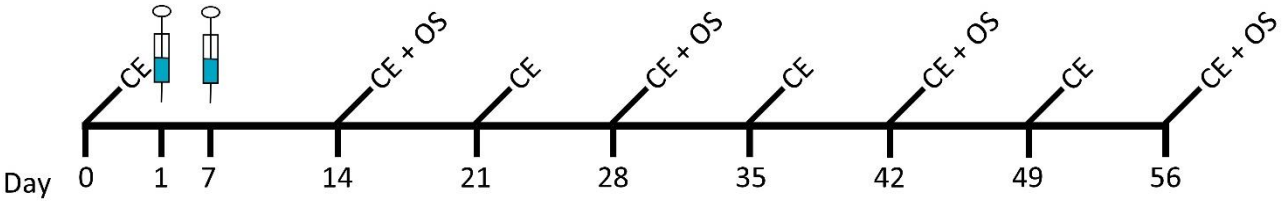

Fig. 6: Scheme of long-term immunization. Initial immunization on day 1 and booster injection on day 7 are indicated by syringes. Clinical evaluation (epitheliopathy and tear secretion; CE) was performed on day 14, 21, 28, 35, 42, 49, and 56. On day 14, 28, 42 and 56 organs required for subsequent analysis were collected (organ sampling; OS).

3.1.2. Desiccating stress model

Acute non-Sjögren's Syndrome dry eye was induced in mice as described below. The used experimental setup is adapted from Dursun et al [137]. C57BL/6 mice were placed in a controlled-environment chamber (CEC) with a relative room humidity maintained at about 30% and a constant temperature of 21 to 23°C. The evaporation of the tear film leads to ocular surface lesions mimicking pathologies found in dry eye patients [112] [138]. To maximize ocular dryness, mice received 100 µl subcutaneous (s.c.) injections of the anti-cholinergic agent scopolamine hydrobromide twice a day, alternating between the left and right flanks with a concentration of 10 mg / ml. This hampers amongst mucosal secretion [137].

To determine the effect of the anti-lymphangiogenic compound Aflibercept in acute non-Sjögren's Syndrome dry eye two experimental setups were used:
A) mice were treated topical beginning on day one for 14 consecutive days (see Fig. 7) while dessicating stress. Topical administration was performed three times a day (40 mg / ml Aflibercept, each 3 µl). Concentrations of the compound was chosen in concordance with the off label concentration used in the clinic.

Control group received an equal volume of saline solution (NaCl, 0.9% (w/v)) and naive mice serve as control for the induction of dry eye. Clinical evaluation (CE) (see 3.2) of epitheliopathy and tear secretion was performed on day 0, 3, 7, 11 and 14 and on final day mice were euthanized and organs required for subsequent analysis collected (organ sampling; OS) (see 3.3).

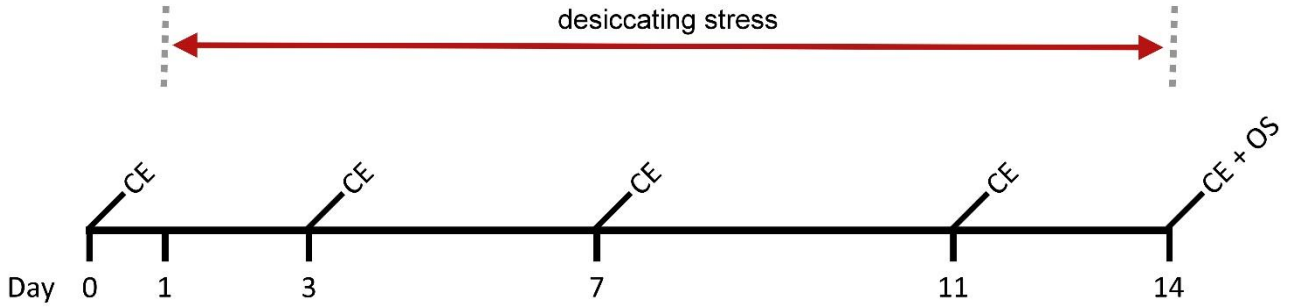

Fig. 7: Scheme of topical administration. Eye drops (3 µl) were administered three times a day (40 mg/ml Aflibercept). Clinical evaluation (epitheliopathy and tear secretion; CE) was performed on day 0, 3, 7, 11 and 14. On final day mice were euthanized and organs required for subsequent analysis collected (organ sampling; OS).

B) mice were treated systemically by two different experimental setups. In the prevention trial mice received intraperitoneally (i.p.) Aflibercept injections on day 1, 3, and 7 while mice were sitting in CEC for 14 days (see Fig. 8). In the therapy trial mice received i.p. Aflibercept injections on day 11 and 13 during dessicating stress. On day 15 mice were transferred to standard animal housing conditions till day 24, receiving i.p. injection on day 17 (see Fig. 9). Mice received 50 µl Aflibercept (25 mg/kg bodyweight) whereas the control group received an equal volume of saline solution (NaCl 0.9% (w/v)). Concentrations of the compounds were chosen in concordance with the off label concentration used in the clinic and previous corneal transplantation experiments performed with Aflibercept. Clinical evaluation (see 3.2) of epitheliopathy and tear secretion was performed on day 0, 3, 7 and 14 in the prevention trial whereas clinical evaluation in the therapy trial was performed on day 0, 7, 11, 13, 17, and 24. On final day mice were euthanized and organs required for subsequent analysis collected (organ sampling; OS) (see 3.3).

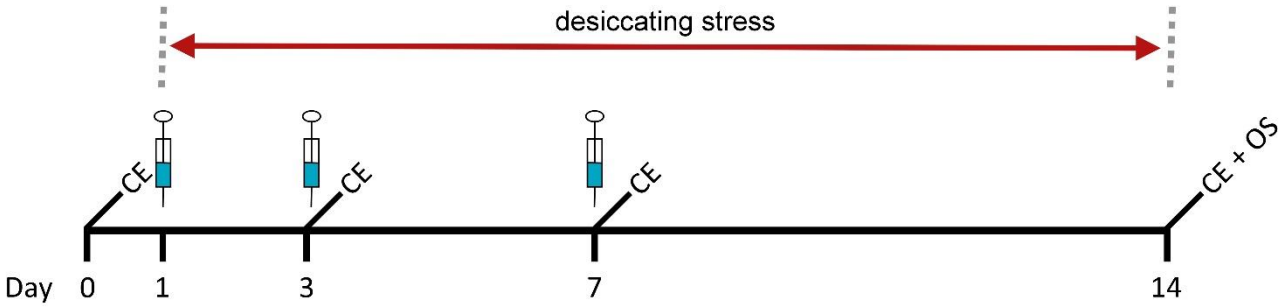

Fig. 8: Scheme of systemically administration regarding prevention. 50 µl Aflibercept (25 mg/kg bodyweight) were injected i.p. on day 1, 3, and 7 during desiccating stress (indicated by syringes). Clinical evaluation (epitheliopathy and tear secretion; CE) was performed on day 0, 3, 7 and 14. On final day mice were euthanized and organs required for subsequent analysis collected (organ sampling; OS).

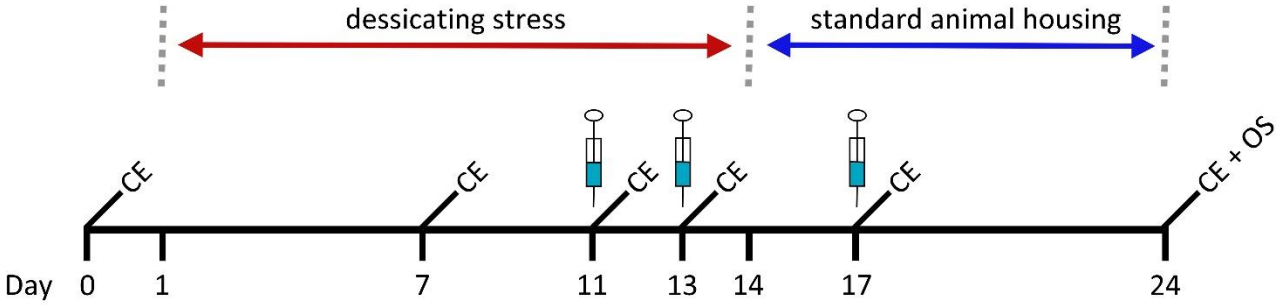

Fig. 9: Scheme of systemically administration regarding therapy. 50 µl Aflibercept (25 mg / kg bodyweight) were injected i.p. on day 11 and 13 during desiccating stress and on day 17 under standard animal housing conditions (indicated by syringes). Clinical evaluation (epitheliopathy and tear secretion; CE) was performed on day 0, 7, 11, 13, 17 and 24. On final day mice were euthanized and organs required for subsequent analysis collected (organ sampling; OS).

3.1.3. Anesthesia

Prior to immunization, mice were deeply anesthetized by mean of the UNO anesthesia machine (UNO BV). First, animals were placed in the induction chamber by a flow rate of 0.7 µl / min and a concentration of 4.5% (v/v) isoflurane. After two min mice were kept out of the chamber and the desired depth of anesthesia maintained with a face mask by a flow rate of 0.25-0.3 µl / min and a concentration of 3% (v/v) isoflurane.

3.2. Clinical evaluation

To monitor disease severity, clinical evaluation by measuring corneal epitheliopathy and tear secretion was performed. Both, fluorescein staining scores and phenol red thread test were validated clinical readouts used in human diagnostics and animal experiments [139] [137]

3.2.1. Fluorescein staining score

Corneal epitheliopathy was measured by staining of epithelial surface defects with a biomicroscope (Illuminator Intensilight C-HGFI (Nikon Instruments Europe B.V)) under cobalt blue light. Two min after topical application of 1% (w/v) fluorescein to the corneal surface, the excessive fluid was removed and the spotted staining recorded with the adapted standard National Eye Institute grading system (NEI, Bethesda, MD) of 0 to 2 for each of the five areas of the cornea – central, superior, inferior, nasal and temporal. Measurements were performed for both eyes and averaged for statistical analysis.

3.2.2. Schirmer test

Measurement of the tear secretion was done by Schirmer test, using cotton phenol red threads (Zone Quick®) which were applied to the lateral canthus of the mouse eye for 15 seconds [140]. Wetting of the threads leads to a change in color and on a millimeter scale, amount of tear secretion was measured. Measurements were performed for both eyes and averaged for statistical analysis.

3.3. Organ sampling

Anatomical dissection of the required organs (cornea, lymph nodes, and lacrimal glands) was performed *post mortem*. Dependent on the subsequent analysis organs were placed in PBS, DMEM-medium (gibco® by life technologies™) or formaldehyde (5% (v/v), Otto Fischar GmbH und Co. KG).

For morphometric analysis of corneal neovascularization corneal wholemounts were excised by carefully cutting the cornea beneath the limbal area. Thereby the limbus is not damaged and can be used for subsequent analysis as the outermost edge. Corneal wholemounts were stored in PBS until immunohistochemical staining (see 3.5.1).

Corneal draining cervical lymph nodes used for flow cytometry analysis were dissected, connective tissue and adhering fat was completely removed and after washing in PBS lymph nodes were stored in DMEM-medium at 4°C until preparation of the single cell suspension (see 3.7.1.1). Lymph nodes were either pooled per group or analyzed per animal.
As lacrimal glands were used for both, flow cytometry analysis (see 3.7.1.2) and paraffin sections staining (see 3.5.2), they were stored in medium at 4°C or in 5% (v/v) formaldehyde. Making a skin incision below the ear, the exorbital lacrimal gland which is located posterior to the eye, is exposed. By cutting the fascia laying around the lacrimal gland it could be dissected, washed in PBS and stored in the required solution.

3.4. Paraffin processing of organ samples

Organs preserved in formaldehyde (5% (v/v), Otto Fischar GmbH und Co. KG) were washed in tap water for 2 to 3 hours (h), replacing the water every 15 min. Afterwards organs were placed in 70% (v/v) alcohol for 60 min, followed by a renewal of the alcohol. For further dehydration and the final infiltration with liquid paraffin, samples were putted in the Leica TP1020 tissue processor (Leica Biosystems Nussloch GmbH) according to manufacturers' guidelines. Tissues were sectioned using the Microtome Microm HM400 (Histo Serve) and 5 to 7 µm sections were obtained. Sections were dried over night at 37°C and stored at room temperature (rT) until immunohistochemical staining (see 3.5.2).

3.5. Immunohistochemical methods

3.5.1. Corneal wholemount immunostaining

Corneal wholemounts were prepared as described previously [141]. Briefly, corneas were excised, rinsed in PBS and fixed in acetone for 30 min. After three washing steps with PBS corneas were blocked with 2% (w/v) BSA in PBS for 2 h at rT. Afterwards corneal wholemounts were stained with rabbit anti *mouse* LYVE-1 antibody (AngioBio) and FITC-conjugated rat anti *mouse* CD31 (BD Bioscience) diluted in PBS (1:200) over night at 4°C. Next day corneal tissue was washed in PBS and LYVE-1 was detected with a Cy3-conjugated secondary antibody (rabbit anti *mouse*; 1 : 500; Dianova).
After a final washing step in PBS corneal wholemounts were transferred to Superfrost Ultra Plus® microscope slides (Thermo Fisher) and covered with DAKO fluorescent mounting medium (DAKO Diagnostic). Stained wholemounts were stored at 4°C in the dark until analysis with a fluorescence microscope (see 3.8.2).

3.5.2. Paraffin section staining with hematoxylin and eosin

For paraffin section staining microsections were first deparaffinised in a descending series of alcohol (100%, 96%, 70% (v/v) alcohol; for 5 min each), starting with xylene (Carl Roth GmbH & Co KG). After washing for 5 min in aqua dest. Nuclei were stained by hematoxylin (Morphisto) for 10 min and washed in running tap water for 10 min. Afterwards connective tissue was counterstained with 1% (v/v) Eosin G (Carl Roth GmbH & Co KG) for 2 min with a following washing step in tap water. Finally, the slides were dehydrated in an ascending series of alcohol (70%, 96%, 100% (v/v); for 2 min each) ending with a 10 min washing step in xylene. Slides were covered with Neo-Mount® mounting medium (Merck Millipore) and stored at 4°C prior to analysis with a light microscope (see 3.8.1).

3.6. Enzymatic methods

3.6.1. Lacrimal gland homogenate

Lacrimal gland homogenate was prepared by means of the Precellys® 24 Homogeniser (Bertin Technologies) and the adapted Nuclear Extract Kit lysis buffer (Active Motif). Dissected and washed lacrimal glands (see 3.3) were weighted and put into an ice cold Precellys tube containing a mixture of 1.4 mm and 2.8 mm ceramic beads. After adding lysis buffer A (Tab. 7) tubes were shaken three times for 10 sec by 5500 rpm 3D speed motion. To avoid reaching of protein-denaturation heat level, tubes were always placed on ice between the shaking steps. After the last shaking step lysis buffer B (Tab. 8) was added and tubes incubated at rT for 2 h with in-between vortexing.
Total protein concentration of the homogenate was quantified by adjusted Pierce BCA Protein assay (Thermo Fisher Scientific) (see 3.6.2).

Tab. 7

Lysis buffer A	µl per 1 mg tissue
10x hypotonic buffer	0.4 µl
Protease Inhibitor Cocktail	0.04 µl
Phosphatase Inhibitor Cocktail	0.4 µl
dH_2O	3.125 µl

Tab. 8

Lysis buffer B	µl per 1 mg tissue
1M DTT	0.004 µl
Detergent	0.004 µl
Precellys Lysis buffer	0.0445 µl

3.6.2. Quantitation of total protein concentration

Quantitation of total protein was performed by the Pierce™ BCA Protein Assay. Manufacturers' protocol was adapted to our needs. For the colorimetric detection the spectrophotometer (Epoch Microplate reader, Bio-Tek) was set on 562 nm. 2 µl of each standard or unknown sample was mixed with 98 µl BCA working reagent (98 µl BCA Reagent A mixed with 2 µl BCA Working Reagent B) and pipetted into a microplate well. Standard was used in a range from 2 to 20 mg / ml. After incubating the plate for 30 min at 37°C, it was cooled down to rT and the absorbance measured.

3.7. Flow cytometry analysis

3.7.1. Single cells suspension

To maintain cell surface marker, preparations of single cell suspensions for flow cytometry analysis were performed immediately after dissecting the tissues. All preparations were performed on ice. During the complete cell separation FACS-medium (DMEM-medium containing 10% (v/v) FCS) was used. For counting and subsequent staining, cells were resuspended in FACS-buffer (HBSS containing 2% (v/v) FCS and 10 mM Hepes).

3.7.1.1. Lymph nodes

Corneal draining cervical lymph nodes, dissected from the animals, were pressed through a 40 µm cell strainer using the plunger of a 3 ml syringe in a 6-well plate containing 3 ml FACS-medium. After rinsing the cell strainers with 2 ml medium, cell suspensions were transferred to 15 ml falcon tubes and centrifuged at 4°C, 300 g for 7 min. Supernatants were removed and 1 ml ice-cold red blood cell lysis buffer (Sigma-Aldrich Chemie GmbH) added to lyse erythrocytes. Suspensions were mixed

for 1 min by gently resuspending on ice. Reaction was stopped by adding 10 ml FACS-medium and cells were spinned down again at 4°C, 300 g for 7 min. After decanting supernatants cells were resuspended in 1 ml FACS-buffer. Single cell suspensions were stored on ice until counting (see 3.7.2).

3.7.1.2. Lacrimal glands

Dissected lacrimal glands stored in medium were minced into 1-2 mm² pieces using a scalpel (disposable, No.11, FEATHER Safety Razor Co., Ltd.). Afterwards lacrimal gland pieces were transferred into small cups and 3 ml of 0.1% (w/v) collagenase 1 (Sigma Aldrich) added. Using a tiny stir bar lacrimal gland pieces were digested for 8 min at rT. Supernatants were transferred into 15 ml falcon tubes containing 5 ml FACS-medium and centrifuged at 4°C, 300 g for 7 min. After spinning down the supernatants were removed and again 5 ml FACS-medium added into the 15 ml falcon tubes. Meanwhile fresh amount of 0.1% (w/v) collagenase 1 (Sigma Aldrich) was added to the lacrimal gland pieces and incubated. After 8 min supernatants were collected again and transferred into the 15 ml falcon tubes containing FACS-medium and cells from the first run. This procedure was repeated a third time, ending with a total volume of 9 ml (0.1% (w/v) collagenase 1, Sigma Aldrich) used for each lacrimal gland.
After the final centrifugation step cells were resuspended in 2 ml FACS-medium and filtered through a 70 µm cell strainer. Cell strainers were rinsed with 2 ml FACS-medium, cell suspensions transferred to a fresh 15 ml falcon tubes, spinned down (4°C, 300 g, 7 min) and cells resuspended in 1 ml FACS-buffer. Single cell suspensions were stored on ice until counting (see 3.7.2).

3.7.2. Cell count

Resuspended cells were counted after staining with trypan blue using the counting chamber according to Neubauer (0.1 mm depth, 0.0025 mm², Karl Hecht GmbH&Co KG)

3.7.3. Immunofluorescence labeling of cells

Flow cytometry was used to detect inflammation typical biomarkers depending on the source of cells. All antibodies used are directly coupled with a fluorophore (see 2.3). As control unstained cells and the appropriate isotype controls were used.

As different setups of markers on different cells were used specific information on the biomarkers used for staining can be found in the results section whereas the basic protocol of the staining is described below.
To block unspecific binding 2 µl rat anti *mouse* CD16/CD32 (Mouse BD Fc Block™, BD Bioscience) was added in each tube before an appropriate number of cells (ca. 200000 cells) were added. After adding the required antibodies, test tubes were incubated for 30 min at 4°C in the dark. To wash cells 2 ml FACS-buffer were added and the cells spinned down at 4°C, 300 g for 7 min. The supernatant was decanted, cells resuspended in 200 µl FACS-buffer and 1 µl 7-AAD Viability staining solution (Biolegend) pipetted in the single stain control tubes and the combination tubes. Finally, cell suspensions were transferred in a 96-well plate for flow cytometry acquisition.

3.7.4. Flow cytometry settings

Cells were analyzed on a BD FACS Canto I™ (BD bioscience) or a Guava easyCyte™ HT flow cytometer (Merck Millipore) with the associated software. For further analysis, the FlowJo v10.0.7 software was used.

3.8. Morphometrically analysis by image acquisition

3.8.1. Morphometric analysis of paraffin sections by light microscopy

Image acquisition of paraffin sections stained with hematoxylin and eosin was performed with light microscope and digital pictures were taken with a 12-bit monochrome CCD camera (ColorViewIII, Olympus Soft Imaging Solutions GmbH). Pictures were taken at 20x magnification.

3.8.2. Morphometric analysis of corneal hem- and lymphangiogenesis by fluorescence microscopy

Image acquisition of double stained wholemounts was performed with a fluorescence microscope (BX51, Olympus Optical Co.) and digital pictures were taken with a 14-bit monochrome CCD camera (XM10, Olympus Soft Imaging Solutions GmbH).
For complete cornea acquisition the full automatic image software CellSense (Olympus Soft Imaging Solutions GmbH) was used whereby cornea was assembled by 24 to 34 pictures taken at 100x magnification. To detect the corneal area covered with blood and lymphatic vessels a semiautomatic image analysis as described previously was used [141].

Briefly, based on the image analysis program CellSense a macro was designed consisting of 5 steps: converting into a grey value picture, differential contrast enhancement, erosion filter, gradient filter and contrast adjustment. Afterwards vessel detection and quantification was performed by setting a threshold whereby bright vessels were included and the dark background excluded. The innermost blood or lymphatic vessel of the limbal arcade was outlined as the border for the region of interest (ROI) and the area covered by vessels was calculated in percentage.

3.9. Statistical analysis

Statistical analysis included Mann-Whitney-U-Test for unpaired, non-normal distributed data; Student t-Test for unpaired normally distributed data with equal variances, and Welch-Test for unpaired normally distributed data with non-equal variances. Furthermore, two-way ANOVA (Two-way analysis of variance) with Bonferroni's Multiple Comparison Post-test was performed. The Gaussian distribution was analyzed by Kolmogorov-Smirnov test.
Statistical analysis was conducted using Graph Pad Prism 6, v6.05 and Graph Pad Instat 3, v3.10.
Graphs were drawn using GraphPad Prism 6, v6.05. GraphPad's definition of p-values is shown below.

p value	*asterisks*
≥ 0.05	ns
0.01 to 0.05	*
0.001 to 0.01	**
0.0001 to 0.001	***
< 0.0001	****

4. Results

4.1. Development of a novel experimentally autoimmune Dry eye model similar to Sjögren's Syndrome dry eye

Purpose of these experiments was to induce a specific autoimmunological lesion of the lacrimal glands, leading to an insufficient tear production resulting in a secondary inflammation of the cornea similar to Sjögren's Syndrome dry eye.
The initial experimental protocol was provided by our cooperation partner Prof. Dr. Masli, Department of Ophthalmology, Boston University Medical Center, Boston, Massachusetts, USA. Thereby, dry eye should be induced by immunization of C57BL/6 mice with an emulsion consisting of syngeneic lacrimal gland homogenate mixed 1:1 (v/v) with complete Freund's adjuvant (CFA). Phenotypically changes of the corneal surface, including a decreased tear production and an increased corneal fluorescein staining was reported on day 14 (data not published).
Experiments carried out on the basis of this protocol did not lead to an induction of dry eye seen by the working group in Boston. Therefore, this protocol was modified multiple times in consultation with the cooperation partner. After the reproducibility still could not be reached, a completely new protocol was established. In addition, as autoimmune driven Sjögren's Syndrome dry eye is characterized by inflammatory infiltrates in the lacrimal glands [117] [118], preparing lacrimal gland single cell suspension for subsequent flow cytometry analysis was established (see 3.7.1.2). Since it is beyond the frame of this work to show all experiments, only the last attempts with the self-generated experimental setup (see 3.1.1) are shown.

Short-term analysis (until day 14) was performed three times (day 7 and day 10: n = 18 mice; day 19: n = 13 mice) while long-term analysis was performed one time (n = 5 mice all timepoints studied). As the administered CFA/IFA and PTX leads to an induction of the innate immune response, control mice receive CFA/IFA mixed with PBS as well as PTX to identify specific immunological reaction.
Common clinical features implying the quantification of corneal epitheliopathy by fluorescein staining scores and the quantification of the tear secretion by Schirmer test (see 3.2) were performed to determine the phenotype. Furthermore, corneal hem- and lymphangiogenesis was determined on different time points (see 3.8.2) to investigate a possible neovascularization as described in experimental DED [109] [110] [111] [76]. Flow cytometry analysis of corneal draining lymph nodes (see 3.7) regarding expression frequencies of CD4, CD8, CD11b/MHC2 and CD11c/MHC2 were performed to analyze the cellular immune response induced by immunization. In addition, as systemic autoimmune driven Sjögren's Syndrome dry eye is characterized by inflammatory infiltrates in the lacrimal glands, flow cytometry analysis of the lacrimal glands

(see 3.7) were performed regarding CD45, CD4 and CD8 expression frequencies. Further on, H&E staining of paraffin embedded lacrimal gland sections (3.8.1) were performed, and viewed regarding inflammatory infiltrates of monocytic cells.

4.1.1. Short-term analysis of experimental induced autoimmune DED

4.1.1.1. Quantification of clinical evaluation after induction of autoimmune DED

Corneal epitheliopathy and tear secretion was analyzed on day 0, 3, 7, 10 and 14. Quantification of both revealed no differences in immunized mice compared to control mice at all time points studied (see Fig. 10).

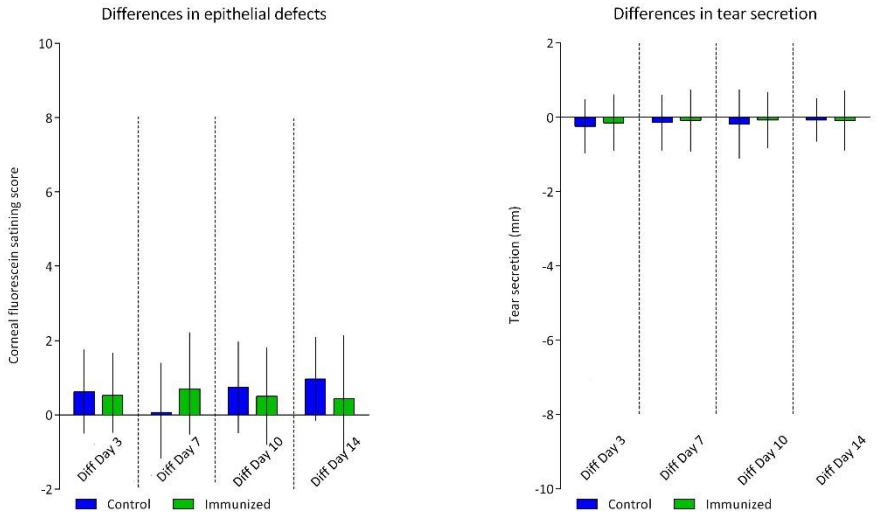

Fig. 10: Quantification of corneal epitheliopathy and tear secretion in control mice (blue bars) and immunized mice (green bars). Statistical analysis of corneal epitheliopathy (depicted on the left) as well as tear secretion (depicted on the right) revealed no significant differences in the immunized group at day 3 (n = 40 mice), day 7 (n = 40 mice), day 10 (n = 27 mice) and day 14 (n = 14 mice) when compared to the control group (day 3, n = 40 mice; day 7, n = 27 mice; day 10, n = 27 mice; day 14, n = 14 mice). Statistical evaluation was done by 2-way analysis of variance (ANOVA) with Bonferroni multiple comparison post test. Significance levels are indicated (p - values: ns = $p > 0.05$). Data are shown as differences of the means ± SD.

4.1.1.2. Morphometric analysis of corneal neovascularization

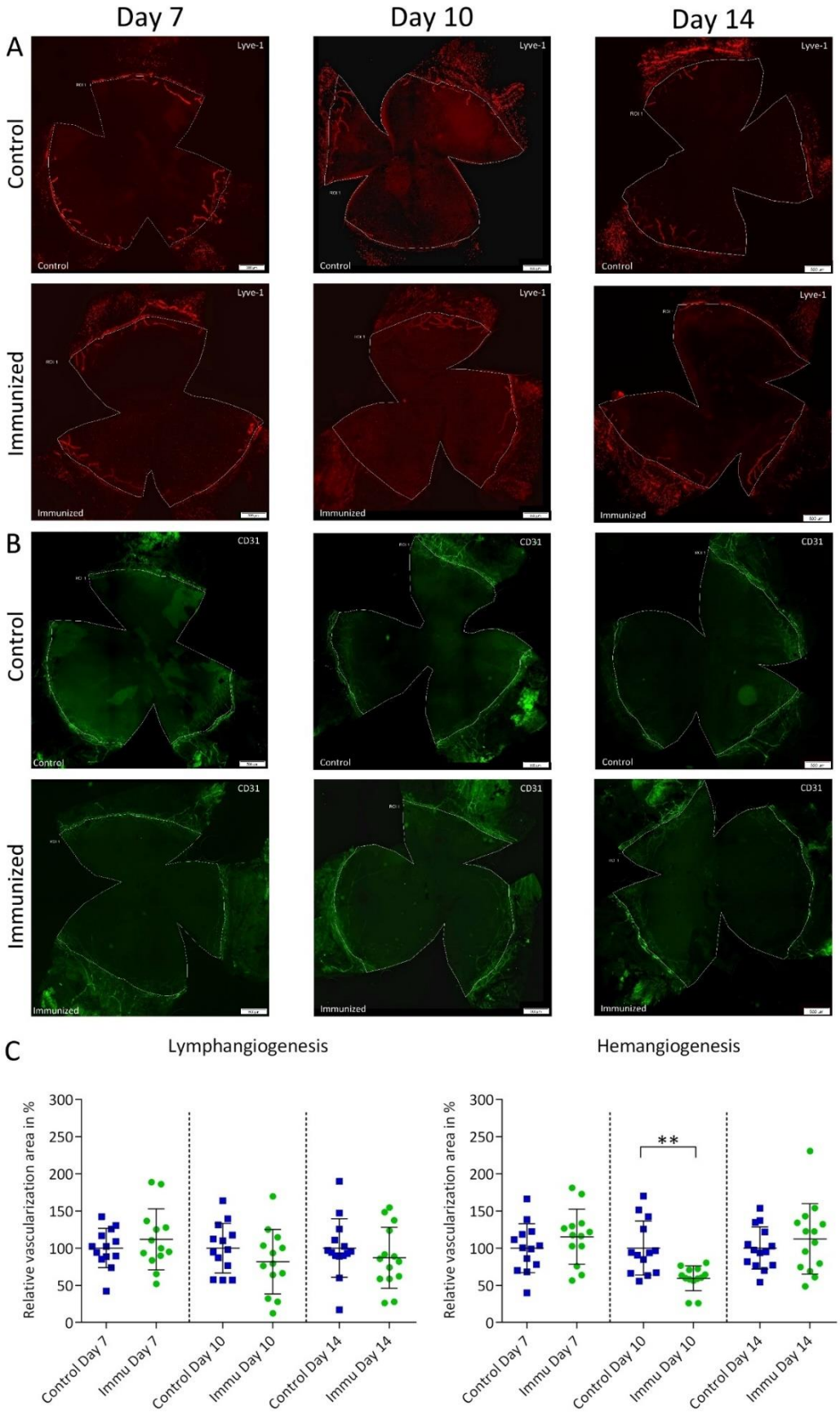

Fig. 11: Quantitative analysis of neovascularization after immunization on day 7, 10 and 14. Representative micrographs (original magnification x 100) of corneal whole mounts on days analyzed (depicted from left to the right) stained for lymphatic vessels with LYVE-1 (*A*) and blood vessels with CD31 (*B*) in control mice and immunized mice are shown (from top downwards). The region of interest for subsequent analysis of vessel area appears as white line. (*C*) Quantitative analysis of relative corneal neovascularization revealed no significant differences in lymphangiogenesis at all time points studied (day 7: 100% ± 26% (n = 13 eyes) for control mice vs. 112% ± 41% (n = 13 eyes) for immunized mice; day 10: 100% ± 33% (n = 13 eyes) for control mice vs. 82% ± 43% (n = 13 eyes) for immunized mice; day 14: 100% ± 39% (n = 14 eyes) for control mice vs. 87% ± 41% (n = 14 eyes) for immunized mice). Analysis of hemangiogenesis also revealed no significant differences in immunized mice compared to control mice on day 7 (100% ± 33% (n = 13 eyes) for control mice vs. 115% ± 37% (n = 13 eyes) for control mice) and day 14 (100% ± 28% (n = 14 eyes) for control mice vs. 112% ± 47% (n = 14 eyes) for immunized mice), expect of day 10 (100% ± 36% (n = 13 eyes) for control mice vs. 59% ± 17% (n = 13 eyes) for immunized mice). Statistical analysis of lymph- and hemangiogenesis was assessed using Mann-Whitney U-test for non-parametric analysis; or student's t-test for parametric analysis. Significance levels versus control mice are indicated (p-values: ** $p < 0.001$). Data are shown as mean ± SD.

The outgrowth area of both, corneal lymphatic and blood vessels was quantitatively analyzed on day 7, day 10 and day 14 (see Fig. 11). Representative wholemounts stained for lymphatic vessels (see Fig. 11 A) and blood vessels (see Fig. 11 B) showed no different extent for lymph- and hemangiogenesis. Quantification of the relative lymph vasculature (see Fig. 11 C) revealed no significant differences between the groups on day 7 (100% ± 26% (n = 13 eyes) for control mice vs. 112% ± 41% (n = 13 eyes) for immunized mice), on day 10 (100% ± 33% (n = 13 eyes) for control mice vs. 82% ± 43% (n = 13 eyes) for immunized) and on day 14 (100% ± 39% (n = 14 eyes) for control mice vs. 87% ± 41% (n = 14 eyes) for immunized mice).
Expect of day 10 (100% ± 36% (n= 13 eyes) for control mice vs. 59% ± 17% (n= 13 eyes) for immunized mice) analysis of the relative blood vessel area (see Fig. 11 C) revealed no significant differences between the groups (day 7:100% ± 33% (n = 13 eyes) for control mice vs. 115% ± 37% (n = 13 eyes) for immunized mice; day 14: 100% ± 28% (n = 14 eyes) for control mice vs. 112% ± 47% (n = 14 eyes) for immunized mice).

4.1.1.3. Quantification of the immune response by flow cytometry analysis of corneal draining lymph nodes

The frequencies of CD4, CD8, CD11b/MHC2 and CD11c/MHC2 positive cells in the corneal draining lymph nodes were analyzed by flow cytometry (see Fig. 12 A) on day 7, day 10 and day 14. Experiment was performed three times and analysis was performed for every single mouse per group (n = 13 mice) and relative percentages of positive stained cells are indicated (see Fig. 12 B).

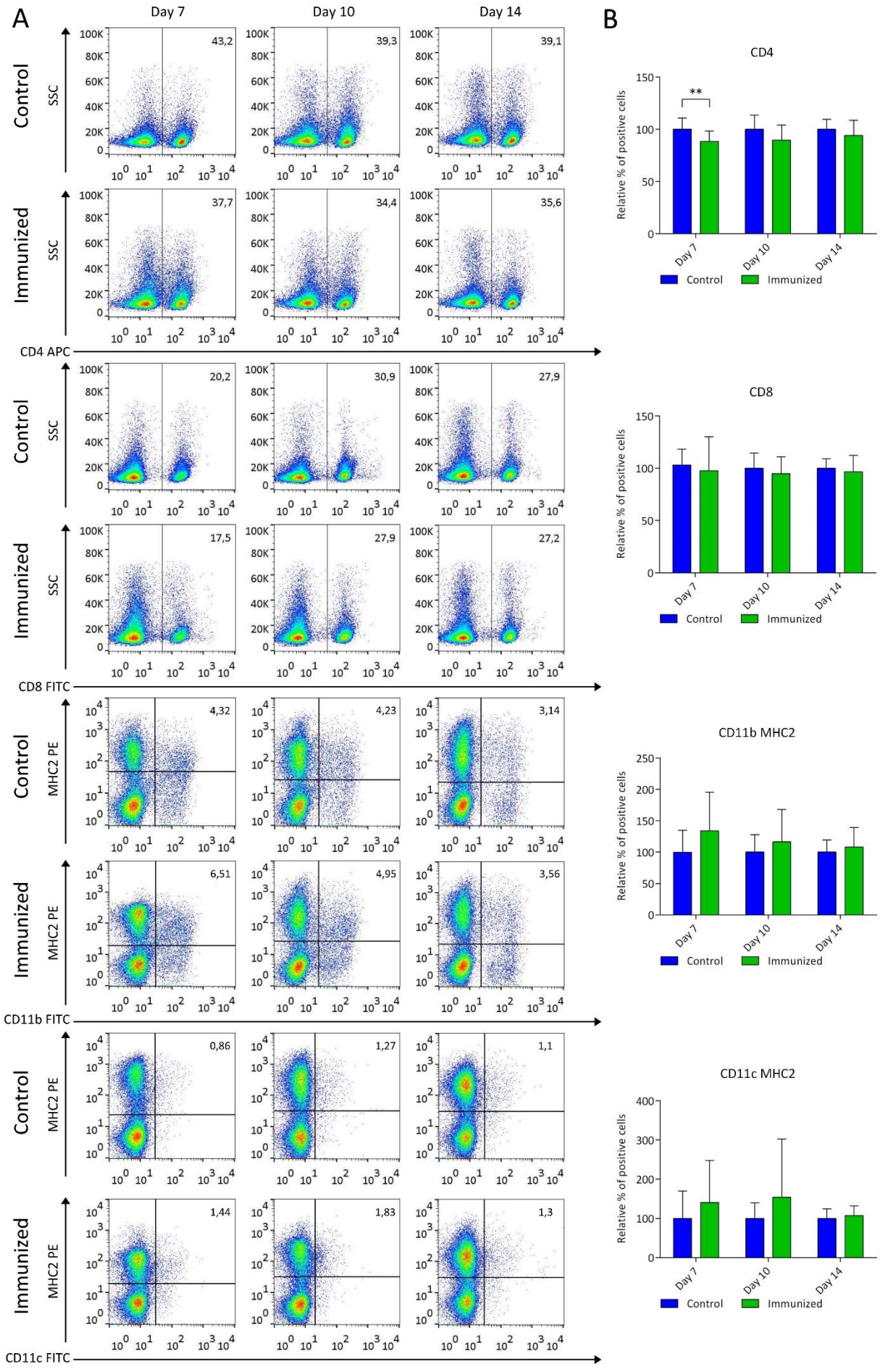
A
Day 7
Day 10
Day 14
Control
Immunized
SSC
CD4 APC
CD8 FITC
MHC2 PE
CD11b FITC
CD11c FITC
43,2
39,3
39,1
37,7
34,4
35,6
20,2
30,9
27,9
17,5
27,9
27,2
4,32
4,23
3,14
6,51
4,95
3,56
0,86
1,27
1,1
1,44
1,83
1,3
B
CD4
CD8
CD11b MHC2
CD11c MHC2
Relative % of positive cells
**
Day 7
Day 10
Day 14
Control
Immunized

Fig. 12: Flow cytometry analysis of corneal draining lymph nodes on day 7, day 10 and day 14. (*A*) Representative histograms of cell surface expression of CD4, CD8, CD11b/MHC2 and CD11c/MHC2 (from the top downwards) in control (blue bars, n = 13 mice) and immunized mice (green bars, n = 13 mice) are shown. The proportion of the cells stained positively is indicated as percent positive cells in the gated region. Quantification of the relative percentage of positive stained cells per group (n = 13 mice) for all days studied is presented on the right (*B*). Significantly decreased expression frequency of CD4 positive cells on day 7 and less detectable frequencies on the other time points studied in immunized mice when compared to control mice were detectable, while CD8 positive cells were not affected. Compared to control mice, analysis of CD11b/MHC2 and CD11c/MHC2 positive cells revealed amplified expression frequencies on day 7 and day 10 in immunized mice. Values represent mean ± SD. Significance levels versus control mice are indicated (p-values: ** = $p > 0.001$).

Quantitative analysis revealed a significantly decreased expression frequency of CD4 positive cells on day 7 and less detectable frequencies on the other time points studied in immunized mice when compared to control mice, while CD8 positive cells were not affected.
In addition, amplified expression frequencies of CD11b/MHC2 and CD11c/MHC2 positive cells in immunized mice compared to control mice on day 7 and day 10 were detectable.

4.1.1.4. Quantification of the immune response by flow cytometry analysis of lacrimal glands

The frequencies of CD45, CD4 and CD8 positive cells in the lacrimal glands were analyzed by flow cytometry (see Fig. 13 A) on day 7, day 10 and day 14. Experiment was performed three times and analysis was performed for every single mouse per group (n = 13 mice) and relative percentages of positive stained cells are indicated (see Fig. 13 B).
Regarding the expression frequency of CD45 positive cells a significant increase of these cells on day 7 and day 14 in immunized mice compared to control mice could be observed, while amplified expression frequency is detectable on day 10.
In addition, analysis of CD4 positive cells in immunized mice compared to control mice revealed increased amount of these cells in the lacrimal glands at all time points studied, while on day 10 a significant difference could be observed. CD8 expression frequency analysis in the lacrimal glands revealed no significant differences.

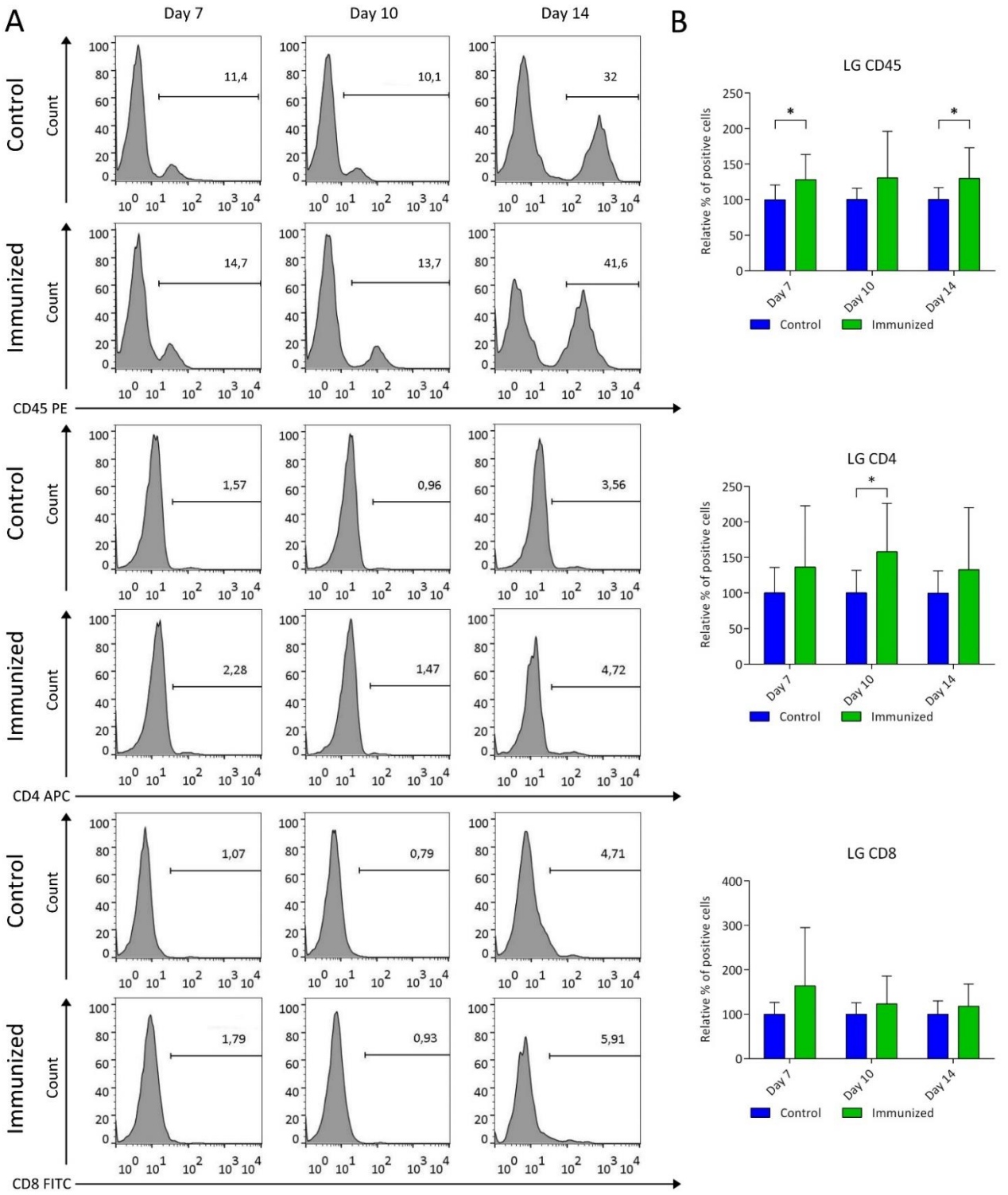

Fig. 13: Flow cytometry analysis of lacrimal glands on day 7, 10 and 14. (*A*) Representative histograms of cell surface expression of CD45, CD4 and CD8 (from the top downwards) in control mice (green bars) and immunized mice (blue bars) are shown. The proportion of the cells stained positively is indicated as percent positive cells in the gated region. Quantification of the relative percentage of positive stained cells per group (day 7, day 10: n = 13 mice per group, day 14: n = 14 mice per group) for all days studied is presented on the right (*B*). Analysis of CD45 expression frequency in immunized compared to control mice revealed a significant increase on day 7 and day 14, while an amplified expression frequency is detectable on day 10. Analysis of CD4 positive cells in immunized mice compared to control mice revealed

increased amount of these cells in the lacrimal glands at all time points studied, while on day 10 a significant difference could be observed. CD8 expression frequency analysis revealed an amplified amount of these cells on day 7, while no significant differences were detectable on the other days. Values represent mean ± SD. Significance levels versus control mice are indicated (p-values: * $p < 0.05$).

To sum up, short-term analysis of experimental induced autoimmune DED provide evidence for a successful induction of a "subclinical" model of DED. Even if clinical evaluation of epithelial defects and tear secretion as well as quantification of corneal neovascularization revealed no differences between control mice and immunized mice, flow cytometry analysis of corneal draining lymph nodes and lacrimal glands revealed an altered immune response in immunized mice, reflecting a specific, but not yet chronically immune response.

4.1.2. Long-term analysis of autoimmune induced dry eye

4.1.2.1. Quantification of clinical evaluation after experimentally induced autoimmune DED

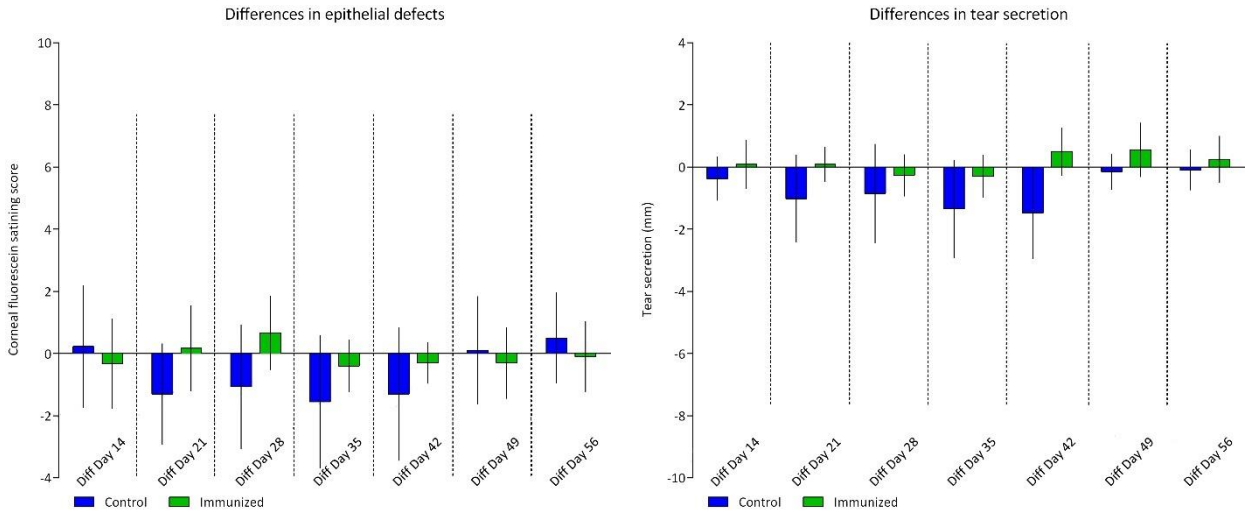

Fig. 14: Quantification of corneal epitheliopathy and tear secretion in control mice (blue bars) and immunized mice (green bars). Statistical analysis of corneal epitheliopathy (depicted on the left) as well as tear secretion (depicted on the right) revealed no significant differences in the immunized group at day 14 (*n* = 20), day 21 (n = 15 mice), day 28 (n = 15 mice), day 35 (n = 10 mice), day 42 (n = 10 mice), day 49 (n = 5 mice) and day 56 (n = 5 mice) when compared to the control group (day 14, n = 20 mice; day 21, n = 15 mice; day 28, n = 15 mice; day 35, n = 10 mice; day 42, n = 10 mice; day 49, n = 5 mice; day 56, n = 5 mice). Statistical evaluation was done by 2-way analysis of variance (ANOVA) with Bonferroni multiple comparison post test. Significance levels are indicated (p - values: ns = $p > 0.05$). Data are shown as differences of the means ± SD.

Corneal epitheliopathy as well as tear secretion was measured on day 0, 14, 21, 28, 35, 42, 49 and 56. Quantification of both revealed no significant differences in immunized mice compared to control mice at all days studied (see Fig. 14).

4.1.2.2. Morphometric analysis of corneal neovascularization

The outgrowth area of both, corneal lymphatic and blood vessels was quantitatively analyzed on day 14, 28, 42 and 56 (see Fig. 15). Representative wholemounts stained for lymphatic vessels (see Fig. 15 A) and blood vessels (see Fig. 15 B) showed no different extent for lymph- and hemangiogenesis. Quantification of the relative lymph vasculature (see Fig. 15 C) revealed non significant differences between the groups on all days studied (day 14: 100% ± 33% (n = 5 eyes) for control mice vs. 77% ± 42% (n = 5 eyes) for immunized mice; day 28: 100% ± 35% (n = 5 eyes) for control mice vs. 107% ± 33% (n = 5 eyes) for immunized; day 42: 100% ± 23% (n = 5 eyes) for control mice vs. 93% ± 40% (n = 5 eyes) for immunized mice; day 56: 100% ± 32% (n = 5 eyes) for control mice vs. 104% ± 17% (n = 5 eyes) for immunized mice).
Analysis of the relative blood vessel area (see Fig. 15 C) also revealed no significant differences between the groups at all days analyzed (day 14: 100% ± 28% (n = 5 eyes) for control mice vs. 80% ± 13% (n = 5 eyes) for immunized mice; day 28 :100% ± 41% (n = 5 eyes) for control mice vs. 89% ± 12% (n = 5 eyes) for immunized mice; day 42: 100% ± 26% (n = 5 eyes) for control mice vs. 103% ± 12% (n = 5 eyes) for immunized mice; day 56: 100% ± 8% (n = 5 eyes) for control mice vs. 93% ± 12% (n = 5 eyes) for immunized mice).

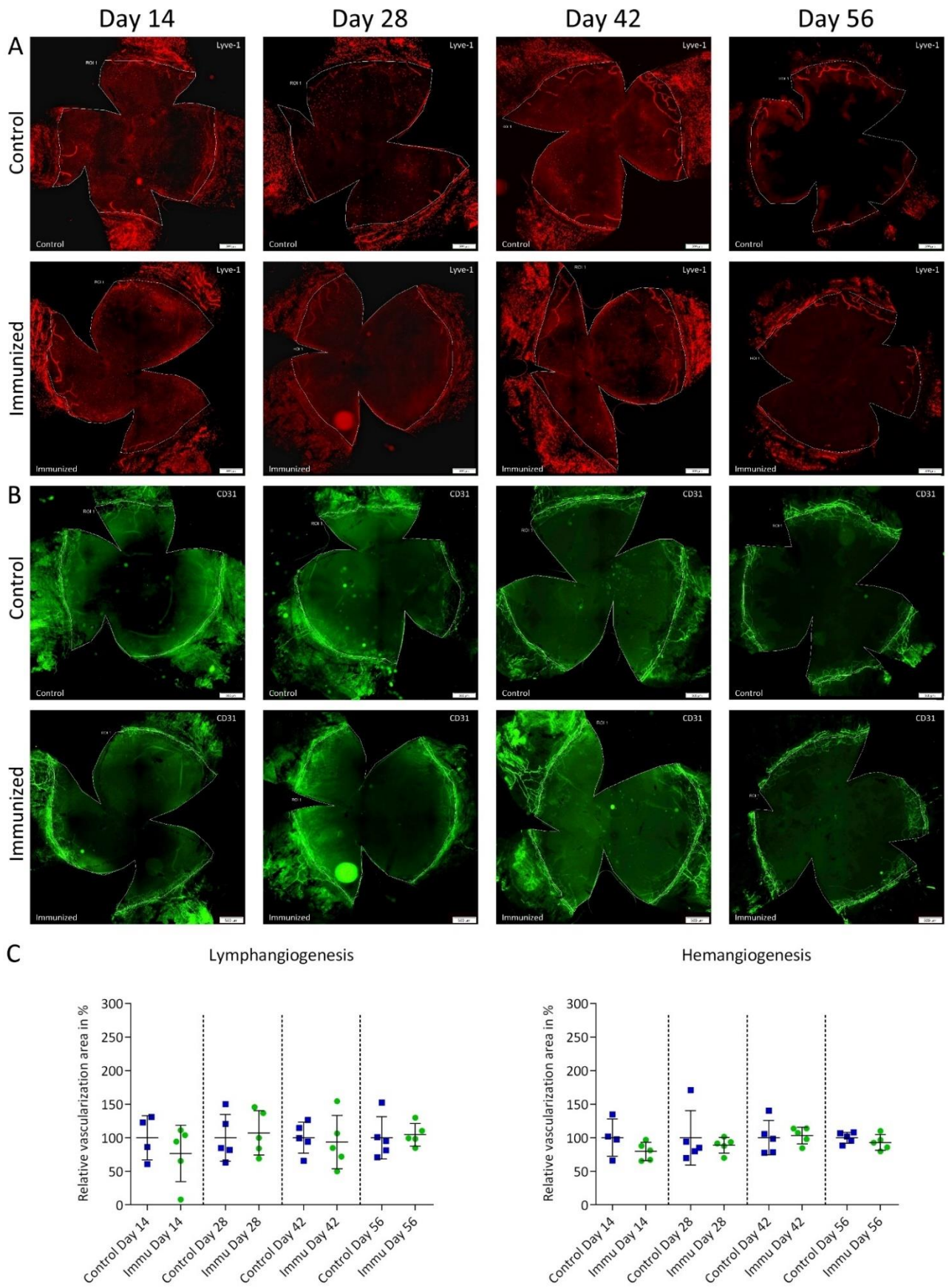

Fig. 15: Quantitative analysis of neovascularization after immunization on day 14, 28, 42 and 56. Representative micrographs (original magnification x 100) of corneal whole mounts (depicted from left to the right) stained for

lymphatic vessels with LYVE-1 (*A*) and blood vessels with CD31 (*B*) in control mice and immunized mice are shown. (*C*) Quantitative analysis of relative corneal neovascularization revealed no significant differences in lymphangiogenesis at all time points studied (day 14: 100% ± 33% (n = 5 eyes) for control mice vs. 77% ± 42% (n = 5 eyes) for immunized mice; day 28: 100% ± 35% (n = 5 eyes) for control mice vs. 107% ± 33% (n = 5 eyes) for immunized mice; day 42: 100% ± 23% (n = 5 eyes) for control mice vs. 93% ± 40% (n = 5 eyes) for immunized mice; day 56: 100% ± 32% (n = 5 eyes) for control mice vs. 104% ± 17% (n = 5 eyes) for immunized mice). Analysis of hemangiogenesis also revealed no significant differences in immunized mice compared to control mice on all analyzed days (day 14: 100% ± 28% (n = 5 eyes) for control mice vs. 80% ± 13% (n = 5 eyes) for immunized mice; day 28: 100% ± 41% (n = 5 eyes) for control mice vs. 89% ± 12% (n = 5 eyes) for immunized mice; day 42: 100% ± 26% (n = 5 eyes) for control mice vs. 103% ± 12% (n = 5 eyes) for immunized mice; day 56: 100% ± 8% (n = 5 eyes) for control mice vs. 93% ± 12% (n = 5 eyes) for immunized mice). Statistical analysis of lymph- and hemangiogenesis was assessed using Mann-Whitney U-test for non-parametric analysis; or student's t-test for parametric analysis. Significance levels versus control mice are indicated (p-values: ns = $p > 0.05$). Data are shown as mean ± SD.

4.1.2.3. Quantification of the immune response by flow cytometry analysis of corneal draining lymph nodes

The frequencies of CD4, CD8, CD11b/MHC2 and CD11c/MHC2 positive cells in the corneal draining lymph nodes on day 14, 28, 42 and 56 were analyzed by flow cytometry (see Fig. 16 A). Analysis was performed for every single mouse per group (n = 5 mice) and relative percentage of positive stained cells are indicated (see Fig. 16 B).

Quantitative analysis revealed significant differences for CD4 and CD8 positive cells on day 56 as well as CD11b/MHC2 positive cells on day 28. CD11c/MHC2 positive cells were amplified on day 28 but no significant level was reached.

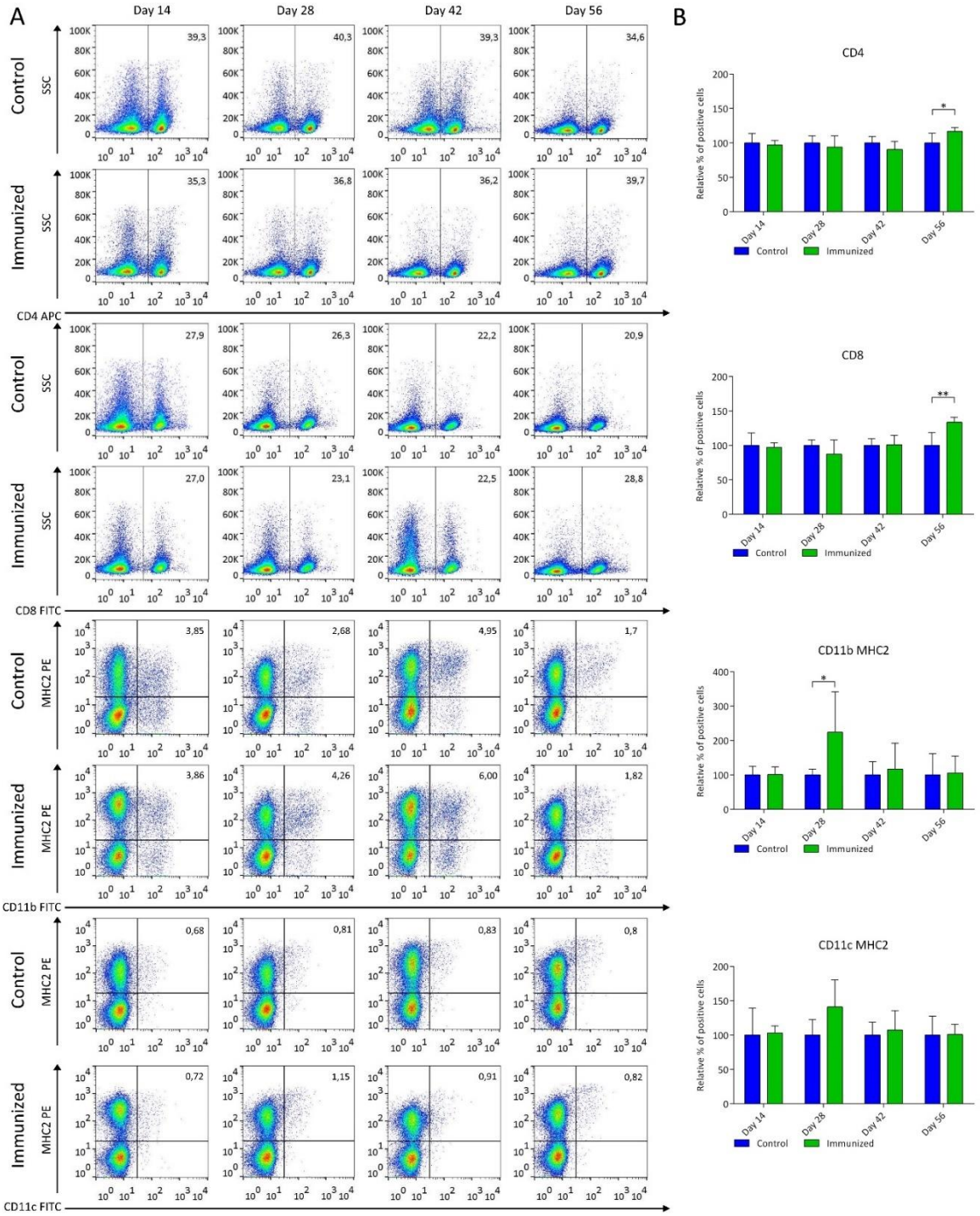

Fig. 16: Flow cytometry analysis of corneal draining lymph nodes on day 14, 28, 42 and 56. (*A*) Representative histograms of cell surface expression of CD4, CD8, CD11b/MHC2 and CD11c/MHC2 (from the top downwards) in control mice (green bars) and immunized mice (blue bars) are shown. The proportion of the cells stained positively is indicated as percent positive cells in the gated region. Quantification of the relative percentage of positive stained cells per group (n = 5 mice) for all days studied is presented on the right (*B*). CD4 and CD8 positive cells were significantly increased in immunized mice on day 56 and CD11b/MHC2 positive cells were significantly increased on day 28 while analysis on all other time points studied revealed no significant differences. Significance levels versus control mice are indicated (p-values: * $p < 0.05$, ** $p < 0.001$). Values represent mean ± SD.

4.1.2.4. Quantification of the immune response by flow cytometry analysis of lacrimal glands

The frequency of CD45, CD4 and CD8 positive cells in the lacrimal glands on day 14, day 28, day 42 and day 56 were analyzed by flow cytometry (see Fig. 17 A). Analysis was performed for every single mouse per group (n = 5 mice) and relative percentage of positive stained cells are indicated (see Fig. 17 B).

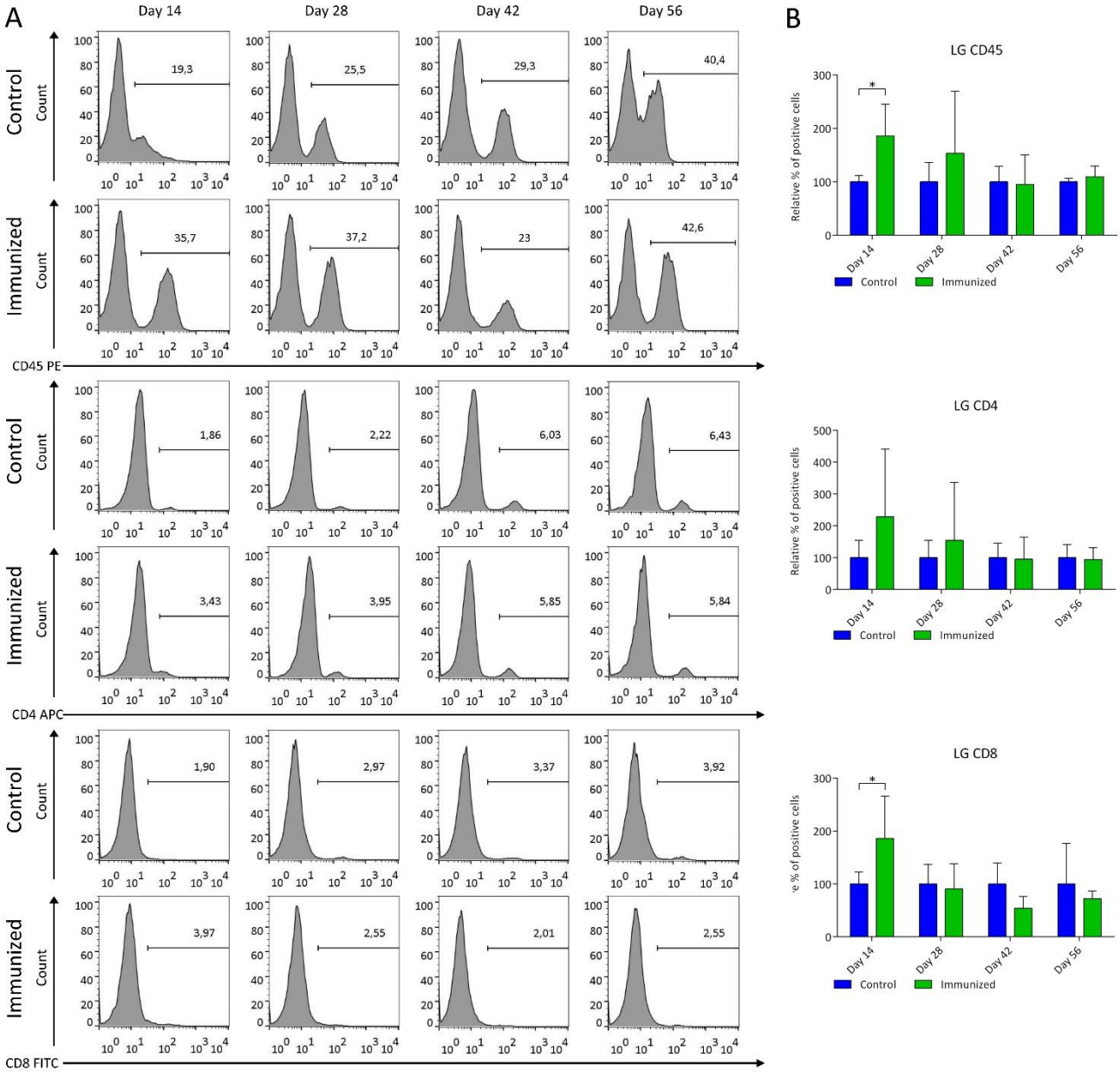

Fig. 17: Flow cytometry analysis of lacrimal glands on day 14, day 28, day 42 and day 56. (*A*) Representative histograms of cell surface expression of CD45, CD4 and CD8 (from the top downwards) in control mice (blue bars) and immunized mice (green bars) are shown. The proportion of the cells stained positively is indicated as percent positive cells in the gated region. Quantification of the relative percentage of positive stained cells per group (n = 5 mice) for all days studied is presented on the right (*B*). A significant increase in CD45 positive cells as well as CD8 positive cells on day 14

in immunized mice compared to control mice was detectable, while expression frequency of CD45 was also amplified on day 28. In addition, analysis of CD4 positive cells also revealed an amplified expression frequency on day 14 and day 28. Significance levels versus control mice are indicated (p-values: * $p < 0.05$). Values represent mean ± SD.

Quantification revealed a significant increase in CD45 positive as well as CD8 positive cells on day 14 in immunized mice compared to control mice, while expression frequency of CD45 was also amplified on day 28. In addition, analysis of CD4 positive cells also revealed an amplified expression frequency on day 14 and day 28.

4.1.2.5. Histological examination of lacrimal gland infiltrates

Histological examination of lacrimal gland infiltrates was performed on serial paraffin sections for day 56 (n = 5 mice per group). Lacrimal gland infiltrates were detectable in all immunized and in two control mice, each one small infiltrate, whereby infiltrates were more distinctive in immunized mice (see Fig. 18).

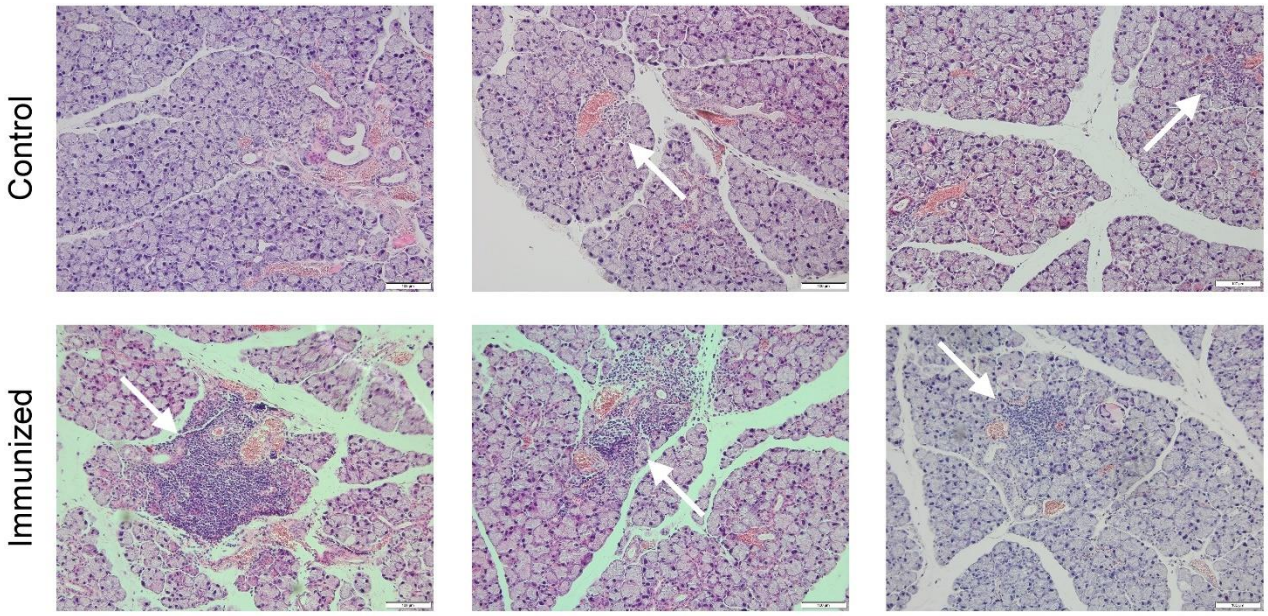

Fig. 18: Histological examination of lacrimal gland infiltrates by H&E staining in serial paraffin sections on day 56. (*A*) Representative lacrimal gland sections from control and immunized mice are depicted. Lacrimal gland infiltrates (white arrows) were detectable in all immunized mice and two control mice, whereby infiltrates were more distinctive in immunized mice.

To sum up, long-term analysis supports the successful induction of an “subclinical” model of DED. Clinical evaluation of epithelial defects and tear secretion as well as quantification of corneal neovascularization revealed no differences between control mice and immunized mice, while flow cytometry analysis of lacrimal glands revealed an altered immune response in immunized mice lasting over a longer periode. Furthermore, inflammatory infiltrates in lacrimal glands of immunized mice were detectable, representing autoimmune driven exocrinopathy occurring in Sjögren’s Syndrome dry eye.

4.2. Effect of topically applied Aflibercept in a desiccating stress model reflecting non-Sjögren's Syndrome dry eye

Purpose of these experiments was to determine the effect of topically administered Aflibercept in a desiccating stress model reflecting non-Sjögren's Syndrome dry eye. Mice exposed to desiccating stress receiving NaCl as eye drops serve as control group to determine the effect of the compound while naive mice serve as control group for the induction of dry eye as well as lymphangiogenesis. The experiment was performed three times, ending up with total number of 25 naive mice, 24 mice exposed to desiccating stress receiving NaCl eye drops and 25 mice exposed to desiccating stress receiving Aflibercept eye drops.

Clinical evaluation implying the quantification of corneal epitheliopathy by fluorescein staining scores and the quantification of the tear secretion by Schirmer test (see 3.2) were performed. These are common clinical features to determine the phenotype as well as the disease progression. Furthermore, corneal hem- and lymphangiogenesis was quantified *post mortem* (see 3.8.2) on day 14, as lymphangiogenesis is shown to peak at this timepoint [109] representing the assumed link to the adaptive immune response we want to disturb. In addition, flow cytometry analysis of corneal draining lymph nodes (see 3.7.1) were performed to analyze the inflammatory response (see Fig. 19). As mainly CD4 positive and CD8 positive T cells are involved in the underlying immune response [112] [113] [114] and while CD11b and CD11c positive cells are shown to activate T cells in the lymphoid compartment, we were interested in the surface expression frequencies of CD4, CD8, CD11b and CD11c.

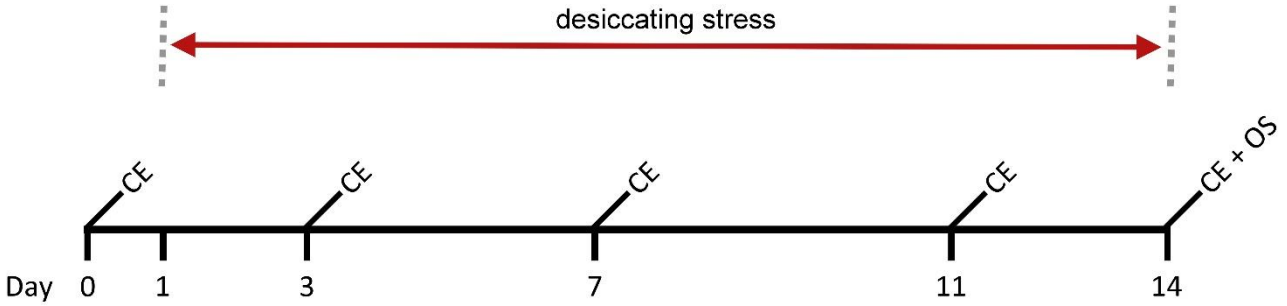

Fig. 19: Scheme of topical administration. Eye drops (3 µl) were administered three times a day (40 mg/ml Aflibercept). Clinical evaluation (epitheliopathy and tear secretion; CE) was performed on day 0, 3, 7, 11 and 14. On final day mice were euthanized and organs required for subsequent analysis collected (organ sampling; OS).

4.2.1. Quantification of clinical evaluation regarding the effect of topically applied Aflibercept

Quantification of clinical evaluation revealed an increased corneal epitheliopathy coupled to a decreased tear secretion in mice exposed to desiccating stress (see Fig. 20). While naive mice (n = 25 mice) showed no changes in corneal fluorescein staining scores, except of day 14, mice exposed to desiccating stress receiving NaCl (n = 24 mice) or Aflibercept (n = 25 mice) as eye drops showed significantly elevated corneal fluorescein staining scores. Concurrently tear secretion significantly decreased in both groups receiving NaCl or Aflibercept as eye drops, from day 3 through the end of the observation period. Thus, induction of dry eye was successful. Regarding the effect of Aflibercept as topically applied therapeutic no improvement of the clinical phenotype was detectable in comparison to the NaCl group.

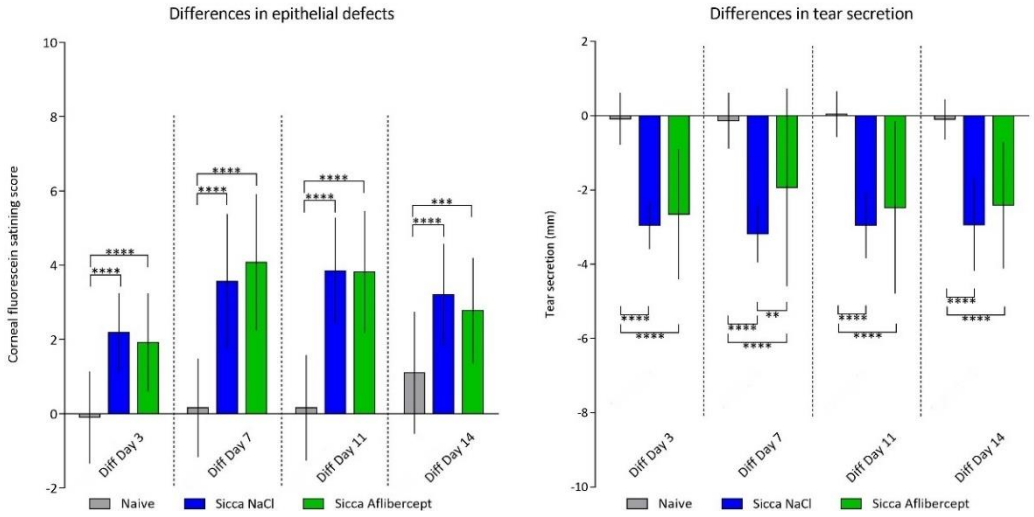

Fig. 20: Quantification of corneal epitheliopathy and tear secretion in naive mice (grey bars, n = 25 mice) and mice exposed to desiccating stress receiving topical application of NaCl (blue bars, n = 24 mice) or Aflibercept (green bars, n = 25 mice). Corneal epitheliopathy (depicted on the left) is significantly increased in both treatment groups over the entire duration. Concurrently tear secretion (depicted on the right) is significantly decreased from day 3 in both treatment groups over the entire duration. Thus receiving Aflibercept as eye drops does not improve clinical phenotype. Statistical evaluation was done by 2-way analysis of variance (ANOVA) with Bonferroni multiple comparison post test. Significance levels are indicated (p - values: ** $p < 0.01$, *** $p < 0.001$, **** $p < 0.0001$). Data are shown as differences of the means ± SD.

4.2.2. Morphometric analysis of neovascularization after topical application of Aflibercept

The outgrowth area of corneal lymph- and blood vessels was quantitatively analyzed *post mortem* on day 14 (see Fig. 21 C). Representative whole mounts stained for lymphatic vessels (see Fig. 21 A) and blood vessels (see Fig. 21 B) showed the outgrowth of vessels from the limbus to the center of the cornea to a different extent. Quantification of the relative lymph vessel area revealed non-

significant differences: 100% ± 24% (n = 24 eyes) for naive mice, followed by mice exposed to desiccating stress receiving NaCl eye drops with 113% ± 24% (n = 24 eyes) and mice exposed to desiccating stress receiving topical applied Aflibercept with 103% ± 25% (n = 25 eyes) (see Fig. 21 C). Analysis of the relative blood vessel area also revealed no significant differences: 100% ± 22% (n = 24 eyes) for naive mice; 99% ± 16% (n = 24 eyes) for mice exposed to desiccating stress receiving NaCl as eye drops and 87% ± 20% (n = 25 eyes) for mice exposed to desiccating stress receiving Aflibercept eye drops (see Fig. 21 C).

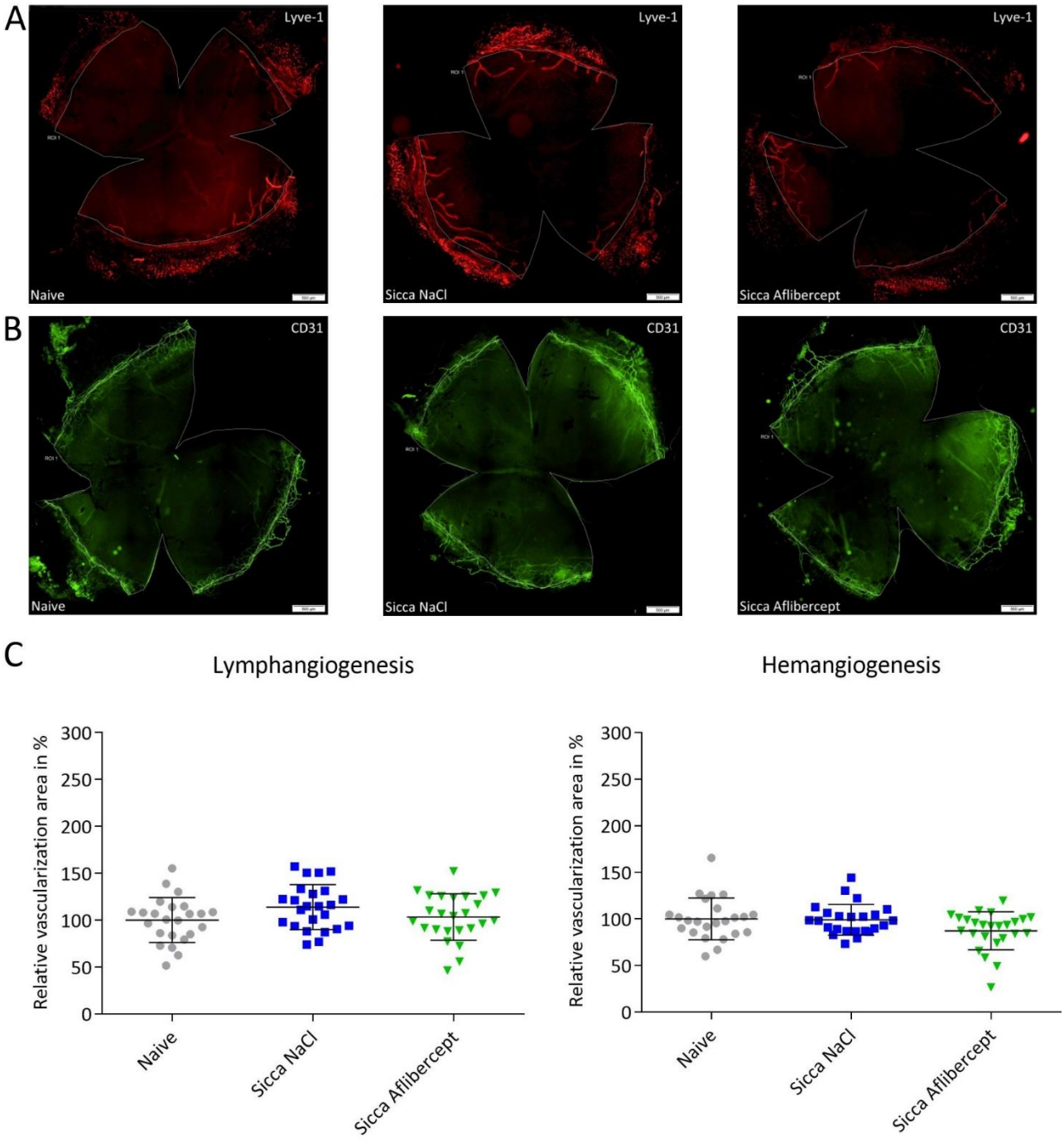

Fig. 21: Quantitative analysis of lymph- and hemangiogenesis after topical application of NaCl or Aflibercept *post mortem* on day 14. Representative micrographs (original magnification x 100) of corneal whole mounts stained for lymphatic vessels with LYVE-1 (*A*) and blood vessels with CD31 (*B*) in naive mice and mice exposed to desiccating stress treated with NaCl or Aflibercept are shown (depicted from left to the right). The region of interest for subsequent analysis of vessel area appears as white line. (*C*) multiple comparison revealed non-significant differences in relative lymphangiogenesis (100% ± 24% (n = 24 eyes) for naive mice; 113% ± 24% (n = 24 eyes) for mice exposed to desiccating stress receiving NaCl as eye drops and 103% ± 25% (n = 25 eyes) for mice exposed to desiccating stress receiving Aflibercept as eye drops), and relative hemangiogenesis (100% ± 22%, (n = 24 eyes) for naive mice; 99% ± 16%, (n = 24 eyes) for mice exposed to desiccating stress receiving NaCl as eye drops and 87 ± 20%, (n = 25 eyes) for mice receiving Aflibercept as eye drops. Statistical analysis was assessed with One-way ANOVA with Bonferroni multiple comparison post test. Data are shown as mean ± SD.

4.2.3. Quantification of the immune response by flow cytometry analysis of corneal draining lymph nodes after topical application of Aflibercept

Using flow cytometry, the frequencies of CD4, CD8, CD11b and CD11c positive cells in the corneal draining lymph nodes were analyzed (see Fig. 22 A). As the experiment was performed three times (n = 3), each time with pooled lymph nodes from each group, relative percentages of positive stained cells are indicated (see Fig. 22 B). Quantification of positive stained cells revealed no significant differences for all analyzed cell markers. Nevertheless, analysis of CD4 and CD8 positive cells revealed diminished expression frequencies while analysis of CD11b and CD11c positive cells revealed amplified expression frequencies in mice exposed to desiccating stress treated with Aflibercept in comparison to naive mice.

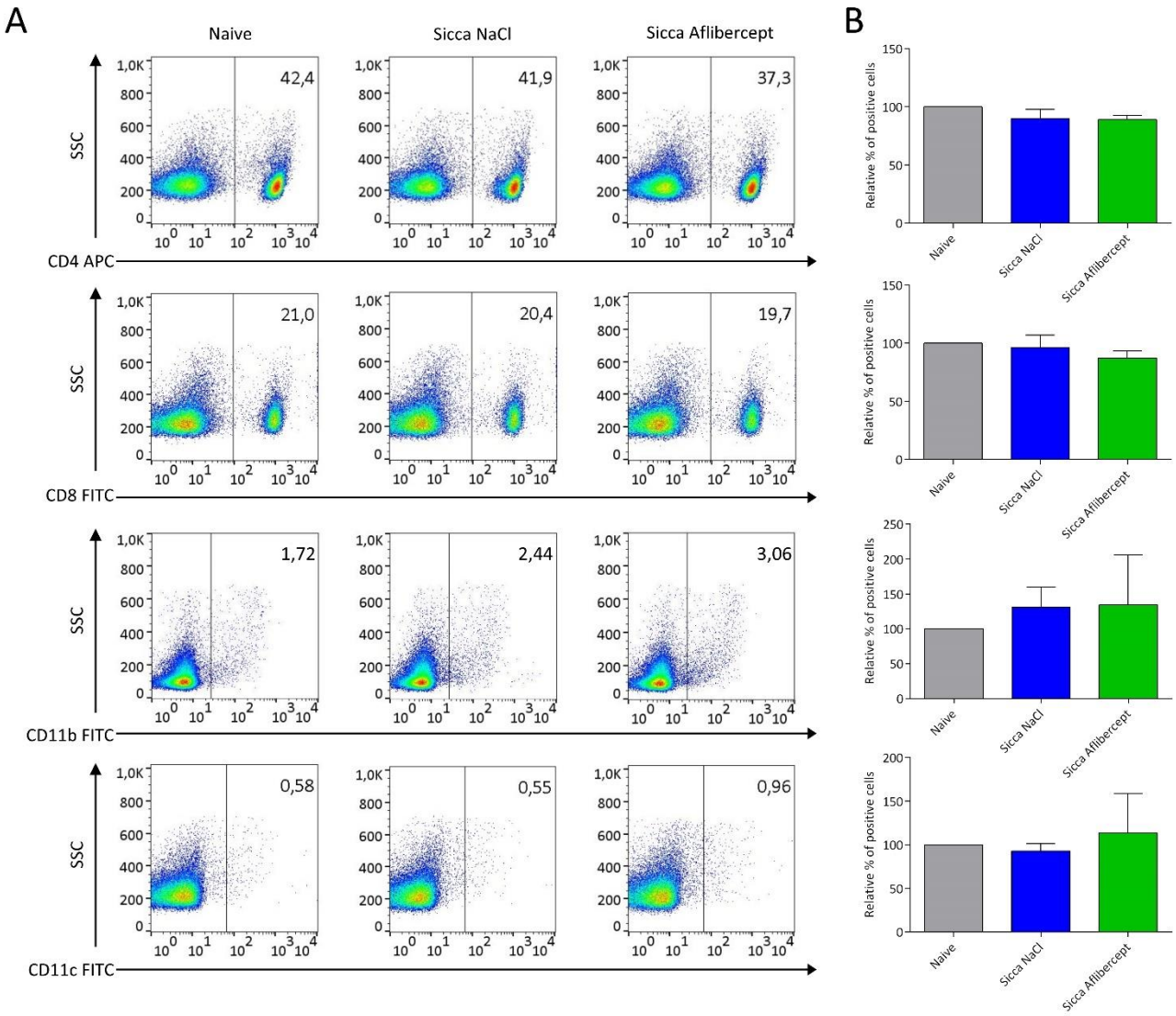

Fig. 22: Flow cytometry analysis of corneal draining lymph nodes. (*A*) Representative histograms of cell surface expression of CD4, CD8, CD11b and CD11c (from the top downwards) in naive mice (grey bars) and mice under desiccating stress treated with topical applied NaCl (blue bars) or Aflibercept (green bars) are shown (depicted from left to the right). The proportion of the cells stained positively is indicated as percent positive cells in the gated region. The experiment was performed three times and quantification of the relative percentage of positive stained cells is presented on the right (*B*). No significant differences were detectable for all surface markers analyzed in mice exposed to desiccating stress treated with Aflibercept in comparison to naive mice. Values represent mean ± SD.

To sum up, topically applied Aflibercept does not ameliorate clinical symptoms of dry eye disease. While corneal neovascularization was not affected, marginally effects on mainly involved immune cells were detectable. Thus, CD4 and CD8 positive T cells were diminished while CD11b and CD11c expression frequencies were amplified.

4.3. Effect of systemically applied Aflibercept in a desiccating stress model reflecting non-Sjögren's Syndrome dry eye

Purpose of these experiments was to determine the effect of systemically applied Aflibercept on non Sjögren's Syndrome dry eye. Unlike the local topical application hereby the whole immune system would be affected. As the induction of dry eye was shown to be successful within our experimental setup and we are interested if Aflibercept has a benefit on the disease outcome, mice exposed to desiccating stress receiving NaCl serve as control group.
Systemically application was performed by two different experimental setups: Aflibercept-injections were performed during desiccating stress representing a prevention trial (see Fig. 23) or after the induction of desiccating stress representing a therapy trial (see Fig. 24).
Both experimental setups were performed two times, ending up with a total number of 20 mice exposed to desiccating stress receiving NaCl injection and 14 mice exposed to desiccating stress receiving Aflibercept injections in the prevention trial and 20 mice per group in the therapy trial.

Again, common clinical features implying the quantification of corneal epitheliopathy by fluorescein staining scores and the quantification of the tear secretion by Schirmer test (see 3.2), were performed to determine the phenotype as well as the disease progression. Corneal hem- and lymphangiogenesis was determined *post mortem* to investigate the effect of Aflibercept on neovascularization (see 3.8.2). Furthermore, flow cytometry analysis of corneal draining lymph nodes (see 3.7.1) regarding expression frequencies of CD4, CD8, CD11b and CD11c were performed, to analyze the effect of Aflibercept on these mainly involved cell types.

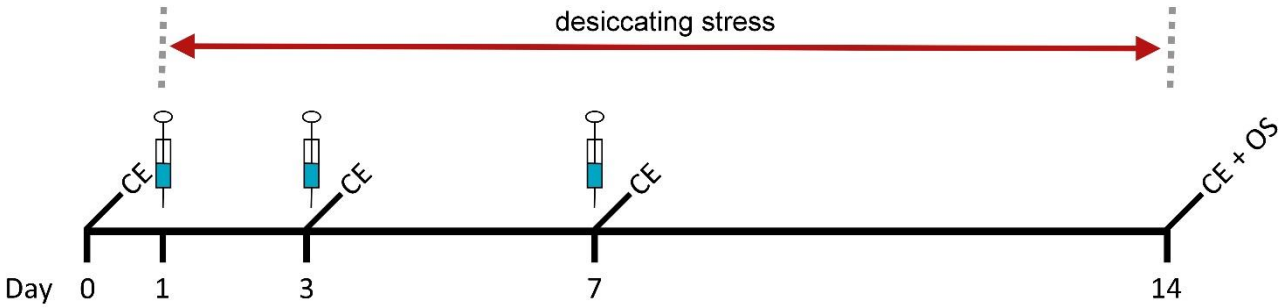

Fig. 23: Scheme of systemically administration regarding prevention. 50 µl Aflibercept (25 mg/kg bodyweight) were injected i.p on day 1, 3, and 7 during desiccating stress (indicated by syringes). Clinical evaluation (epitheliopathy and tear secretion; CE) was performed on day 0, 3, 7 and 14. On final day mice were euthanized and organs required for subsequent analysis collected (organ sampling; OS).

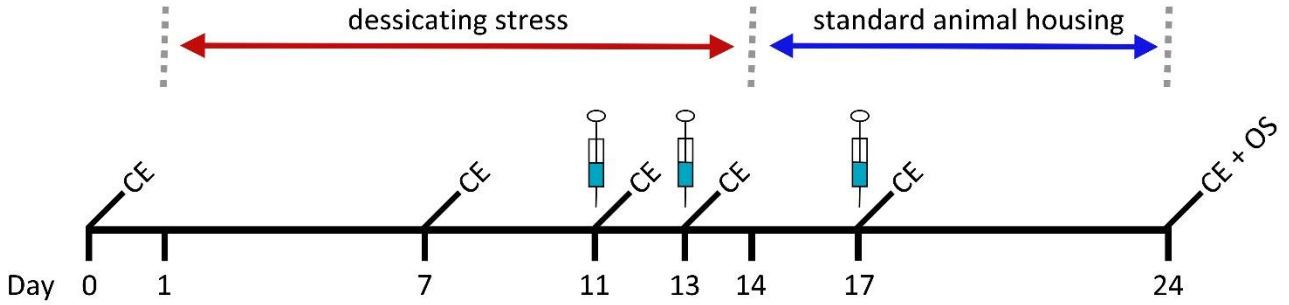

Fig. 24: Scheme of systemically administration regarding therapy. 50 µl Aflibercept (25 mg / kg bodyweight) were injected i.p on day 11 and 13 during desiccating stress and on day 17 under standard animal housing conditions (indicated by syringes). Clinical evaluation (epitheliopathy and tear secretion; CE) was performed on day 0, 7, 11, 13, 17 and 24. On final day mice were euthanized and organs required for subsequent analysis collected (organ sampling; OS).

4.3.1. Preventive effect of systemically applied Aflibercept on DED

4.3.1.1. Quantification of clinical evaluation

Quantification of clinical evaluation revealed an increased corneal fluorescein staining score as well as a decreased tear secretion in mice exposed to desiccating stress independent from their treatment with NaCl (n = 14 mice) or Aflibercept (n = 20 mice) over the entire duration (see Fig. 25). As clinical signs changed in both groups in the same amount no improvement of the phenotype by systemically applied Aflibercept was detectable.

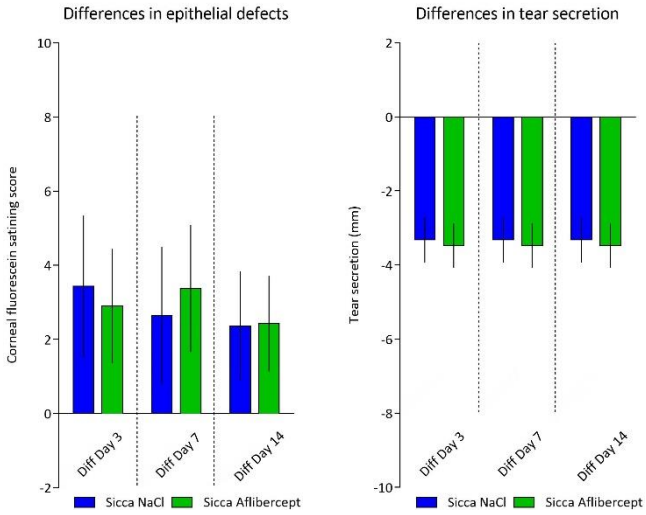

Fig. 25: Quantification of corneal epitheliopathy and tear secretion after systemically application of Aflibercept in the prevention trial. Analysis of corneal epitheliopathy (depicted on the left) revealed no significantly differences between

mice exposed to desiccating stress receiving NaCl injections (blue bars, n= 14 mice) and mice exposed to desiccating stress receiving Aflibercept injections (green bars, n= 20 mice). Meanwhile tear secretion (depicted on the right) is decreased in both groups in the same mass. Statistical analysis was assessed by 2-way ANOVA with Bonferroni multiple comparison post test (p - values: ns = $p > 0.05$). Data are shown as differences of the means ± SD.

4.3.1.2. Morphometric analysis of neovascularization

The outgrowth area of both, corneal lymphatic and blood vessels was quantitatively analyzed *post mortem* on day 14 (see Fig. 26 C). Representative wholemounts stained for lymphatic vessels (see Fig. 26 A) and blood vessels (see Fig. 26 B) showed mild ingrowths of both vessel types in mice exposed to desiccating stress receiving Aflibercept injections.

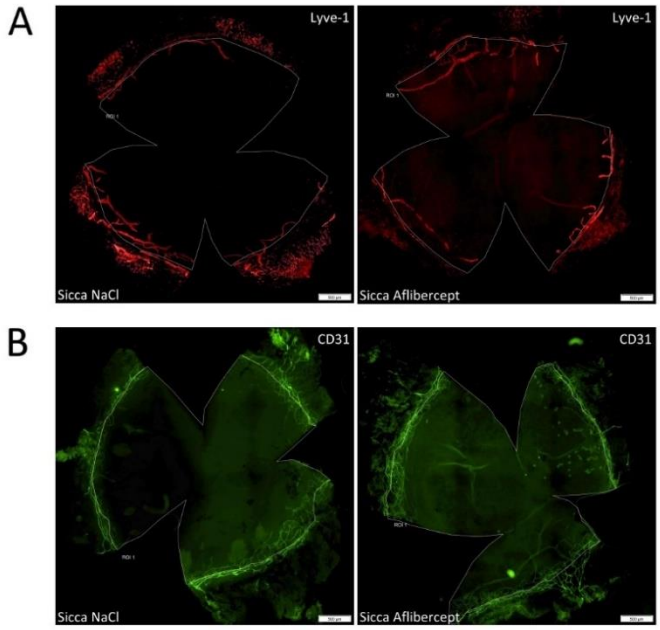

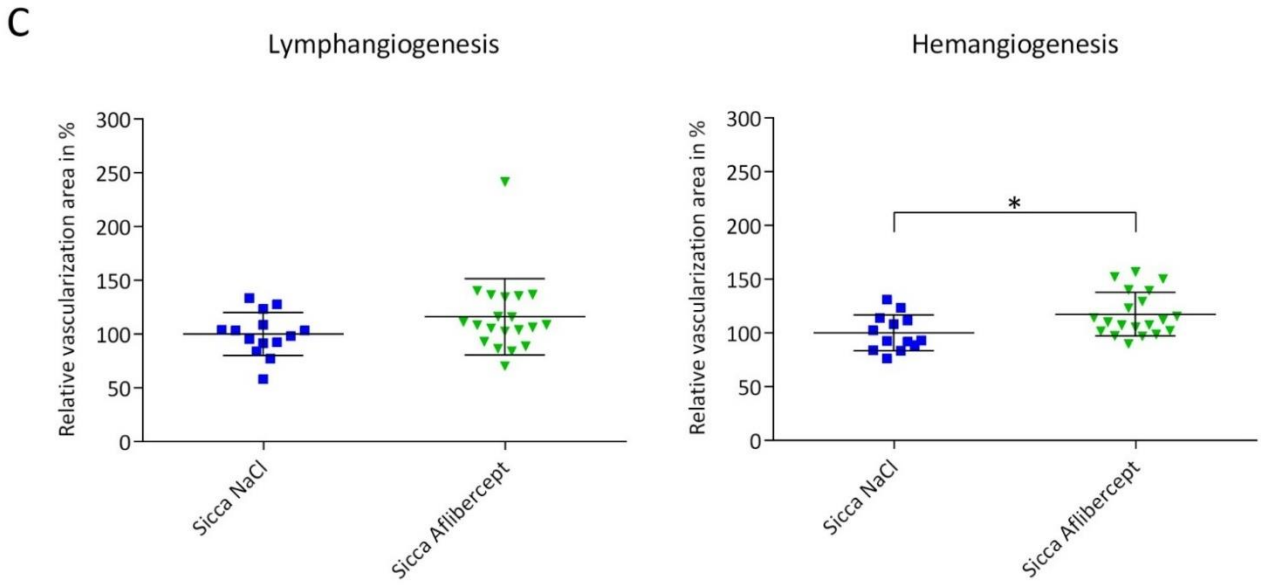

Fig. 26: Quantitative analysis of neovascularization after systemic application of NaCl and Aflibercept *post mortem* on day 14. Representative micrographs (original magnification x 100) of corneal whole mounts stained for lymphatic vessels with LYVE-1 (*A*) and blood vessels with CD31 (*B*) in mice exposed to desiccating stress receiving NaCl injections or Aflibercept injections (depicted from left to the right) are shown. The region of interest for subsequent analysis of vessel area appears as white line. *C*, Quantitative analysis revealed no significant differences in lymphangiogenesis (100% ± 20% (n= 14 eyes) for mice exposed to desiccating stress receiving NaCl injections vs. 116% ± 35% (n = 20 eyes) for mice exposed to desiccating stress receiving Aflibercept injections), while hemangiogenesis in Aflibercept treated mice was significantly increased compared to the control group (1.2-fold; *, $p < 0.05$). Statistical analysis of lymphangiogenesis was assessed using Mann-Whitney U-test for non-parametric analysis; statistical analysis of hemangiogenesis was assessed using student's t-test. Significance levels versus control mice are indicated (p-values: * $p < 0.05$). Data are shown as mean ± SD.

Quantification of the relative lymph vasculature revealed non-significant differences between the groups (100% ± 20% (n = 14 eyes) for mice exposed to desiccating stress receiving NaCl injections vs. 116% ± 35% (n = 20 eyes) for mice exposed to desiccating stress receiving Aflibercept injections), while analysis of the relative blood vessel area resulted in a significant increase (1.2 fold increase) of blood vessels in mice exposed to desiccating stress receiving Aflibercept injections (100% ± 17% (n = 13 eyes) vs. 117% ± 20% (n = 20 eyes)) (see Fig. 26 C).

4.3.1.3. Quantification of the immune response by flow cytometry analysis of corneal draining lymph nodes

The frequencies of CD4, CD8, CD11b and CD11c positive cells in the corneal draining lymph nodes were analyzed by flow cytometry (see Fig. 27 A). As the experiment was performed two times (n = 2), each time with pooled lymph nodes from each group, relative percentages of positive stained cells are indicated (see Fig. 27 B).
Quantitative analysis revealed diminished expression frequencies of CD4 and CD8 positive cells while CD11b and CD11c positive cells revealed also a diminished amount of these cells, in contrast to the topical application experiment.

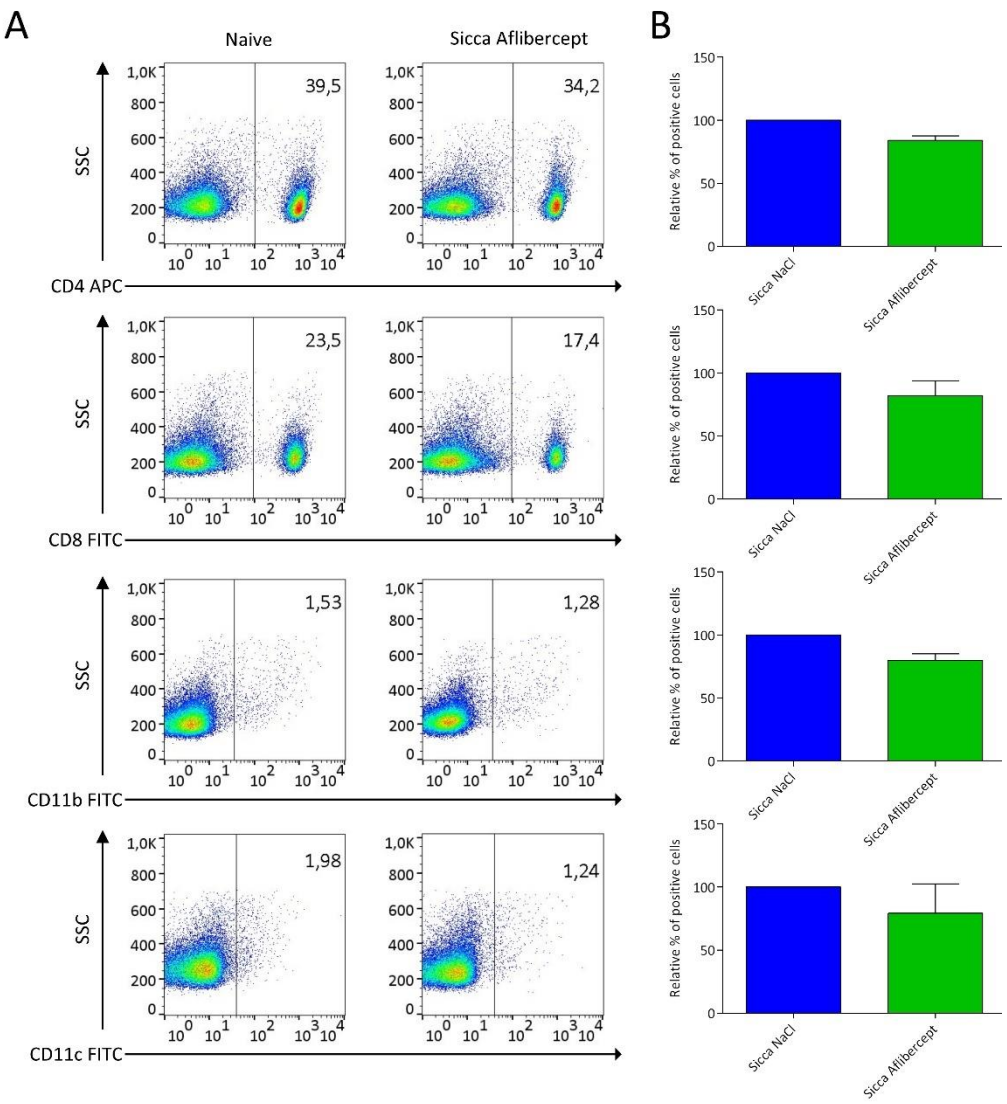

Fig. 27: Flow cytometry analysis of corneal draining lymph nodes on day 14 after systemic applied NaCl or Aflibercept in the prevention trial. (*A*) Representative histograms of cell surface expression of CD4, CD8, CD11b and CD11c (from the top downwards) in mice under desiccating stress receiving NaCl or Aflibercept injections during induction of DED are shown. The proportion of the cells stained positively is indicated as percent positive cells in the gated region. The experiment was performed two times and quantification of the relative percentage of positive stained cells is presented on the right (*B*). Quantitative analysis revealed diminished expression frequencies of CD4 and CD8 positive cells while CD11b and CD11c positive cells revealed also a diminished amount of these cells in mice exposed to desiccating stress treated with Aflibercept (green bars) in comparison to mice under desiccating stress receiving NaCl injections (blue bars). Values represent mean ± SD.

4.3.2. Therapeutic effect of systemically applied Aflibercept on DED

4.3.2.1. Quantification of clinical evaluation

Quantification of clinical evaluation revealed no significant differences in corneal epitheliopathy and tear secretion for the entire duration of the experiment (see Fig. 28). Corneal fluorescein staining increased during desiccating stress (till day 14) and decreased to baseline under standard animal housing conditions (day 15 till day 24) in both groups (n = 20 mice) in the same amount. Quantitative analysis of the tear secretion shows a similar pattern: while desiccating stress (till day 14) tear secretion goes down and returned to normal level under standard animal housing conditions (day 15 till day 24).

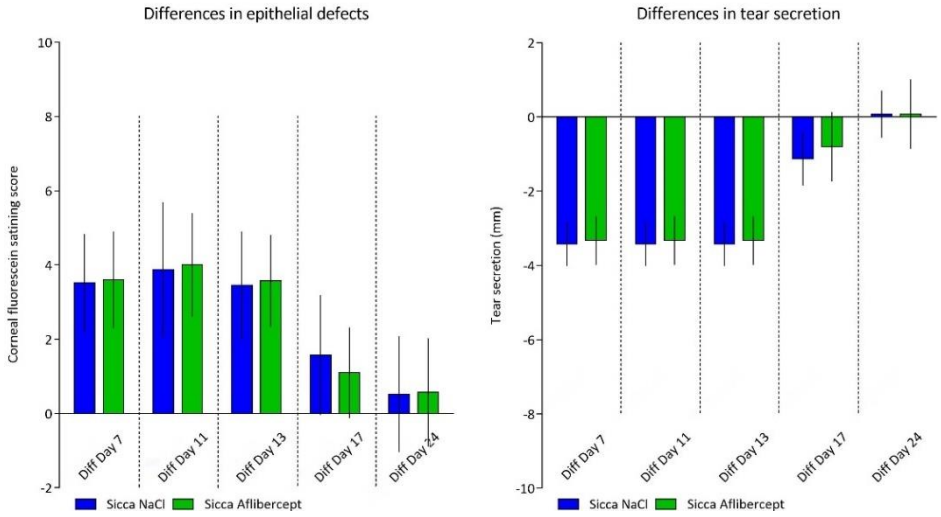

Fig. 28: Quantification of corneal epitheliopathy and tear secretion after systemically application of Aflibercept in the therapy trial. Analysis of corneal epitheliopathy (depicted on the left) and tear secretion (depicted on the right) revealed no differences between mice receiving NaCl injections (blue bars, n = 20 mice) and mice receiving Aflibercept injections (green bars, n = 20 mice). Both groups show the same clinical disease outcome with a recovery to baseline after desiccating stress. Statistical analysis was assessed by 2-way ANOVA with Bonferroni multiple comparison post test (p - values: ns = $p > 0.05$). Data are shown as differences of the means ± SD.

4.3.2.2. Morphometric analysis of neovascularization

The outgrowth area of lymphatic and blood vessels was quantitatively analyzed *post mortem* on day 24 (see Fig. 29 C). Representative wholemounts stained for lymphatic vessels (see Fig. 29 A) and blood vessels (see Fig. 29 B) showed no different extent for lymph- and hemangiogenesis. Quantification of the relative lymph vasculature revealed no significant differences between the groups (100% ± 33% (n = 20 eyes) for mice exposed to desiccating stress receiving NaCl injections vs. 105% ± 33% (n = 20 eyes) for mice exposed to desiccating stress receiving Aflibercept

injections), while analysis of the relative blood vessel area resulted in a significant decrease in mice exposed to desiccating stress receiving Aflibercept injections (94% ± 11% (n = 20 eyes) vs. 100% ± 19% (n = 20 eyes)) (see Fig. 29 C, D).

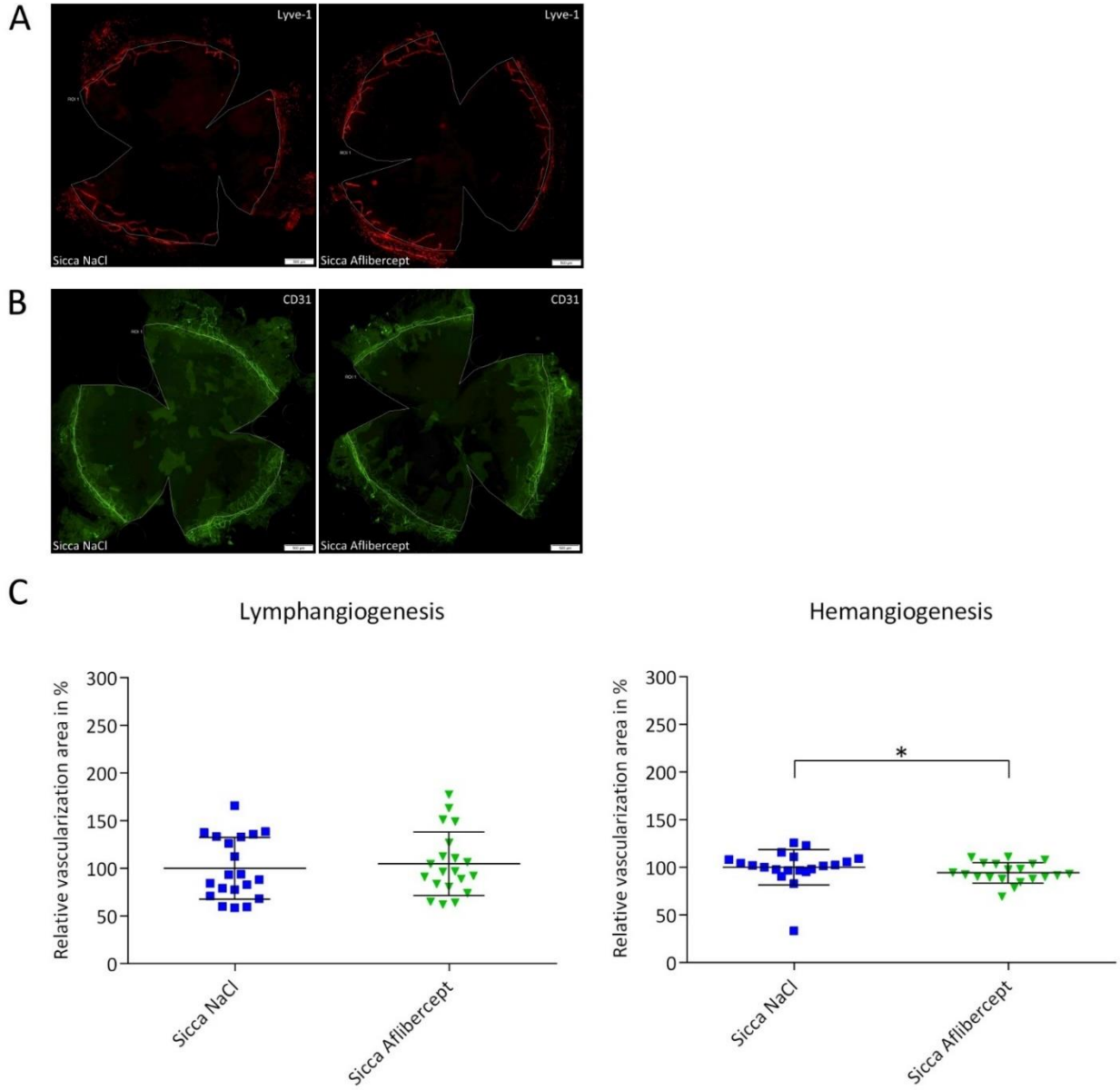

Fig. 29: Quantitative analysis of lymph- and hemangiogenesis after systemic application of NaCl or Aflibercept *post mortem* on day 24. Representative micrographs (original magnification x 100) of corneal whole mounts stained for lymphatic vessels with LYVE-1 (*A*) and blood vessels with CD31 (*B*) in naive mice and mice exposed to desiccating stress treated with Aflibercept injections (depicted from left to the right) are shown. The region of interest for subsequent analysis of vessel area appears as white line. (*C*) Quantitative analysis of the relative lymphangiogenesis revealed no significant differences between the groups (100% ± 33% (n = 20 eyes) for mice exposed to desiccating stress receiving NaCl injections vs. 104% ± 33% (n = 20 eyes) for mice exposed to desiccating stress receiving Aflibercept injections), while relative hemangiogenesis in Aflibercept treated mice was significantly decreased compared to the control group (1.3-fold; *, $p < 0.05$). Statistical analysis of relative lymphangiogenesis was assessed using student's t-test; statistical analysis of relative hemangiogenesis was assessed using Mann-Whitney U-test for non-parametric analysis. Significance levels versus control mice are indicated (p-values: * $p < 0.05$). Data are shown as mean ± SD.

4.3.2.3. Quantification of the immune response by flow cytometry analysis of corneal draining lymph nodes

The frequencies of CD4, CD8, CD11b and CD11c positive cells in the corneal draining lymph nodes were analyzed by flow cytometry (see Fig. 30 A). As the experiment was performed two times (n = 2), each time with pooled lymph nodes from each group, relative percentages of positive stained cells are indicated (see Fig. 30 B).

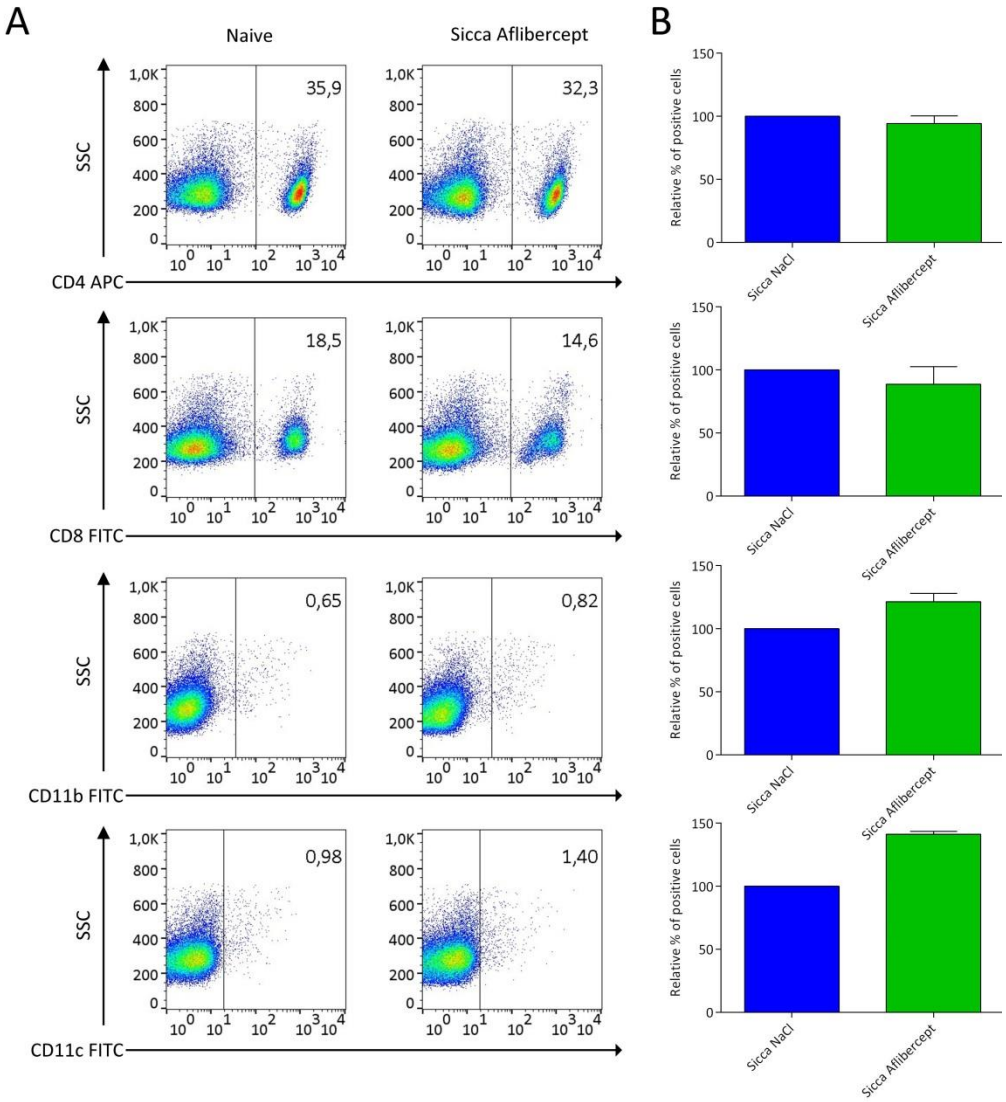

Fig. 30: Flow cytometry analysis of corneal draining lymph nodes on day 24 after systemic applied NaCl or Aflibercept in the therapy trial. (*A*) Representative histograms of cell surface expression of CD4, CD8, CD11b and CD11c (from the top downwards) in mice receiving NaCl or Aflibercept injections at the end of the desiccating stress induction are shown. The proportion of the cells stained positively is indicated as percent positive cells in the gated region. The experiment was performed two times and quantification of the relative percentage of positive stained cells is presented on the right (*B*). Analysis revealed diminished frequencies of CD4 and CD8 positive T cells, while expression frequencies of CD11b and CD11c positive cells are amplified in mice exposed to desiccating stress receiving Afliberceot injections (blue bars) compared to mice receiving NaCl injections (green bars). Values represent mean ± SD.

Quantitative analysis revealed no significant results for all analyzed cells markers in mice exposed to desiccating stress treated with Aflibercept in comparison to control mice. Just as in the topical experiments, analysis revealed a diminished frequency of CD4 and CD8 positive T cells while expression frequencies of CD11b and CD11c positive cells are amplified in mice exposed to desiccating stress compared to control mice.

To sum up, systemically applied Aflibercept has an effect on the immune repsonse depending on the day of application. Thus, injection of Aflibercept starting with desiccating stress has no effects on clinical signs as well as on corneal neovascularization, but expression frequencies of CD4, CD8, CD11b and CD11c positive cells in corneal draining lymph nodes were diminished. Starting injections of Aflibercept after the induction of DED leads to effects similar to those seen by topically application. Clinical evaluation as well as analysis of corneal neovascularization revealed no differences between control mice and mice treated with Aflibercept, while flow cytometry analysis of corneal draining lymph nodes revealed diminished expression frequencies of CD4 and CD8 positive T cells as well as amplified frequencies of CD11b and CD11c positive cells.

5. Discussion

5.1. Novel experimental autoimmune Dry eye model similar to Sjögren's Syndrome dry eye representing a sub-clinical model

Dry eye is not only induced by environmental stress, like in the desiccating stress model reflecting the non-Sjögren's Syndrome dry eye, but also manifest itself as an inflammatory autoimmune disorder. In this case it is described as an autoimmune epithelitis, wherein the exocrine glands (salivary and lacrimal glands) are infiltrated by lymphocytic and plasma cells [110] [111] [118], leading to a glandular destruction of the tissue. Thereby, the underlying exocrinopathy can be encountered alone, like in the primary Sjögren's Syndrome dry eye or in association with other autoimmune disorders, like rheumatoid arthritis (secondary Sjögren's Syndrome dry eye) [9].

Thus, the establishment of an experimental autoimmune mouse model is an essential need to further delineate the role of autoimmunity in dry eye disease. In such a model, the exocrinopathy would be induced due to an autoimmunological lesion of the lacrimal glands, leading to an insufficient tear production. The following secondary inflammation of the cornea should be similar to Sjögren's Syndrome dry eye.

As already mentioned before, first experiments were performed using a protocol provided by our cooperation partner Prof. Dr. Masli, Department of Ophthalmology, Boston University Medical Center, Boston, Massachusetts, USA. In this experimental setup mice were immunized with a syngeneic emulsion of lacrimal gland homogenate and CFA (mixed 1:1 (v/v), lacrimal gland homogenate: 240 µg / µl protein concentration). As the provided protocol was not reproducible, a new self-generated protocol had to be established and short-term analysis after 14 days as well as long-term analysis after 56 days was performed (see 3.1.1).

Short-term analysis was carried out in accordance to the reported induction of dry eye, including increased epitheliopathy and decreased tear secretion, seen by the working group in Boston and long-term analysis was performed as chronic autoimmune disorders manifest itself over a long time more pronounced.

The common phenotypically features like epitheliopathy as well as decreased tear secretion were not seen in any of my experiments (see Fig. 10, Fig. 14). Short-term as well as long-term analysis revealed no differences neither in epithelial defects nor in tear secretion at all time points studied. Furthermore, corneal lymphangiogenesis was also not induced in any of the experimental setups at any time point studied (see Fig. 11, Fig. 15). But however, while clinical manifestation was not seen during the investigated period, an immunological reaction due to the immunization was detectable.

Flow cytometry analysis of corneal draining lymph nodes (see Fig. 12) in the short-term experiment revealed amplified expression frequencies of CD11b/MHC2 and CD11c/MHC2 positive cells in immunized mice compared to control mice on day 7 and day 10. Although the differences do not

reach a significant level an increased migration of mature APCs and an induction of the immune reaction could be assumed. CD4 positive cells were significantly decreased on day 7 and less detectable on the other time points studied in mice immunized, while CD8 positive cells were not affected. However, as Sjögren's Syndrome dry eye manifests itself by an exocrinopathy and the infiltration of monocytic cells in the lacrimal glands, the flow cytometric analysis of the lacrimal glands represents a more interestingly read out parameter (see Fig. 13). Regarding the expression frequencies of CD45 positive cells a significant increase of these cells on day 7 and day 14 in immunized mice compared to control mice could be observed. On day 10 differences reached no significant level but the increasing tendency was clearly recognizable. In addition, analysis of CD4 positive cells in immunized mice compared to control mice revealed increased amount of these cells in the lacrimal glands at all time points studied, while on day 10 a significant difference could be observed. With respect to the analysis of the corneal draining lymph nodes and the diminished amount recognized, the migration of CD4 positive cells from the corneal draining lymph nodes to the lacrimal glands could be assumed. CD8 expression frequency analysis in the lacrimal glands revealed no significant differences.

Long-term analysis starting at day 14 revealed similar results for this day, as seen in the short-term analysis. Thus, CD4 and CD8 expression frequencies in the corneal draining lymph nodes of immunized mice were diminished compared to control mice (see Fig. 16), while CD11b/MHC2 and CD11c/MHC2 expression frequencies were increased (see Fig. 17) in the corneal draining lymph nodes of immunized mice compared to control mice. The less pronounced differences could be due to a comparatively small number of animals per group. Further on, the significant increase in CD45 positive cells in the lacrimal glands as well as the amplified expression frequencies of CD4 and CD8 positive cells in the lacrimal glands in immunized mice compared to control mice were reproducible, while the increase in CD8 expression frequencies reached a significant level (see Fig. 17).

Regarding expression frequency analysis of CD4 and CD8 positive cell in the corneal draining lymph nodes at the other time points studied, no differences where detectable, expect of day 56 revealing a significant increase of these cells in immunized mice (see Fig. 16). Analysis of CD11b/MHC2 and CD11b/MCH2 expression frequencies revealed no differences, expect of day 28, on which both cell types were increased. Lacrimal gland flow cytometry analysis at the other days investigated, revealed increased expression frequencies for CD45 and CD4 positive cells on day 28, while other days revealed no significant differences (see Fig. 17). Thus, it may well be the immunological reaction initiated due to the immunization has not reached a chronic autoimmune state.

However, lacrimal glands of immunized mice were not only enlarged (data not shown) but also inflammatory infiltrates were detectable in all immunized mice (see Fig. 18). Small infiltrates were also found in two control mice, but infiltrates detectable in immunized mice were more pronounced (see Fig. 18). Thus, specific autoimmunological infiltrates in the lacrimal glands as

described in humans [117] [110] [111] [112] and other experimental Sjögren's Syndrome dry eye models [118], are detectable.
Hence, the described protocol does not fully mimic the human pathology seen in Sjögren's Syndrome dry eye, but reflects the autoimmunological destruction and the inflammatory infiltrates in the lacrimal glands. It may well be, that the period investigated was not long enough for the manifestation of the clinical signs, as the secondary inflammation of the corneal surface would start after the altered tear secretion induced due to the destruction of the lacrimal glands. Corneal lymphangiogenesis, described in experimental dry eye models, would also be a secondary phenotype, which may be needs elongated inflammation of the corneal surface to be initiated.
Further experiments over a longer time period may lead to phenotypica changes and corneal lymphangiogenesis as the autoimmunological destruction of the lacrimal glands would be strengthened. Furthermore, experiments using a specific antigen, already identified for Sjögren's Syndrome dry eye, would be a possibility to intensify the specificity of the immunological reaction against the lacrimal glands leading to a more chronic state of the disease.
Nonetheless this novel "subclinical" model may be of great use in the future to study the also usually subclinical course of most milde forms of DED in patients.

5.2. Topically applied Aflibercept as novel treatment strategy for non-Sjögren's Syndrome dry eye

At its simplest, non-Sjögren's Syndrome dry eye is a chronic inflammatory ocular surface disorder characterized by tear hyperosmolarity and surface symptoms. Almost all experimental induced models are characterized by an increased corneal fluorescein staining and a decreased aqueous tear secretion mimicking clinical features [112] [137] [140]. As epitheliopathy increased over time meanwhile tear secretion decreased over time (see 4.2.1) in all mice exposed to desiccating stress, it can be considered that the induction of DED was successful in the study presented here (see Fig. 20).
Even if nowadays a more comprehensive understanding of the pathophysiology of dry eye exist, the first line therapy of dry eye are artificial tears that moisturize the ocular surface, reduce tear osmolarity and protect from further desiccation [142] [143] [144] [145]. There is a general consensus that the use of this preparations ameliorates clinical symptoms and improves patient's condition [146]. For more severe forms of dry eye, anti-inflammatory therapies like corticosteroids-, cyclosporine- and autologous serum- eye drops are known to improve clinical symptoms and ocular surface dye staining [147]. In the study presented here, it was expected that NaCl, mimicking a simple lubricant, has no effect on the clinical signs, while Aflibercept could maybe ameliorate clinical signs due to the disruption of the vicious circle by inhibiting lymphangiogenesis assumed as

the link to the adaptive immunity [109]. But interestingly, the data obtained revealed no improvement in the clinical phenotype in the Aflibercept treated group (see Fig. 20).
Moreover, no secondarily invasion of lymphatic vessels in the control group exposed to desiccating stress receiving NaCl as eye drops was detectable (100 ± 24% for naive mice, 113 ± 24% for mice exposed to desiccating stress receiving NaCl as eye drops) (see Fig. 21). As NaCl should have no direct influence on the underlying molecular mechanisms relating to lymphangiogenesis, a massive increase in lymphangiogenesis still would have to take place in mice receiving NaCl. But however, no increased lymphangiogenesis was measured in any experimental induced DED during my research period. Thus the data are inconsistent with the prevailing assumption that dry eye disease is a prolymphangiogenic condition [109] [110] [111]. They are much more likely to agree with the recent publication demonstrating no secondary lymphangiogenesis in dry eye disease [148]. Despite the assumption that corneal lymphangiogenesis is maybe not a common feature of DED, several reasons could be taken into account: i) mice's genetic background and ii) state of corneal neovascularization prior the experiment. Regarding mice's genetic background a strain-dependency in the murine corneal lymphangiogenesis was already demonstrated [149] [150]. It may also well be, that there are differences in the same strain between different continents, due to the different breeding strategies. Further on, the state of corneal vascularization prior the experiment has an effect on neovascularization. If mice grow up under non-perfect conditions regarding the room humidity, corneal neovascularization could be induced due to the desiccating stress. These mice then already suffer from an elevated lymphangiogenesis by delivery, which no longer allows the experimental induction and the inhibition of lymphangiogenesis by any compound. As only a few limited studies are available on secondarily lymphangiogenesis occurring in DED, further investigations have to clarify if a selective lymphangiogenesis occurs in experimental induced dry eye independent from the mice's genetic background, their age or their corneal predisposition.
Further on, no significant inhibition on corneal lymphangiogenesis (113% ± 24% for mice exposed to desiccating stress receiving NaCl as eye drops and 103% ± 25% for mice exposed to desiccating stress receiving Aflibercept as eye drops) as well as hemangiogenesis (99% ± 16% for mice exposed to desiccating stress receiving NaCl as eye drops and 87% ± 20% for mice exposed to desiccating stress receiving Aflibercept eye drops) was detectable by topical application of Aflibercept during desiccating stress (see Fig. 21). In the suture induced inflammatory neovascularization model [135] [126] as well as after keratoplasty [127] [128] [129] systemically applied Aflibercept is shown to reduce both, lymph- and hemangiogenesis. In addition, a good penetration of topically applied Aflibercept is demonstrated in the chemical burn-induced neovascularization model [136], wherein the corneal epithelial barrier function is reduced to a minimum. But however, it may be that the integrity of the ocular surface is not enough disrupted after 14 days of desiccating stress, leading to an insufficient penetration. Therefore, further investigations regarding the ability for entering the cornea during desiccating stress has to be performed.

With respect to the purpose of the study presented here, the potential effect of Aflibercept on the immunopathogenesis was examined by flow cytometry analysis of the corneal draining lymph nodes (see Fig. 22). As it is shown that mainly CD4 positive and CD8 positive T cells are involved in the underlying immune response [112] [113] [114] and that CD11b and CD11c positive cells lead to the activation of autoreactive T cells in the lymphoid compartment, we were interested in the surface expression frequencies of CD4, CD8, CD11b and CD11c (see 4.2.3).

A decreasing tendency for CD4 as well as CD8 positive T cells in both treatment groups compared to naive mice could be observed. Schaumburg et al demonstrated a significantly increase in CD4 positive as well as CD8 positive T cells in mice exposed to desiccating stress on day 10 compared to naive mice [151]. In comparison to mice exposed to desiccating stress on day 7 the amount of these cells was lower [151]. Thus it might well be that the decreasing tendency is continued due to the started migration of these cells toward the corneal surface.

Furthermore, as already published by Goyal et al., an increased homing of mature CD11b positive cells in the corneal draining lymph nodes of mice exposed to desiccating stress occurs [109]. Thus, the data received in this study are in line with this report and an increased presentation of ocular antigens could be assumed. Nevertheless, it is quite surprisingly that mice receiving Aflibercept had a higher expression frequency as mice receiving NaCl. Further on, CD11c expression frequencies for mice exposed to desiccating stress receiving NaCl as eye drops revealed a decreasing tendency consistent with the report by Schaumburg et al. [151]. Therein, a decrease of CD11c positive cells in the corneal draining lymph nodes on day 10 was demonstrated.

Regarding the CD11c expression frequency of mice exposed to desiccating stress receiving Aflibercept as eye drops no difference compared to the naive group but a slightly increase in comparison to the control group could be demonstrated. In terms of tumor diseases, VEGF-A was demonstrated to exhibits immunosuppressive properties like the inhibition of dendritic cell as well as macrophage maturation [152] [153]. Transferring this to the obtained data, the increased frequencies of CD11b positive cells in the Aflibercept treated group could be due to the prevented inhibitory effect of VEGF-A on the maturation of these cells. Furthermore, as the maturation of dendritic cells (CD11c) could also not be inhibited by VEGF-A, the amount of these cells could be higher as in the control group leading to an increased expansion of these cells in the corneal draining lymph nodes. Nevertheless, it has to be kept in mind, that pooled lymph nodes for each group were used for flow cytometry analysis which in turn does not allow to perform statistically analysis. Further experiments including a group of mice exposed to desiccating stress without any treatment and investigations on different timepoints, e.g. day 10 and day 16, would allow more information about the effect of topically applied Aflibercept with a better insight on the immunopathogenesis.

Taken together the data obtained herein revealed a successful induction of the desiccating stress model reflecting non-Sjögren's syndrome dry eye. Furthermore, the data provide evidence that topical administered Aflibercept does not ameliorate clinical symptoms of dry eye, because no

lymph- and hemangiogenesis takes place. It was assumed that inhibiting lymphangiogenesis interfere with the vicious circle by inhibiting the access of antigenic material to the regional lymph nodes providing a better outcome of the disease. Now, it is quite unclear if trapping VEGF-A due to topical application of Aflibercept leads to a weaker immune response improving disease outcome. Nevertheless, our data do not support the hypothesis of a significant role of pathological corneal lymphangiogenesis in DED induction and maintenance.

5.3. Systemically applied Aflibercept as novel treatment strategy for non-Sjögren's Syndrome dry eye

As already mentioned before, non-Sjögren's Syndrome dry eye is characterized by increased epithelial defects as well as an decreased tear volume [112] [140] [137]. In both experiments, performing systemical application of Aflibercept, these typically clinical signs in mice exposed to desiccating stress independent from their treatment were induced. Thus, the induction of dry eye was successful in the studies presented here. Nevertheless, again no improvement of the clinical phenotype was reached by systemically application of Aflibercept during desiccating stress (see Fig. 25., Fig. 28). Furthermore, fluorescein staining scores as well as tear secretion recovered to baseline after desiccating stress in both groups in the same amount (see Fig. 28). Thus, systemic Aflibercept neither seems to have an inhibiting effect on the development of clinical signs nor an accelerating effect on the recovery of the clinical signs.

Regarding corneal lymphangiogenesis, again in both treatment regimes no decrease of the lymph vasculature in mice exposed to desiccating stress receiving Aflibercept was detectable (therapy trial: 100% ± 20% for mice exposed to desiccating stress receiving NaCl injections and 116% ± 35% for mice exposed to desiccating stress receiving Aflibercept injections; prevention trial: 100% ± 32% for mice exposed to desiccating stress receiving NaCl injections and 104% ± 33% for mice exposed to desiccating stress receiving Aflibercept injections) (see Fig. 26, Fig. 29). Thus the anti-lymphangiogenic properties of Aflibercept [135] [126] [127] [128] [129] once more were not reproducible, maybe due to a missing induction of lymphangiogenesis as seen in the topical experiments.

Interestingly, quantification of hemangiogenesis revealed an adverse impact of systemically applied Aflibercept in the two experimental setups (see Fig. 26, Fig. 29). Application of Aflibercept starting simultaneously with desiccation stress leads to an increased hemangiogenesis (100% ± 16% for mice exposed to desiccating stress receiving NaCl injections and 117% ± 20% for mice exposed to desiccating stress receiving Aflibercept injections) contrarily to the demonstrated anti-hemangiogenic effect of Aflibercept, while application of Aflibercept after the induction of DED leads to a decrease of hemangiogenesis (100% ± 18% for mice exposed to desiccating stress receiving NaCl injections and 94% ± 10% for mice exposed to desiccating stress receiving Aflibercept

injections) (see Fig. 26, Fig. 29). It may well be that the local inflammatory stimuli on the corneal surface induce endogenous VEGF-A expression, like by the corneal epithelium [154]. This in turn could lead to the induction of corneal hemangiogenesis. In contrast, as the mice are no longer exposed to desiccating stress in the therapy trial, the local inflammatory stimuli are no longer furthered and the endogenous expression of VEGF-A would be stopped. Application of Aflibercept in this period may result in a decreased hemangiogenesis.

Furthermore, quantification of the flow cytometry analysis revealed a decreasing tendency for CD4 positive T cells as well as CD8 positive T cells for Aflibercept treated mice in both systemically treatment regimes (see Fig. 27, Fig. 30). Therefore, a decreased expansion of these cells as well as an already started migration towards the corneal surface could be possible explanations.

In addition, regarding CD11b and CD11c expression frequencies, adverse results for the different treatment regimes were observed. Systemically application of Aflibercept starting with desiccating stress leads to diminished expression frequencies, while systemically application of Aflibercept after the induction of DED leads to amplified expression frequencies (see Fig. 27, Fig. 30).

VEGF-A is shown to mobilize hematopoietic stem cells from the bone marrow to the peripheral circulation under steady state conditions [155] [156]. In addition, VEGFR-1 signaling is demonstrated to promote the mobilization of macrophage lineage cells [157], whereas VEGFR-2 signaling is involved in the accumulation of myeloid precursor cells in the bone marrow [158]. Thus, it could be concluded that trapping VEGF-A simultaneously with the induction of DED, when inflammatory state is not reached yet, leads to a repressed immune response due to the missing recruitment of the precursor cells. The data obtained by systemically Aflibercept injections after the induction of DED, when the immune response is already initiated, looks quite similar to those obtained by topical application of Aflibercept. The observed increasing tendencies of CD11b and CD11c positive cells in mice exposed to desiccating stress receiving Aflibercept in topical treatment regime are more pronounced in this experiment. Thus, the systemically application after the induction of the immune response, again appears to prevent the reported inhibitory effect of VEGF-A on the maturation of CD11b and CD11c positive cells [152] [153], thereby leading to an increased activation and expansion of those cells in the corneal draining lymph nodes [107]. In addition, the decreasing tendency of hemangiogenesis reached a significant level by this treatment regime. Thus, it looks like the effect of topical local applied Aflibercept is amplified by this systemical application. Nevertheless, it has to be kept in mind, that again only pooled lymph nodes for each group were used for flow cytometry analysis which in turn does not allow to perform statistically analysis. Additionally, due to the missing naive group no final conclusion could be given.

Taken together, the data obtained herein provide evidence that systemically administered Aflibercept does not ameliorate clinical symptoms of dry eye at any treatment regime. Nevertheless, the findings of this study for the first time provide indications that VEGF-A has immunoregulatory properties, including immunosuppressive as well as immunosupporting properties, eligible for dry eye. Further experiments including a group of mice exposed to

desiccating stress without any treatment and investigations on different timepoints, e.g. day 10 and day 16, would allow more information about the effect of systemically applied Aflibercept with a better insight on the immunopathogenesis.

6. References

1. Moss, S.E., R. Klein, and B.E. Klein, *Long-term incidence of dry eye in an older population.* Optom Vis Sci, 2008. **85**(8): p. 668-74.
2. Clegg, J.P., et al., *The annual cost of dry eye syndrome in France, Germany, Italy, Spain, Sweden and the United Kingdom among patients managed by ophthalmologists.* Ophthalmic Epidemiol, 2006. **13**(4): p. 263-74.
3. Moss, S.E., R. Klein, and B.E. Klein, *Prevalence of and risk factors for dry eye syndrome.* Arch Ophthalmol, 2000. **118**(9): p. 1264-8.
4. Schaumberg, D.A., et al., *Prevalence of dry eye syndrome among US women.* Am J Ophthalmol, 2003. **136**(2): p. 318-26.
5. Schaumberg, D.A., et al., *Prevalence of dry eye disease among US men: estimates from the Physicians' Health Studies.* Arch Ophthalmol, 2009. **127**(6): p. 763-8.
6. Stern, M.E., et al., *The pathology of dry eye: the interaction between the ocular surface and lacrimal glands.* Cornea, 1998. **17**(6): p. 584-9.
7. Roger, W.B., et al., *The Lacrimal Functional Unit*, in *Dry Eye and Ocular Surface Disorders*. 2004, CRC Press. p. 11-39.
8. Gipson, I.K., *The ocular surface: the challenge to enable and protect vision: the Friedenwald lecture.* Invest Ophthalmol Vis Sci, 2007. **48**(10): p. 4390; 4391-8.
9. *The definition and classification of dry eye disease: report of the Definition and Classification Subcommittee of the International Dry Eye WorkShop (2007).* Ocul Surf, 2007. **5**(2): p. 75-92.
10. Pflugfelder, S.C. and M.E. Stern, *Dry Eye: Inflammation of the Lacrimal Functional Unit*, in *Uveitis and Immunological Disorders*, G.K. Krieglstein, et al., Editors. 2005, Springer Berlin Heidelberg: Berlin, Heidelberg. p. 11-24.
11. Pflugfelder, S., R. Bauerman, and M.E. Stern, *Dry Eye and Ocular Surface Disorders*. 2004: Taylor & Francis.
12. Benitez-del-Castillo, J.M. and M.A. Lemp, *Ocular surface disorders*. 2013, London: JP Medical.
13. Cursiefen, C., *Immune privilege and angiogenic privilege of the cornea.* Chem Immunol Allergy, 2007. **92**: p. 50-7.
14. Haque, S., et al., *Corneal and epithelial thickness changes after 4 weeks of overnight corneal refractive therapy lens wear, measured with optical coherence tomography.* Eye Contact Lens, 2004. **30**(4): p. 189-93; discussion 205-6.
15. Li, H.F., et al., *Epithelial and corneal thickness measurements by in vivo confocal microscopy through focusing (CMTF).* Curr Eye Res, 1997. **16**(3): p. 214-21.
16. Beuerman, R.W. and L. Pedroza, *Ultrastructure of the human cornea.* Microsc Res Tech, 1996. **33**(4): p. 320-35.
17. Nichols, B., C.R. Dawson, and B. Togni, *Surface features of the conjunctiva and cornea.* Invest Ophthalmol Vis Sci, 1983. **24**(5): p. 570-6.
18. Gipson, I.K., *Distribution of mucins at the ocular surface.* Exp Eye Res, 2004. **78**(3): p. 379-88.
19. Haaskjold, E., et al., *The early cell kinetic response during healing of corneal epithelial wounds.* Ophthalmic Surg, 1992. **23**(10): p. 680-4.
20. Sandvig, K.U., et al., *Cell kinetics of conjunctival and corneal epithelium during regeneration of different-sized corneal epithelial defects.* Acta Ophthalmol (Copenh), 1994. **72**(1): p. 43-8.
21. Schermer, A., S. Galvin, and T.T. Sun, *Differentiation-related expression of a major 64K corneal keratin in vivo and in culture suggests limbal location of corneal epithelial stem cells.* J Cell Biol, 1986. **103**(1): p. 49-62.
22. Schlotzer-Schrehardt, U. and F.E. Kruse, *Identification and characterization of limbal stem cells.* Exp Eye Res, 2005. **81**(3): p. 247-64.
23. Pearlman, J.V.F.A.D.D.P.G.M.F.R.E., *The eye: Basic Sciences in Pratice*. Vol. 4. 2016.

24. Dartt, D.A., *Neural regulation of lacrimal gland secretory processes: relevance in dry eye diseases.* Prog Retin Eye Res, 2009. **28**(3): p. 155-77.
25. Linsen, C. and L. Missotten, *Physiology of the lacrimal system.* Bull Soc Belge Ophtalmol, 1990. **238**: p. 35-44.
26. Asbell, P.A. and M.A. Lemp, *Dry Eye Disease: The Clinician's Guide to Diagnosis and Treatment*. 2006: Thieme.
27. Medawar, P.B., *Immunity to homologous grafted skin; the fate of skin homografts transplanted to the brain, to subcutaneous tissue, and to the anterior chamber of the eye.* Br J Exp Pathol, 1948. **29**(1): p. 58-69.
28. Cousins, S.W., et al., *Identification of transforming growth factor-beta as an immunosuppressive factor in aqueous humor.* Invest Ophthalmol Vis Sci, 1991. **32**(8): p. 2201-11.
29. Apte, R.S. and J.Y. Niederkorn, *Isolation and characterization of a unique natural killer cell inhibitory factor present in the anterior chamber of the eye.* J Immunol, 1996. **156**(8): p. 2667-73.
30. Apte, R.S., et al., *Cutting edge: role of macrophage migration inhibitory factor in inhibiting NK cell activity and preserving immune privilege.* J Immunol, 1998. **160**(12): p. 5693-6.
31. Taylor, A.W., D.G. Yee, and J.W. Streilein, *Suppression of nitric oxide generated by inflammatory macrophages by calcitonin gene-related peptide in aqueous humor.* Invest Ophthalmol Vis Sci, 1998. **39**(8): p. 1372-8.
32. Goslings, W.R., et al., *A small molecular weight factor in aqueous humor acts on C1q to prevent antibody-dependent complement activation.* Invest Ophthalmol Vis Sci, 1998. **39**(6): p. 989-95.
33. Kaiser, C.J., B.R. Ksander, and J.W. Streilein, *Inhibition of lymphocyte proliferation by aqueous humor.* Reg Immunol, 1989. **2**(1): p. 42-9.
34. Griffith, T.S., et al., *Fas ligand-induced apoptosis as a mechanism of immune privilege.* Science, 1995. **270**(5239): p. 1189-92.
35. Yoshida, M., M. Takeuchi, and J.W. Streilein, *Participation of pigment epithelium of iris and ciliary body in ocular immune privilege. 1. Inhibition of T-cell activation in vitro by direct cell-to-cell contact.* Invest Ophthalmol Vis Sci, 2000. **41**(3): p. 811-21.
36. Yoshida, M., T. Kezuka, and J.W. Streilein, *Participation of pigment epithelium of iris and ciliary body in ocular immune privilege. 2. Generation of TGF-beta-producing regulatory T cells.* Invest Ophthalmol Vis Sci, 2000. **41**(12): p. 3862-70.
37. Sugita, S. and J.W. Streilein, *Iris pigment epithelium expressing CD86 (B7-2) directly suppresses T cell activation in vitro via binding to cytotoxic T lymphocyte-associated antigen 4.* J Exp Med, 2003. **198**(1): p. 161-71.
38. Williamson, J.S., D. Bradley, and J.W. Streilein, *Immunoregulatory properties of bone marrow-derived cells in the iris and ciliary body.* Immunology, 1989. **67**(1): p. 96-102.
39. Steptoe, R.J., P.G. Holt, and P.G. McMenamin, *Functional studies of major histocompatibility class II-positive dendritic cells and resident tissue macrophages isolated from the rat iris.* Immunology, 1995. **85**(4): p. 630-7.
40. Wilbanks, G.A. and J.W. Streilein, *Studies on the induction of anterior chamber-associated immune deviation (ACAID). 1. Evidence that an antigen-specific, ACAID-inducing, cell-associated signal exists in the peripheral blood.* J Immunol, 1991. **146**(8): p. 2610-7.
41. Wilbanks, G.A., M. Mammolenti, and J.W. Streilein, *Studies on the induction of anterior chamber-associated immune deviation (ACAID). II. Eye-derived cells participate in generating blood-borne signals that induce ACAID.* J Immunol, 1991. **146**(9): p. 3018-24.
42. Wilbanks, G.A. and J.W. Streilein, *Macrophages capable of inducing anterior chamber associated immune deviation demonstrate spleen-seeking migratory properties.* Reg Immunol, 1992. **4**(3): p. 130-7.
43. Sonoda, K.H., et al., *CD1-reactive natural killer T cells are required for development of systemic tolerance through an immune-privileged site.* J Exp Med, 1999. **190**(9): p. 1215-26.
44. Faunce, D.E., K.H. Sonoda, and J. Stein-Streilein, *MIP-2 recruits NKT cells to the spleen during tolerance induction.* J Immunol, 2001. **166**(1): p. 313-21.

45. D'Orazio, T.J. and J.Y. Niederkorn, *Splenic B cells are required for tolerogenic antigen presentation in the induction of anterior chamber-associated immune deviation (ACAID).* Immunology, 1998. **95**(1): p. 47-55.
46. Sonoda, K.H. and J. Stein-Streilein, *CD1d on antigen-transporting APC and splenic marginal zone B cells promotes NKT cell-dependent tolerance.* Eur J Immunol, 2002. **32**(3): p. 848-57.
47. Masli, S., et al., *Expression of thrombospondin in TGFbeta-treated APCs and its relevance to their immune deviation-promoting properties.* J Immunol, 2002. **168**(5): p. 2264-73.
48. Takeuchi, M., P. Alard, and J.W. Streilein, *TGF-beta promotes immune deviation by altering accessory signals of antigen-presenting cells.* J Immunol, 1998. **160**(4): p. 1589-97.
49. Sonoda, K.H., et al., *NK T cell-derived IL-10 is essential for the differentiation of antigen-specific T regulatory cells in systemic tolerance.* J Immunol, 2001. **166**(1): p. 42-50.
50. Niederkorn, J.Y. and J.W. Streilein, *Alloantigens placed into the anterior chamber of the eye induce specific suppression of delayed-type hypersensitivity but normal cytotoxic T lymphocyte and helper T lymphocyte responses.* J Immunol, 1983. **131**(6): p. 2670-4.
51. Wilbanks, G.A. and J.W. Streilein, *Characterization of suppressor cells in anterior chamber-associated immune deviation (ACAID) induced by soluble antigen. Evidence of two functionally and phenotypically distinct T-suppressor cell populations.* Immunology, 1990. **71**(3): p. 383-9.
52. Niederkorn, J.Y. and J. Mellon, *Anterior chamber-associated immune deviation promotes corneal allograft survival.* Invest Ophthalmol Vis Sci, 1996. **37**(13): p. 2700-7.
53. Cursiefen, C., et al., *Lymphatic vessels in vascularized human corneas: immunohistochemical investigation using LYVE-1 and podoplanin.* Invest Ophthalmol Vis Sci, 2002. **43**(7): p. 2127-35.
54. Cursiefen, C., et al., *Corneal lymphangiogenesis: evidence, mechanisms, and implications for corneal transplant immunology.* Cornea, 2003. **22**(3): p. 273-81.
55. Cursiefen, C., et al., *[Angiogenesis and lymphangiogenesis in the cornea. Pathogenesis, clinical implications and treatment options].* Ophthalmologe, 2003. **100**(4): p. 292-9.
56. Cursiefen, C., et al., *Absence of blood and lymphatic vessels in the developing human cornea.* Cornea, 2006. **25**(6): p. 722-6.
57. Ambati, B.K., et al., *Corneal avascularity is due to soluble VEGF receptor-1.* Nature, 2006. **443**(7114): p. 993-7.
58. Ambati, B.K., et al., *Soluble vascular endothelial growth factor receptor-1 contributes to the corneal antiangiogenic barrier.* Br J Ophthalmol, 2007. **91**(4): p. 505-8.
59. Albuquerque, R.J., et al., *Alternatively spliced vascular endothelial growth factor receptor-2 is an essential endogenous inhibitor of lymphatic vessel growth.* Nat Med, 2009. **15**(9): p. 1023-30.
60. Singh, N., et al., *Soluble vascular endothelial growth factor receptor 3 is essential for corneal alymphaticity.* Blood, 2013. **121**(20): p. 4242-9.
61. Maurice, D.M., *The location of the fluid pump in the cornea.* J Physiol, 1972. **221**(1): p. 43-54.
62. Maurice, D.M., *The structure and transparency of the cornea.* J Physiol, 1957. **136**(2): p. 263-86.
63. Cogan, D.G., *Vascularization of the Cornea. Its Experimental Induction by Small Lesions and a New Theory of Its Pathogenesis.* Trans Am Ophthalmol Soc, 1948. **46**: p. 457-71.
64. Langham, M., *Observations on the growth of blood vessels into the cornea; application of a new experimental technique.* Br J Ophthalmol, 1953. **37**(4): p. 210-22.
65. Kim, Y.M., et al., *Endostatin blocks vascular endothelial growth factor-mediated signaling via direct interaction with KDR/Flk-1.* J Biol Chem, 2002. **277**(31): p. 27872-9.
66. Dhanabal, M., et al., *Endostatin induces endothelial cell apoptosis.* J Biol Chem, 1999. **274**(17): p. 11721-6.
67. Armstrong, L.C. and P. Bornstein, *Thrombospondins 1 and 2 function as inhibitors of angiogenesis.* Matrix Biol, 2003. **22**(1): p. 63-71.
68. Lawler, J., *Thrombospondin-1 as an endogenous inhibitor of angiogenesis and tumor growth.* J Cell Mol Med, 2002. **6**(1): p. 1-12.
69. Moser, T.L., et al., *Angiostatin binds ATP synthase on the surface of human endothelial cells.* Proc Natl Acad Sci U S A, 1999. **96**(6): p. 2811-6.

70. Ambati, B.K., et al., *Angiostatin inhibits and regresses corneal neovascularization.* Arch Ophthalmol, 2002. **120**(8): p. 1063-8.
71. Gabison, E., et al., *Anti-angiogenic role of angiostatin during corneal wound healing.* Exp Eye Res, 2004. **78**(3): p. 579-89.
72. Karakousis, P.C., et al., *Localization of pigment epithelium derived factor (PEDF) in developing and adult human ocular tissues.* Mol Vis, 2001. **7**: p. 154-63.
73. Meyer, C., L. Notari, and S.P. Becerra, *Mapping the type I collagen-binding site on pigment epithelium-derived factor. Implications for its antiangiogenic activity.* J Biol Chem, 2002. **277**(47): p. 45400-7.
74. Shao, X.J. and X.Y. Chi, *Influence of angiostatin and thalidomide on lymphangiogenesis.* Lymphology, 2005. **38**(3): p. 146-55.
75. Cursiefen, C., et al., *Roles of thrombospondin-1 and -2 in regulating corneal and iris angiogenesis.* Invest Ophthalmol Vis Sci, 2004. **45**(4): p. 1117-24.
76. Cursiefen, C., et al., *Thrombospondin 1 inhibits inflammatory lymphangiogenesis by CD36 ligation on monocytes.* J Exp Med, 2011. **208**(5): p. 1083-92.
77. Dana, M.R. and J.W. Streilein, *Loss and restoration of immune privilege in eyes with corneal neovascularization.* Invest Ophthalmol Vis Sci, 1996. **37**(12): p. 2485-94.
78. Hos, D. and C. Cursiefen, *Lymphatic vessels in the development of tissue and organ rejection.* Adv Anat Embryol Cell Biol, 2014. **214**: p. 119-41.
79. Kaplan, H.J., J.W. Streilein, and T.R. Stevens, *Transplantation immunology of the anterior chamber of the eye. II. Immune response to allogeneic cells.* J Immunol, 1975. **115**(3): p. 805-10.
80. Lemp, M.A., *Report of the National Eye Institute/Industry workshop on Clinical Trials in Dry Eyes.* CLAO J, 1995. **21**(4): p. 221-32.
81. Li, D.Q., et al., *Stimulation of matrix metalloproteinases by hyperosmolarity via a JNK pathway in human corneal epithelial cells.* Invest Ophthalmol Vis Sci, 2004. **45**(12): p. 4302-11.
82. Luo, L., et al., *Hyperosmolar saline is a proinflammatory stress on the mouse ocular surface.* Eye Contact Lens, 2005. **31**(5): p. 186-93.
83. De Paiva, C.S., et al., *Corticosteroid and doxycycline suppress MMP-9 and inflammatory cytokine expression, MAPK activation in the corneal epithelium in experimental dry eye.* Exp Eye Res, 2006. **83**(3): p. 526-35.
84. Yeh, S., et al., *Apoptosis of ocular surface cells in experimentally induced dry eye.* Invest Ophthalmol Vis Sci, 2003. **44**(1): p. 124-9.
85. Kunert, K.S., A.S. Tisdale, and I.K. Gipson, *Goblet cell numbers and epithelial proliferation in the conjunctiva of patients with dry eye syndrome treated with cyclosporine.* Arch Ophthalmol, 2002. **120**(3): p. 330-7.
86. Argueso, P., et al., *Decreased levels of the goblet cell mucin MUC5AC in tears of patients with Sjogren syndrome.* Invest Ophthalmol Vis Sci, 2002. **43**(4): p. 1004-11.
87. Nakamura, H., A. Kawakami, and K. Eguchi, *Mechanisms of autoantibody production and the relationship between autoantibodies and the clinical manifestations in Sjogren's syndrome.* Transl Res, 2006. **148**(6): p. 281-8.
88. Hayashi, Y., R. Arakaki, and N. Ishimaru, *The role of caspase cascade on the development of primary Sjogren's syndrome.* J Med Invest, 2003. **50**(1-2): p. 32-8.
89. Mathers, W.D., J.A. Lane, and M.B. Zimmerman, *Tear film changes associated with normal aging.* Cornea, 1996. **15**(3): p. 229-34.
90. Patel, S. and J.C. Farrell, *Age-related changes in precorneal tear film stability.* Optom Vis Sci, 1989. **66**(3): p. 175-8.
91. Sullivan, B.D., et al., *Influence of aging on the polar and neutral lipid profiles in human meibomian gland secretions.* Arch Ophthalmol, 2006. **124**(9): p. 1286-92.
92. Chen, Y., et al., *Interferon-gamma-secreting NK cells promote induction of dry eye disease.* J Leukoc Biol, 2011. **89**(6): p. 965-72.
93. Zhang, X., et al., *NK cells promote Th-17 mediated corneal barrier disruption in dry eye.* PLoS One, 2012. **7**(5): p. e36822.

94. De Paiva, C.S., et al., *Dry eye-induced conjunctival epithelial squamous metaplasia is modulated by interferon-gamma.* Invest Ophthalmol Vis Sci, 2007. **48**(6): p. 2553-60.
95. De Paiva, C.S., et al., *IL-17 disrupts corneal barrier following desiccating stress.* Mucosal Immunol, 2009. **2**(3): p. 243-53.
96. Stern, M.E., et al., *Conjunctival T-cell subpopulations in Sjogren's and non-Sjogren's patients with dry eye.* Invest Ophthalmol Vis Sci, 2002. **43**(8): p. 2609-14.
97. Luo, L., et al., *Experimental dry eye stimulates production of inflammatory cytokines and MMP-9 and activates MAPK signaling pathways on the ocular surface.* Invest Ophthalmol Vis Sci, 2004. **45**(12): p. 4293-301.
98. Li, D.Q., et al., *JNK and ERK MAP kinases mediate induction of IL-1beta, TNF-alpha and IL-8 following hyperosmolar stress in human limbal epithelial cells.* Exp Eye Res, 2006. **82**(4): p. 588-96.
99. Luo, L., D.Q. Li, and S.C. Pflugfelder, *Hyperosmolarity-induced apoptosis in human corneal epithelial cells is mediated by cytochrome c and MAPK pathways.* Cornea, 2007. **26**(4): p. 452-60.
100. Corrales, R.M., et al., *Desiccating stress stimulates expression of matrix metalloproteinases by the corneal epithelium.* Invest Ophthalmol Vis Sci, 2006. **47**(8): p. 3293-302.
101. Hamrah, P., et al., *The corneal stroma is endowed with a significant number of resident dendritic cells.* Invest Ophthalmol Vis Sci, 2003. **44**(2): p. 581-9.
102. Hamrah, P., et al., *Alterations in corneal stromal dendritic cell phenotype and distribution in inflammation.* Arch Ophthalmol, 2003. **121**(8): p. 1132-40.
103. Yoon, K.C., et al., *Expression of Th-1 chemokines and chemokine receptors on the ocular surface of C57BL/6 mice: effects of desiccating stress.* Invest Ophthalmol Vis Sci, 2007. **48**(6): p. 2561-9.
104. Yoon, K.C., et al., *Expression of CXCL9, -10, -11, and CXCR3 in the tear film and ocular surface of patients with dry eye syndrome.* Invest Ophthalmol Vis Sci, 2010. **51**(2): p. 643-50.
105. Choi, W., et al., *Expression of CCR5 and its ligands CCL3, -4, and -5 in the tear film and ocular surface of patients with dry eye disease.* Curr Eye Res, 2012. **37**(1): p. 12-7.
106. Pisella, P.J., et al., *Flow cytometric analysis of conjunctival epithelium in ocular rosacea and keratoconjunctivitis sicca.* Ophthalmology, 2000. **107**(10): p. 1841-9.
107. Gao, J., et al., *ICAM-1 expression predisposes ocular tissues to immune-based inflammation in dry eye patients and Sjogrens syndrome-like MRL/lpr mice.* Exp Eye Res, 2004. **78**(4): p. 823-35.
108. Jin, Y., et al., *The chemokine receptor CCR7 mediates corneal antigen-presenting cell trafficking.* Mol Vis, 2007. **13**: p. 626-34.
109. Goyal, S., et al., *Evidence of corneal lymphangiogenesis in dry eye disease: a potential link to adaptive immunity?* Arch Ophthalmol, 2010. **128**(7): p. 819-24.
110. Goyal, S., S.K. Chauhan, and R. Dana, *Blockade of prolymphangiogenic vascular endothelial growth factor C in dry eye disease.* Arch Ophthalmol, 2012. **130**(1): p. 84-9.
111. Chen, Y., et al., *Chronic dry eye disease is principally mediated by effector memory Th17 cells.* Mucosal Immunol, 2014. **7**(1): p. 38-45.
112. Niederkorn, J.Y., et al., *Desiccating stress induces T cell-mediated Sjogren's Syndrome-like lacrimal keratoconjunctivitis.* J Immunol, 2006. **176**(7): p. 3950-7.
113. El Annan, J., et al., *Characterization of effector T cells in dry eye disease.* Invest Ophthalmol Vis Sci, 2009. **50**(8): p. 3802-7.
114. Chauhan, S.K., et al., *Autoimmunity in dry eye is due to resistance of Th17 to Treg suppression.* J Immunol, 2009. **182**(3): p. 1247-52.
115. Massingale, M.L., et al., *Analysis of inflammatory cytokines in the tears of dry eye patients.* Cornea, 2009. **28**(9): p. 1023-7.
116. Kang, M.H., et al., *Interleukin-17 in various ocular surface inflammatory diseases.* J Korean Med Sci, 2011. **26**(7): p. 938-44.
117. Fox, R.I., *Sjogren's syndrome.* Lancet, 2005. **366**(9482): p. 321-31.
118. Turpie, B., et al., *Sjogren's syndrome-like ocular surface disease in thrombospondin-1 deficient mice.* Am J Pathol, 2009. **175**(3): p. 1136-47.

119. Bacman, S., et al., *Muscarinic acetylcholine receptor antibodies as a new marker of dry eye Sjogren syndrome.* Invest Ophthalmol Vis Sci, 2001. **42**(2): p. 321-7.
120. Gao, J., et al., *Detection of anti-type 3 muscarinic acetylcholine receptor autoantibodies in the sera of Sjogren's syndrome patients by use of a transfected cell line assay.* Arthritis Rheum, 2004. **50**(8): p. 2615-21.
121. Iwasaki, K., et al., *Detection of anti-SS-A/Ro and anti-SS-B/La antibodies of IgA and IgG isotypes in saliva and sera of patients with Sjogren's syndrome.* Nihon Rinsho Meneki Gakkai Kaishi, 2003. **26**(6): p. 346-54.
122. Haneji, N., et al., *Identification of alpha-fodrin as a candidate autoantigen in primary Sjogren's syndrome.* Science, 1997. **276**(5312): p. 604-7.
123. Chauhan, S.K., et al., *A novel pro-lymphangiogenic function for Th17/IL-17.* Blood, 2011. **118**(17): p. 4630-4.
124. Steven, P., et al., *Intravital two-photon microscopy of immune cell dynamics in corneal lymphatic vessels.* PLoS One, 2011. **6**(10): p. e26253.
125. von Andrian, U.H. and T.R. Mempel, *Homing and cellular traffic in lymph nodes.* Nat Rev Immunol, 2003. **3**(11): p. 867-78.
126. Dietrich, T., et al., *Cutting edge: lymphatic vessels, not blood vessels, primarily mediate immune rejections after transplantation.* J Immunol, 2010. **184**(2): p. 535-9.
127. Cursiefen, C., et al., *Inhibition of hemangiogenesis and lymphangiogenesis after normal-risk corneal transplantation by neutralizing VEGF promotes graft survival.* Invest Ophthalmol Vis Sci, 2004. **45**(8): p. 2666-73.
128. Bachmann, B.O., et al., *Promotion of graft survival by vascular endothelial growth factor a neutralization after high-risk corneal transplantation.* Arch Ophthalmol, 2008. **126**(1): p. 71-7.
129. Bachmann, B.O., et al., *Transient postoperative vascular endothelial growth factor (VEGF)-neutralisation improves graft survival in corneas with partly regressed inflammatory neovascularisation.* Br J Ophthalmol, 2009. **93**(8): p. 1075-80.
130. Yamagami, S., M.R. Dana, and T. Tsuru, *Draining lymph nodes play an essential role in alloimmunity generated in response to high-risk corneal transplantation.* Cornea, 2002. **21**(4): p. 405-9.
131. *Aflibercept: AVE 0005, AVE 005, AVE0005, VEGF Trap - Regeneron, VEGF Trap (R1R2), VEGF Trap-Eye.* Drugs R D, 2008. **9**(4): p. 261-9.
132. Papadopoulos, N., et al., *Binding and neutralization of vascular endothelial growth factor (VEGF) and related ligands by VEGF Trap, ranibizumab and bevacizumab.* Angiogenesis, 2012. **15**(2): p. 171-85.
133. Saishin, Y., et al., *VEGF-TRAP(R1R2) suppresses choroidal neovascularization and VEGF-induced breakdown of the blood-retinal barrier.* J Cell Physiol, 2003. **195**(2): p. 241-8.
134. Nork, T.M., et al., *Prevention of experimental choroidal neovascularization and resolution of active lesions by VEGF trap in nonhuman primates.* Arch Ophthalmol, 2011. **129**(8): p. 1042-52.
135. Cursiefen, C., et al., *VEGF-A stimulates lymphangiogenesis and hemangiogenesis in inflammatory neovascularization via macrophage recruitment.* J Clin Invest, 2004. **113**(7): p. 1040-50.
136. Sella, R., et al., *Efficacy of topical aflibercept versus topical bevacizumab for the prevention of corneal neovascularization in a rat model.* Exp Eye Res, 2016. **146**: p. 224-232.
137. Dursun, D., et al., *A mouse model of keratoconjunctivitis sicca.* Investigative Ophthalmology & Visual Science, 2002. **43**(3): p. 632-638.
138. Dursun, D., et al., *Experimentally induced dry eye produces ocular surface inflammation and epithelial disease.* Adv Exp Med Biol, 2002. **506**(Pt A): p. 647-55.
139. *Methodologies to diagnose and monitor dry eye disease: report of the Diagnostic Methodology Subcommittee of the International Dry Eye WorkShop (2007).* Ocul Surf, 2007. **5**(2): p. 108-52.
140. Barabino, S., et al., *The controlled-environment chamber: a new mouse model of dry eye.* Invest Ophthalmol Vis Sci, 2005. **46**(8): p. 2766-71.
141. Bock, F., et al., *Improved semiautomatic method for morphometry of angiogenesis and lymphangiogenesis in corneal flatmounts.* Exp Eye Res, 2008. **87**(5): p. 462-70.
142. Liu, Z. and S.C. Pflugfelder, *Corneal surface regularity and the effect of artificial tears in aqueous tear deficiency.* Ophthalmology, 1999. **106**(5): p. 939-43.

143. Huang, F.C., et al., *Effect of artificial tears on corneal surface regularity, contrast sensitivity, and glare disability in dry eyes.* Ophthalmology, 2002. **109**(10): p. 1934-40.
144. Lopez Bernal, D. and J.L. Ubels, *Artificial tear composition and promotion of recovery of the damaged corneal epithelium.* Cornea, 1993. **12**(2): p. 115-20.
145. Gilbard, J.P. and R.L. Farris, *Tear osmolarity and ocular surface disease in keratoconjunctivitis sicca.* Arch Ophthalmol, 1979. **97**(9): p. 1642-6.
146. McCann, L.C., et al., *Effectiveness of artificial tears in the management of evaporative dry eye.* Cornea, 2012. **31**(1): p. 1-5.
147. *Management and therapy of dry eye disease: report of the Management and Therapy Subcommittee of the International Dry Eye WorkShop (2007).* Ocul Surf, 2007. **5**(2): p. 163-78.
148. Cho, Y.K., B. Archer, and B.K. Ambati, *Dry eye predisposes to corneal neovascularization and lymphangiogenesis after corneal injury in a murine model.* Cornea, 2014. **33**(6): p. 621-7.
149. Regenfuss, B., et al., *Genetic heterogeneity of lymphangiogenesis in different mouse strains.* Am J Pathol, 2010. **177**(1): p. 501-10.
150. Regenfuß, B., *Strain-Dependent Differences in Lymphangiogenesis among Inbred Mouse Strains*. 2012, Friedrich-Alexander-Universität Erlangen-Nürnberg.
151. Schaumburg, C.S., et al., *Ocular surface APCs are necessary for autoreactive T cell-mediated experimental autoimmune lacrimal keratoconjunctivitis.* J Immunol, 2011. **187**(7): p. 3653-62.
152. Gabrilovich, D., et al., *Vascular endothelial growth factor inhibits the development of dendritic cells and dramatically affects the differentiation of multiple hematopoietic lineages in vivo.* Blood, 1998. **92**(11): p. 4150-66.
153. Oyama, T., et al., *Vascular endothelial growth factor affects dendritic cell maturation through the inhibition of nuclear factor-kappa B activation in hemopoietic progenitor cells.* J Immunol, 1998. **160**(3): p. 1224-32.
154. Mastyugin, V., et al., *Corneal epithelial VEGF and cytochrome P450 4B1 expression in a rabbit model of closed eye contact lens wear.* Curr Eye Res, 2001. **23**(1): p. 1-10.
155. Hattori, K., et al., *Vascular endothelial growth factor and angiopoietin-1 stimulate postnatal hematopoiesis by recruitment of vasculogenic and hematopoietic stem cells.* J Exp Med, 2001. **193**(9): p. 1005-14.
156. Heissig, B., et al., *Recruitment of stem and progenitor cells from the bone marrow niche requires MMP-9 mediated release of kit-ligand.* Cell, 2002. **109**(5): p. 625-37.
157. Muramatsu, M., et al., *Vascular endothelial growth factor receptor-1 signaling promotes mobilization of macrophage lineage cells from bone marrow and stimulates solid tumor growth.* Cancer Res, 2010. **70**(20): p. 8211-21.
158. Larrivee, B., I. Pollet, and A. Karsan, *Activation of vascular endothelial growth factor receptor-2 in bone marrow leads to accumulation of myeloid cells: role of granulocyte-macrophage colony-stimulating factor.* J Immunol, 2005. **175**(5): p. 3015-24.

7. Abbreviation Index

α	anti
Ag	antigen
ANOVA	analysis of variance
APCs	antigen presenting cells
BSA	bovine serum albumin
C57BL/6	C57BL/6NCrl
ca.	circa
CD	cluster of differentiation
CEC	controlled environment chamber
DC	dendritic cell
e.g.	for example
FBS	Fetal bovine serum
Fig.	figure
h	hours
HA	hemangiogenesis
i.p.	intraperitonial
kg	Kilogram
l	liter
LA	lymphangiogenesis
Li	limbus
LYVE-1	Lymphatic Vessel Endothelial hyaluronan Receptor 1
µg	microgram
mg	milligram
MHC	major Histocompatibility Complex
min	minute
µl	microliter
mm	millimeter
n.s.	not significant
NV	neovascularization
p	p-value
PBS	phosphate-buffered saline solution
PBSA	phosphate-buffered saline (PBS), containing 2% (w/v) BSA
PFA	paraformaldehyde
ROI	region of interest
rpm	rounds per minute
rT	room temperature
S	stroma
SD	standard deviation
s.c.	subcutaneous

Tab.	table
t-Test	students t-Test
VEGF	vascular endothelial growth factor
VEGFR	vascular endothelial growth factor receptor
vs	versus.

8. Danksagung

An dieser Stelle danke ich all jenen Menschen, die mir bei der Erstellung dieser Arbeit auf alle nur erdenklichen Arten geholfen haben.

An erster Stelle möchte ich Herr *Prof. Dr. Cursiefen* für die Bereitstellung des Promotionsthemas und die Möglichkeit diese Doktorarbeit in seinem Labor durchführen zu können bedanken. Außerdem bedanke ich mich für die Möglichkeit auf verschiedenen internationalen Kongressen Forschungsergebnisse präsentieren zu dürfen und einen wissenschaftlichen Artikel verfassen und veröffentlichen zu dürfen.

Ich bedanke mich bei *PD Dr. Bock* für die persönliche Betreuung im Labor und die Einarbeitung in ein neues Thema mit neuen faszinierenden Techniken.

Nicht weniger bedanke ich mich bei *Prof. Langmann* und *Prof. Neundorf* für die hilfsbereite und unkomplizierte Betreuung sowie die Begutachtung dieser Arbeit.

Des Weiteren danke ich dem *Graduiertenprogramm Pharmacology and experimental Therapeutics* der Universitätsklinik Köln und der Bayer Health Care AG für die Finanzierung meiner Stelle. Durch die vielen zusätzlichen Möglichkeiten an Kursen und Fortbildungen konnte man sich stets, auch Abseits des eigenen Forschungsbereich, weiterentwickeln.

Ich danke auch *PD Dr. Steven* und *Dr. Gehlsen*, für die Hilfe bei meinem Forschungsprojekt und die anregenden Diskussionen.

Ein ganz herzlicher Dank geht an alle, die die letzten drei Jahre mit mir zusammen im Labor gearbeitet haben. Insbesondere möchte ich mich bei *Gabriele Braun* bedanken: Du warst nicht nur der Stützpfeiler aller organistorischen Dinge im Labor, sondern hast mich auch stets mit deinen helfenden Händen unterstützt und immer ein offenes Ohr für mich gehabt. Bei *Nasrin Refaian*: Getreu dem Motto “Halbes Leid, geteiltes Leid”, konnte ich immer auf deine moralische Unterstützung zählen. Unsere gemeinsamen Kaffepausen und Überstunden haben meinen Laboralltag versüsst!

Bedanken möchte ich mich auch bei *Dr. Rebecca Scholz* und *Dr. Anika Lückoff*, die mich stets mit unerschütterlicher Hingabe motiviert haben und auch abseits dieser Arbeit mein Leben bereichern.

Abschließend möchte ich meiner Familie danken! *Mum, Dad* euch danke ich für die unerschütterliche und ausdauernde Unterstützung die Ihr mir schon mein ganzes Leben entgegenbringt. *Daniel*, dir danke ich für deine motivierenden Worte und dein Interesse an mir und meiner Arbeit! *Hedi*, dir danke ich dafür, dass ich darauf vertrauen kann, dass du immer für mich da bist und mich mein ganzes weiteres Leben unterstützen wirst. *Björn*, dir danke ich für deine Ausdauer und dein Vertrauen in mich. Du hast viel ertragen müssen und dich nie beschwert!

Erklärung

Ich versichere, dass ich die mir vorgelegte Dissertation selbständig angefertigt, die benutzten Quellen und Hilfsmittel vollständig angegeben und die Stellen der Arbeit - einschließlich Tabellen, Karten, und Abbildungen - , die anderen Werken im Wortlaut oder dem Sinn nach entnommen sind, in jedem Einzelfall als Entlehnung kenntlich gemacht habe; dass diese Dissertation noch keiner anderen Fakultät oder Universität zur Prüfung vorgelegen hat; dass sie – abgesehen von unten angegebenen Teilpublikationen – noch nicht veröffentlicht worden ist sowie, dass ich eine solche Veröffentlichung vor Abschluss des Promotionsverfahrens nicht vornehmen werde.
Die Bestimmungen dieser Promotionsordnung sind mir bekannt. Die von mir vorgelegte Dissertation ist von Prof. Dr. med. Claus Cursiefen (Zentrum für Augenheilkunde) betreut worden.

Übersicht der Publikationen:
nicht zutreffend

Ich versichere, dass ich alle Angaben wahrheitsgemäß nach bestem Wissen und Gewissen gemacht habe und verpflichte mich, jedmögliche, die obigen Angaben betreffenden Veränderungen, dem Promotionsausschuss unverzüglich mitzuteilen.

Köln, den 24. Oktober 2016 

Laura Schöllhorn